

A THREE-POSITION SPECTRAL LINE SURVEY OF SAGITTARIUS B2 BETWEEN 218 AND 263 GHz. I. THE OBSERVATIONAL DATA

A. NUMMELIN, P. BERGMAN, AND Å. HJALMARSON

Onsala Space Observatory, S-439 92 Onsala, Sweden; albert@oso.chalmers.se, bergman@oso.chalmers.se, hjalmar@oso.chalmers.se

P. FRIBERG

Joint Astronomy Centre, 660 North A'ohoku Place, University Park, Hilo, HI 96720; friberg@jach.hawaii.edu

W. M. IRVINE

FCRAO, 619 Lederle GRC, University of Massachusetts, Amherst, MA 01003; irvine@fcrao1.phast.umass.edu

T. J. MILLAR

Department of Physics, UMIST, P.O. Box 88, Manchester M60 1QD, England; tjm@saturn.phy.umist.ac.uk

M. OHISHI

Nobeyama Radio Observatory, Nobeyama, Minamimaki, Minamisaku, Nagano 384-13, Japan; ohishi@nro.nao.ac.jp

AND

S. SAITO

Institute for Molecular Science, Myodaiji, Okazaki 444, Japan; saito@ims.ac.jp

Received 1998 January 12; accepted 1998 March 12

ABSTRACT

We have surveyed the frequency band 218.30–263.55 GHz toward the core positions N and M and the quiescent cloud position NW in the Sgr B2 molecular cloud using the Swedish-ESO Submillimetre Telescope. In total 1730, 660, and 110 lines were detected in N, M, and NW, respectively, and 42 different molecular species were identified. The number of unidentified lines are 337, 51, and eight. Toward the N source, spectral line emission constitutes 22% of the total detected flux in the observed band, and complex organic molecules are the main contributors. Toward M, 14% of the broadband flux is caused by lines, and SO₂ is here the dominant source of emission. NW is relatively poor in spectral lines and continuum. In this paper we present the spectra together with tables of suggested line identifications.

Subject headings: ISM: individual (Sagittarius B2) — ISM: molecules — line: identification — surveys

1. INTRODUCTION

When the decision was made to survey the 1.3 mm spectrum toward the Sgr B2 molecular cloud, the dense core positions Sgr B2(N) and Sgr B2(M) were rather obvious choices based upon the high-resolution data of Goldsmith et al. (1987a) and Vogel, Genzel, & Palmer (1987). These cores are the two main centers of massive star formation in Sgr B2 but appear to be rather different in chemistry and structure. In addition to N and M, a third position toward the surrounding cloud, Sgr B2(NW) or northwest, was selected since it was indicated from Nobeyama observations as having a large column of gas (Ohishi 1992). The same positions have also been observed in a survey of the bands 30–50 and 79–116 GHz made at Nobeyama Radio Observatory (Ohishi, Ishikawa, & Kaifu 1998). Observations of these three positions therefore enable comparison of physics and chemistry between molecular gas in different evolutionary stages and physical environments.

Traditionally, lower frequency surveys of Sgr B2 have been performed toward a more southern source position, Sgr B2(OH), located about 30" south of M (Cummins, Linke, & Thaddeus 1986; Turner 1989, 1991). More recently Sutton et al. (1991) surveyed the 330–350 GHz band toward Sgr B2(M) and also made comparisons with some bands taken toward the N position.

The present work is the first comprehensive survey of the N and NW positions and the first survey of any of the three positions in the 1.3 mm band. In this paper we describe the observational details and present the spectra together with tabulations of the proposed line identifications. Data

analysis, results, and a more detailed discussion of the data will follow in a separate paper (Nummelin et al. 1998; hereafter Paper II).

2. OBSERVATIONS AND DATA REDUCTION

The observations were performed with the 15 m Swedish ESO-Submillimetre Telescope (SEST)¹ at La Silla during 11 observing sessions between 1990 August and 1997 June. Three positions (see Table 1) were observed: Sgr B2(N), Sgr B2(M), and Sgr B2(NW). The frequency band covered is 218.30–263.55 GHz (1.14–1.37 mm) although the coverage for Sgr B2(NW) is somewhat incomplete. Toward this position there are five gaps of in total 8 GHz between 229.9 and 243.8 GHz, the reason being that the decision to observe the Sgr B2(NW) position was made in 1991, after the survey was commenced.

The original SEST 230 GHz Schottky receiver, which was used in the 1990 observing session, gave system temperatures (T_{sys}^*) typically around 1300 K. In 1991 the Schottky receiver was replaced by an SIS receiver that gave system temperatures around 600 K. Both receivers were tuned to single-sideband operation, with an image sideband suppression of about 20 dB. A confirmation of the high image-band rejection is given by the intensity of the observed line features ($T_{\text{mb}} \lesssim 0.4$ K) around 222.66 GHz from the CO($J = 2 \rightarrow 1$) line in the upper (image) sideband,

¹ The Swedish-ESO Submillimetre Telescope is operated jointly by ESO and the Swedish National Facility for Radio Astronomy, Onsala Space Observatory, at Chalmers University of Technology.

TABLE 1
SOURCE COORDINATES AND V_{LSR} ADOPTED

Source	$\alpha(1950.0)$	$\delta(1950.0)$	V_{LSR} (km s $^{-1}$)
Sgr B2(N)	17 44 10.1	-28 21 17.0	+62
Sgr B2(M)	17 44 10.4	-28 22 03.0	+62
Sgr B2(NW).....	17 44 06.6	-28 21 20.0	+62

NOTE.—Units of right ascension are hours, minutes, and seconds, and units of declination are degrees, arcminutes, and arcseconds.

which indicates an image rejection ratio of approximately 20 dB. Because of the high image-band rejection, no post-processing treatment of the data to separate the sideband responses was necessary.

Three different acousto-optical spectrometers (AOS) have been used. The AOS used between 1990 and 1992 had a bandwidth of 500 MHz, while those used in subsequent observing sessions each had 1 GHz bandwidth. All three spectrometers had nominal channel separations of 0.7 MHz, but, owing to the channel correlation, the actual frequency resolution obtained is about 1.4 MHz, and the resulting velocity resolution is 1.8 km s $^{-1}$ at 230 GHz. The data presented here have been filtered to 1.0 MHz channel separation. The local oscillator frequency settings were chosen so that consecutive scans overlapped by 50 MHz. A radial velocity relative to the local standard of rest, $V_{\text{LSR}} = +62 \text{ km s}^{-1}$, was used toward all three sources throughout the survey.

The data were calibrated on-line using the standard chopper-wheel method described by Kutner & Ulich (1981), and the raw data obtained at the telescope were given in the atmosphere-corrected antenna temperature scale, T_A^* .

From La Silla the Sgr B2 region is at observable elevation, between 25° and 80°, for 9 hr per day, and at SEST observations are carried out daytime as well as nighttime. The telescope pointing was checked 2–3 times before and after transit toward the SiO masers in VX Sgr and AH Sco, located about 10° from Sgr B2, or toward suitable planets. The relative offsets were in general within 5''. After dawn and dusk the subreflector focusing was also checked after the regular pointing checks owing to the change in ambient temperature. The consistency of the pointing and calibration was also checked directly toward the Sgr B2(M) and Sgr B2(N) sources through observations of the strong emission from CH₃CN($J = 13 \rightarrow 12$) at 239 GHz. Another consistency confirmation was the continuum level measured in each spectrum. We estimate the uncertainty in the antenna temperature due to pointing and calibration errors to be within 30%.

The observations were performed in wide dual beam-switch mode, with an azimuthal beam throw of 11.6. The only exception to this is the 244.75–245.40 GHz band toward the N and M positions, which was observed in position-switch mode with the reference position at $\alpha(1950.0) = 17^{\text{h}}42^{\text{m}}10^{\text{s}}.4$, $\delta(1950.0) = -27^{\circ}52'03.0'$. These data were obtained during a mapping study of CS($J = 5 \rightarrow 4$) in 1997 June and replaced the older data that suffered from poor signal-to-noise ratio. The line emission from CO and ^{13}CO certainly is more extended than the beam throw, the result being distorted line profiles and incorrect line intensities. This has also been commented on in the tables.

The full half-power beamwidth (FHPBW) of the SEST antenna is 22'' at 230 GHz, and the corresponding linear resolution at Sgr B2 is 0.9 pc, assuming a distance of 8.0 kpc. The FHPBW varies between 19'' and 23'' over the frequency range covered. By comparison of spectra containing strong lines in the N core with those taken toward the NW position, we conclude that the relative response of the sidelobes of the telescope is at least less than 5% at 50'' angular offset from the on-source position. The separation between the N and M positions is similar to the N-NW separation.

The intensity scale used in the spectra and tables is main-beam brightness temperature, which for a uniformly bright source that exactly fills the main beam is equal to the true brightness temperature of the source (in the Rayleigh-Jeans limit). The main-beam brightness temperature (T_{mb}) was calculated as

$$T_{\text{mb}} = \frac{T_A^*}{\eta_{\text{mb}}},$$

where T_A^* is the calibrated and atmosphere-corrected antenna temperature, and η_{mb} is the main-beam efficiency as defined by Mangum (1993). Furthermore, the elevation dependence of η_{mb} at 1.3 mm wavelength, which was determined toward Uranus (see the SEST Handbook), has been corrected for. It can be written as

$$\eta_{\text{mb}} = \eta_{\text{mb}}^0 [\cos^2(\epsilon - 64.9) + 0.31 \sin^2(\epsilon - 64.9)],$$

where $\eta_{\text{mb}}^0 = 0.6$ is the nominal value of the main-beam efficiency at elevations where the gain-elevation curve peaks, and ϵ is the telescope elevation in degrees. The T_{mb} scale is appropriate here since the angular extent of the emission regions in Sgr B2 is comparable to (and often smaller than) the size of the SEST main beam. The true (source-averaged) brightness temperature can subsequently be obtained by correcting for the beam-filling of the source, if known.

The average rms noise measured in the spectra is about 60 mK per 1 MHz channel (T_{mb}), with 80% of the scans falling in the 30–80 mK range. In some of the spectra, in particular from the N source, it was difficult to find bands free from emission lines for accurate noise estimates.

The baselines in the spectra are in general very flat, and hence only the continuum levels were subtracted before the Gaussian fitting procedure was applied in order to determine the peak main-beam brightness temperature, center frequency, and velocity width of each line feature. The only exception to this is the 244.7–245.4 GHz position-switched band, where a third-order polynomial baseline was subtracted. However, because spectral lines occupy such a large fraction of the spectra, the proper levels of the baselines were difficult to estimate in some frequency bands. Toward the M source we estimate that the uncertainty in the peak antenna temperature due to an incorrectly subtracted baseline is less than 0.1 K (T_{mb}), which generally causes us to underestimate the line brightness temperatures. Toward the N source it is sometimes exceptionally difficult to estimate the level of the true baseline since it is easy to mistake a line forest for a possible baseline curvature. In some frequency bands, the suspected bad baselines turned out to be line forests when they were reobserved because of this suspicion. In the N spectra we estimate that the accuracy of the baseline level in general is better than 0.2 K, and we also tend to underestimate the true antenna temperatures. In the

TABLE 2
SUMMARY OF DETECTED MOLECULAR SPECIES AND SPECTROSCOPIC REFERENCES

MOLECULE	LINES DETECTED			REMARKS	TABLE	REFERENCES
	N	M	NW			
CN	Absorption features	...	1
CO	4	4	3	^{13}C , ^{18}O , ^{17}O	6	1
NO	9	7	5		7	1
CS	5	5	2	^{13}C , ^{34}S , ^{33}S , $^{13}\text{C}^{34}\text{S}$	6	2
SiO	1	3	1	^{29}Si , ^{30}Si	6	2
NS	4	3	2		8	3
SO	8	15	4	^{34}S , ^{33}S , ^{18}O	9	1, 4
SO ⁺	2	...		10	1
HDO	2	2	...		11	1
C ₂ H	2	3	2		12	1
HCN	2	2	2	Only ^{13}C , ^{15}N	13	1
HNC	1	1	1	Only ^{13}C	14	1
HCO ⁺	2	3	1	Only ^{13}C , ^{18}O , ^{17}O	15	1, 5
N ₂ O	1	1	...		16	1
HCS ⁺	1	1	1		17	1
OCS	13	9	3	^{13}C , ^{34}S , ^{18}O	18	1
SO ₂	48	125	6	^{34}S , ^{33}S , SO ^{18}O	19	1, 6
HCNH ⁺	1		20	1
H ₂ CO	6	4	3	^{13}C , HDCO	21	1
HNCO	12	11	6		22	1
HOCO ⁺	4	4	1		23	1
H ₂ CS	7	6	4		24	1
CH ₂ NH	11	7	5		25	1
c-C ₃ H ₂	5	5	4		26	1
CH ₂ CN	9		27	7
CH ₂ CO	14	11	...		28	1
NH ₂ CN	8	4	...		29	1
HCOOH	8		30	1
HC ₃ N	52	46	3	^{13}C isotopomers	31	8
CH ₃ OH	152	78	30	^{13}C , ^{18}O , CH ₃ OD	32	9–12
CH ₃ CN	107	56	5	^{13}C , ^{15}N	33	1
NH ₂ CHO	53	26	...		34	1, 5
CH ₃ SH	15	10	...		35	13
CH ₃ NH ₂	41		36	14
CH ₃ C ₂ H	16	14	6	$^{13}\text{CH}_3\text{C}_2\text{H}$	37	1
CH ₃ CHO	70	26	...		38	15
c-C ₂ H ₄ O	4		39	16
C ₂ H ₅ CN	212	37	...		40	1, 17
CH ₃ OCHO	255	25	...		41	1, 21
C ₂ H ₅ OH	106	19	5		42	18
CH ₃ OCH ₃	75	14	...		43	1, 19
C ₂ H ₅ CN	178	47	...		44	1
Recombination lines	1	3	...		45	20
Unidentified	337	51	8		46	...

REFERENCES.—(1) Poynter & Pickett 1985; (2) Lovas & Krupenie 1974; (3) Lee, Ozeki, & Saito 1995; (4) Klaus et al. 1996; (5) Lovas 1984; (6) Lovas 1985; (7) Saito & Yamamoto 1997; (8) Lafferty & Lovas 1978; (9) E. Herbst 1996, private communication; (10) Anderson, Herbst, & De Lucia 1990; (11) Hoshino et al. 1996; (12) Anderson et al. 1988; (13) K. V. L. N. Sastry & E. Herbst 1997, private communication; (14) K. Takagi 1997, private communication; (15) Kleiner, Lovas, & Godefroid 1996; (16) Dickens et al. 1997; (17) Demaison et al. 1994; (18) J. C. Pearson 1997, private communication; (19) Groner et al. 1997; (20) Towle, Feldman, & Watson 1996; (21) Plummer, Herbst, & De Lucia 1987.

very few bands for which we are hesitant about the baselines, we have refrained from assigning lines of low intensity.

3. LINE IDENTIFICATIONS

The primary source of data for the spectral line identification process has been the JPL catalog² (Poynter & Pickett 1985). A summary of the spectroscopic references used for the various species can be found in Table 2.

During the final stages of the identification work, which was highly iterative, we used a local thermodynamical equilibrium (LTE) analysis method ("rotation diagram") to determine the rotation temperatures and column densities

of the different molecular species. This was done only for molecules with sufficient number of lines observed in a sufficiently large range of upper-state energies. Optical depths were calculated and corrected for when appropriate. The primary purpose of this analysis was to predict the intensities of all spectral lines in the frequency band covered for each species analyzed. This LTE model could therefore be used to find misidentifications, blends, and other inconsistencies in the line identifications. However, it also became clear that an LTE model may not be sufficient for an accurate analysis of the excitation of some of the complex molecules, for example CH₃OCHO. This has been noticed in previous spectral surveys (Turner 1991).

Comparison of the observed line intensities in the N and M positions was also a valuable help in the identification

² The updated version is available on the internet at <http://spec.jpl.nasa.gov>.

TABLE 3
LINE IDENTIFICATIONS TOWARD SAGITTARIUS B2(N) ORDERED BY FREQUENCY

Observed Frequency (MHz)	T_{mb} (K)	Δv (km s ⁻¹)	Orion Reference	Identification	Remarks
218321.....	3.01	19	S85	HC ₃ N	
218337.....	0.69	12	...	HC ₃ N v_5	

NOTE.—Table 3 appears in its entirety in the electronic edition of the *Astrophysical Journal Supplement Series*.

REFERENCES.—S85: Sutton et al. 1985. Additional references appear in the electronic edition of the table.

TABLE 4
LINE IDENTIFICATIONS TOWARD SAGITTARIUS B2(M) ORDERED BY FREQUENCY

Observed Frequency (MHz)	T_{mb} (K)	Δv (km s ⁻¹)	Orion Reference	Identification	Remarks
218325.....	2.23	18	S85	HC ₃ N	
218398.....	0.21	20	...	C ₂ H ₅ CN	

NOTE.—Table 4 appears in its entirety in the electronic edition of the *Astrophysical Journal Supplement Series*.

REFERENCES.—S85: Sutton et al. 1985. Additional references appear in the electronic edition of the table.

TABLE 5
LINE IDENTIFICATIONS TOWARD SAGITTARIUS B2(NW) ORDERED BY FREQUENCY

Observed Frequency (MHz)	T_{mb} (K)	Δv (km s ⁻¹)	Orion Reference	Identification	Remarks
218319.....	0.31	20	S85	HC ₃ N	
218433.....	2.31	...	S85	CH ₃ OH	Not Gaussian

NOTE.—Table 5 appears in its entirety in the electronic edition of the *Astrophysical Journal Supplement Series*.

REFERENCES.—S85: Sutton et al. 1985. Additional references appear in the electronic edition of the table.

process, especially for the SO₂ lines, which are much stronger toward M than N, in contrast to the lines from most other species.

A difficulty with the line identifications in Sgr B2 is of course the vast number of broad emission lines, which makes this survey “confusion-limited” rather than noise-limited, at least in several bands in the N position. In addition, many molecules systematically exhibit peculiar line profiles, for example C₂H₅CN and HC₃N toward Sgr B2(N). Therefore no unidentified lines have been assigned in case the line features are intermixed with strong C₂H₅CN or HC₃N lines, nor have we indicated U-lines that overlap strong CH₃OH lines since these frequently have wing emission. However, expected transitions from already identified species have sometimes been marked even if overlapping strong lines.

4. DATA PRESENTATION

4.1. Explanation of the Line Identification Tables

The line identifications have been tabulated in three ways. First, a summary of all molecules detected in the survey and the number of lines detected in each of the sources is listed in Table 2. Second, frequency-sorted lists of all detected lines for each of the three positions can be found

in Tables 3, 4, and 5.³ These tabulate the line parameters from the Gaussian fit (observed frequency, peak main-beam brightness temperature, and velocity width) for each detected line, together with suggested identifications. For each line, its detection or absence in the line surveys toward Orion (Sutton et al. 1985; Blake et al. 1986; Greaves & White 1991) have also been noted.

Third, the lines are listed species by species (Tables 6–45). In these tables the transition data, i.e., the rest frequency, quantum numbers, upper state energy (E_u), and A -coefficient (A_{ul}), are listed for each detected transition, together with the observed integrated intensities for the three positions. These tables are ordered by the number of atomic nuclei per molecule. Finally, in Table 46, we list all unidentified lines detected.

In several cases we have not been able to assign uniquely an observed spectral line to a single molecule because there is more than one possible identification, each alternative equally plausible. If our LTE analysis predicts frequency-coincident transitions from two (or more) molecules to have equal intensity, we have tabulated both (all) of these mol-

³ Tables 3–46 appear in their entirety in the electronic edition of the *Astrophysical Journal Supplement Series*.

TABLE 6
 $^1\Sigma$ DIATOMIC SPECIES

REST FREQUENCY (MHz)	MOLECULE	TRANSITION (J)	E_u (K)	A_{ul} (s $^{-1}$)	$\int T_{mb} dv$ (K km s $^{-1}$)			REMARKS
					N	M	NW	
230538.0.....	CO	2 → 1	17	6.92×10^{-7}	1250.0 ^a	1430.0 ^a	...	Emission in ref. beam (N,M,NW)
220398.7.....	^{13}CO	2 → 1	16	6.08×10^{-7}	270.0 ^a	530.0 ^a	410.0 ^a	Emission in ref. beam (N,M,NW)

NOTE.—Table 6 appears in its entirety in the electronic edition of the *Astrophysical Journal Supplement Series*.

^a Line intensity incorrect due to emission in ref. beam.

TABLE 7
NO

REST FREQUENCY (MHz)	STATE	TRANSITION (J _F)	E_u (K)	A_{ul} (s $^{-1}$)	$\int T_{mb} dv$ (K km s $^{-1}$)			REMARKS
					N	M	NW	
250436.9.....	$^2\Pi_{1/2}^+$	$5/2_{7/2} \rightarrow 3/2_{5/2}$	19	1.84×10^{-6}	39.7	41.3	20.9	b C ₂ H ₅ CN (N)
250440.7.....	$^2\Pi_{1/2}^+$	$5/2_{5/2} \rightarrow 3/2_{3/2}$	19	1.55×10^{-6}	↑	↑	↑	

NOTE.—Table 7 appears in its entirety in the electronic edition of the *Astrophysical Journal Supplement Series*.

TABLE 8
NS

REST FREQUENCY (MHz)	STATE	TRANSITION (J _F)	E_u (K)	A_{ul} (s $^{-1}$)	$\int T_{mb} dv$ (K km s $^{-1}$)			REMARKS
					N	M	NW	
253570.5.....	$^2\Pi_{1/2}^+$	$11/2_{13/2} \rightarrow 9/2_{11/2}$	40	2.83×10^{-4}	59.6	42.0	6.3	
253570.5.....	$^2\Pi_{1/2}^+$	$11/2_{11/2} \rightarrow 9/2_{9/2}$	40	2.73×10^{-4}	↑	↑	↑	

NOTE.—Table 8 appears in its entirety in the electronic edition of the *Astrophysical Journal Supplement Series*.

TABLE 9
SO

REST FREQUENCY (MHz)	TRANSITION (N _J)	E_u (K)	A_{ul} (s $^{-1}$)	$\int T_{mb} dv$ (K km s $^{-1}$)			REMARKS
				N	M	NW	
219949.4.....	$6_5 \rightarrow 5_4$	35	1.36×10^{-4}	89.6	195.7	27.7	
236452.3.....	$1_2 \rightarrow 2_1$	16	1.45×10^{-6}	...	2.8	...	

NOTE.—Table 9 appears in its entirety in the electronic edition of the *Astrophysical Journal Supplement Series*.

TABLE 10
SO⁺

REST FREQUENCY (MHz)	STATE	TRANSITION (J)	E_u (K)	A_{ul} (s $^{-1}$)	$\int T_{mb} dv$ (K km s $^{-1}$)			REMARKS
					N	M	NW	
254977.9.....	$^2\Pi_{1/2}$	e $11/2 \rightarrow 9/2$	39	8.77×10^{-5}	...	15.4	...	b C ₂ H ₅ CN/C ₃ H ₂
255353.2.....	$^2\Pi_{1/2}$	f $11/2 \rightarrow 9/2$	39	8.81×10^{-5}	...	8.2	...	

NOTE.—Table 10 appears in its entirety in the electronic edition of the *Astrophysical Journal Supplement Series*.

TABLE 11
HDO

REST FREQUENCY (MHz)	TRANSITION (J _{K_a, K_c})	E_u (K)	A_{ul} (s $^{-1}$)	$\int T_{mb} dv$ (K km s $^{-1}$)			REMARKS
				N	M	NW	
225896.7.....	$3_{1,2} \rightarrow 2_{2,1}$	168	1.32×10^{-5}	7.9	5.2	...	Poor S/N (N)
241561.6.....	$2_{1,1} \rightarrow 2_{1,2}$	95	1.19×10^{-5}	9.1	5.5	...	

NOTE.—Table 11 appears in its entirety in the electronic edition of the *Astrophysical Journal Supplement Series*.

TABLE 12
 C_2H

REST FREQUENCY (MHz)	TRANSITION (N_J)	E_u (K)	A_{ul} (s $^{-1}$)	$\int T_{mb} dv$ (K km s $^{-1}$)			REMARKS
				N	M	NW	
262005.3.....	$3_{7/2} \rightarrow 2_{5/2}$	25	5.74×10^{-5}	18.1	48.8	22.6	Not Gaussian (N,M,NW)
262066.1.....	$3_{5/2} \rightarrow 2_{3/2}$	25	5.28×10^{-5}	16.2	31.9	17.1	Not Gaussian (N,M,NW)
262208.4.....	$3_{5/2} \rightarrow 2_{5/2}$	25	4.28×10^{-6}	...	3.2	...	

NOTE.—Table 12 appears in its entirety in the electronic edition of the Astrophysical Journal Supplement Series.

TABLE 13
HCN ISOTOPOMERS

REST FREQUENCY (MHz)	SPECIES	TRANSITION (J)	E_u (K)	A_{ul} (s $^{-1}$)	$\int T_{mb} dv$ (K km s $^{-1}$)			REMARKS
					N	M	NW	
259011.8.....	H^{13}CN	$3 \rightarrow 2$	25	7.72×10^{-4}	13.9	67.3	9.6	Self-absorbed (N,M)
258154.7.....	HC^{15}N	$3 \rightarrow 2$	25	7.64×10^{-4}	26.4	21.5	4.9	

NOTE.—Table 13 appears in its entirety in the electronic edition of the Astrophysical Journal Supplement Series.

TABLE 14
 HN^{13}C

REST FREQUENCY (MHz)	TRANSITION (J)	E_u (K)	A_{ul} (s $^{-1}$)	$\int T_{mb} dv$ (K km s $^{-1}$)			REMARKS
				N	M	NW	
261263.3.....	$3 \rightarrow 2$	25	6.48×10^{-4}	15.7	22.4	8.9	Not Gaussian (N,M,NW)

NOTE.—Table 14 appears in its entirety in the electronic edition of the Astrophysical Journal Supplement Series.

TABLE 15
HCO $^+$ ISOTOPOMERS

REST FREQUENCY (MHz)	SPECIES	TRANSITION (J)	E_u (K)	A_{ul} (s $^{-1}$)	$\int T_{mb} dv$ (K km s $^{-1}$)			REMARKS
					N	M	NW	
260255.5.....	H^{13}CO^+	$3 \rightarrow 2$	25	9.65×10^{-4}	13.7	69.9	14.3	b CH_3OCHO (N); not Gaussian (NW)
255480.2.....	HC^{18}O^+	$3 \rightarrow 2$	25	9.13×10^{-4}	6.2	17.3	...	

NOTE.—Table 15 appears in its entirety in the electronic edition of the Astrophysical Journal Supplement Series.

TABLE 16
 N_2O

REST FREQUENCY (MHz)	TRANSITION (J)	E_u (K)	A_{ul} (s $^{-1}$)	$\int T_{mb} dv$ (K km s $^{-1}$)			REMARKS
				N	M	NW	
226094.0.....	$9 \rightarrow 8$	54	1.65×10^{-6}	6.6	4.2	...	

NOTE.—Table 16 appears in its entirety in the electronic edition of the Astrophysical Journal Supplement Series.

TABLE 17
 HCS^+

REST FREQUENCY (MHz)	TRANSITION (J)	E_u (K)	A_{ul} (s $^{-1}$)	$\int T_{mb} dv$ (K km s $^{-1}$)			REMARKS
				N	M	NW	
256027.1.....	$6 \rightarrow 5$	43	4.13×10^{-4}	15.1	12.6	3.4	

NOTE.—Table 17 appears in its entirety in the electronic edition of the Astrophysical Journal Supplement Series.

ecules in their respective tables. For each of these transitions, the alternative identifications have been listed as ambiguous ("a") in the Remarks columns.

If, on the other hand, coincident transitions from two (or

more) different molecules are indicated by our LTE analysis to have significantly different intensities, we have listed only the species that, given the column density and rotation temperature estimated from other lines, produces the strongest

TABLE 18
OCS

REST FREQUENCY (MHz)	TRANSITION (J)	E_u (K)	A_{ul} (s ⁻¹)	$\int T_{mb} dv$ (K km s ⁻¹)			REMARKS
				N	M	NW	
218903.4.....	18 → 17	100	3.04×10^{-5}	66.5	41.4	10.9	
231061.0.....	19 → 18	111	3.58×10^{-5}	69.4	43.3	...	

NOTE.—Table 18 appears in its entirety in the electronic edition of the Astrophysical Journal Supplement Series.

TABLE 19
SO₂

REST FREQUENCY (MHz)	TRANSITION (J_{K_a, K_c})	E_u (K)	A_{ul} (s ⁻¹)	$\int T_{mb} dv$ (K km s ⁻¹)			REMARKS
				N	M	NW	
219276.0.....	$22_{7,15} \rightarrow 23_{6,18}$	353	2.13×10^{-5}	5.3	21.8	...	
221965.2.....	$11_{1,11} \rightarrow 10_{0,10}$	60	1.14×10^{-4}	35.8	127.0	4.1	

NOTE.—Table 19 appears in its entirety in the electronic edition of the Astrophysical Journal Supplement Series.

TABLE 20
HCNH⁺

REST FREQUENCY (MHz)	TRANSITION (J)	E_u (K)	A_{ul} (s ⁻¹)	$\int T_{mb} dv$ (K km s ⁻¹)			REMARKS
				N	M	NW	
222329.4.....	3 → 2	21	4.93×10^{-6}	6.2	Not Gaussian

NOTE.—Table 20 appears in its entirety in the electronic edition of the Astrophysical Journal Supplement Series.

TABLE 21
H₂CO

REST FREQUENCY (MHz)	TRANSITION (J_{K_a, K_c})	E_u (K)	A_{ul} (s ⁻¹)	$\int T_{mb} dv$ (K km s ⁻¹)			REMARKS
				N	M	NW	
218475.6.....	$3_{2,2} \rightarrow 2_{2,1}$	68	1.57×10^{-4}	28.6	32.0	18.4	Not Gaussian (N,NW)
218760.1.....	$3_{2,1} \rightarrow 2_{2,0}$	68	1.58×10^{-4}	37.7	35.4	19.0	Self-absorbed (N); not Gaussian (M)

NOTE.—Table 21 appears in its entirety in the electronic edition of the Astrophysical Journal Supplement Series.

TABLE 22
HNCO

REST FREQUENCY (MHz)	TRANSITION (J_{K_a, K_c})	E_u (K)	A_{ul} (s ⁻¹)	$\int T_{mb} dv$ (K km s ⁻¹)			REMARKS
				N	M	NW	
218981.2.....	$10_{1,10} \rightarrow 9_{1,9}$	101	1.48×10^{-4}	32.6	22.5	4.9	Not Gaussian (NW)
219656.7.....	$10_{3,7/8} \rightarrow 9_{3,6/7}$	447	1.37×10^{-4}	22.6	10.0	...	

NOTE.—Table 22 appears in its entirety in the electronic edition of the Astrophysical Journal Supplement Series.

TABLE 23
HOCH⁺

REST FREQUENCY (MHz)	TRANSITION (J_{K_a, K_c})	E_u (K)	A_{ul} (s ⁻¹)	$\int T_{mb} dv$ (K km s ⁻¹)			REMARKS
				N	M	NW	
235114.3.....	$11_{2,10} \rightarrow 10_{2,9}$	216	2.80×10^{-4}	1.8	
235119.8.....	$11_{2,9} \rightarrow 10_{2,8}$	216	2.80×10^{-4}	↑	

NOTE.—Table 23 appears in its entirety in the electronic edition of the Astrophysical Journal Supplement Series.

TABLE 24
H₂CS

REST FREQUENCY (MHz)	TRANSITION (J _{K_a,K_c})	E _u (K)	A _{ul} (s ⁻¹)	$\int T_{mb} dv$ (K km s ⁻¹)			REMARKS
				N	M	NW	
236726.8.....	7 _{1,7} → 6 _{1,6}	59	1.91 × 10 ⁻⁴	68.3	36.2	...	
240266.3.....	7 _{0,7} → 6 _{0,6}	46	2.04 × 10 ⁻⁴	45.8	20.4	6.3	

NOTE.—Table 24 appears in its entirety in the electronic edition of the Astrophysical Journal Supplement Series.

TABLE 25
CH₂NH

REST FREQUENCY (MHz)	TRANSITION (J _{K_a,K_c})	E _u (K)	A _{ul} (s ⁻¹)	$\int T_{mb} dv$ (K km s ⁻¹)			REMARKS
				N	M	NW	
225555.0.....	1 _{1,1} → 0 _{0,0}	11	1.04 × 10 ⁻⁴	-32.9	-24.8	-1.9	Not Gaussian (N,M)
226549.0.....	6 _{1,5} → 6 _{0,6}	75	1.33 × 10 ⁻⁴	32.6	11.2	1.5	b CH ₃ CHO (N,M)

NOTE.—Table 25 appears in its entirety in the electronic edition of the Astrophysical Journal Supplement Series.

TABLE 26
c-C₃H₂

REST FREQUENCY (MHz)	TRANSITION (J _{K_a,K_c})	E _u (K)	A _{ul} (s ⁻¹)	$\int T_{mb} dv$ (K km s ⁻¹)			REMARKS
				N	M	NW	
218732.7.....	7 _{1/2,6} → 7 _{0/1,7}	61	9.82 × 10 ⁻⁵	5.4	o H ₂ CO (N)
227169.1.....	4 _{3,2} → 3 _{2,1}	29	3.42 × 10 ⁻⁴	6.8	7.9	2.9	b C ₂ H ₅ CN (N)

NOTE.—Table 26 appears in its entirety in the electronic edition of the Astrophysical Journal Supplement Series.

TABLE 27
CH₂CN

REST FREQUENCY (MHz)	TRANSITION ^a (N _{K_a,K_c})	E _u (K)	A _{ul} (s ⁻¹)	$\int T_{mb} dv$ (K km s ⁻¹)			REMARKS
				N	M	NW	
221241.5.....	11 _{0,11} → 10 _{0,10}	F ₁	64	7.44 × 10 ⁻⁴	6.4
223326.0.....	11 _{1,10} → 10 _{1,9}	F ₁	78	7.59 × 10 ⁻⁴	5.0

NOTE.—Table 27 appears in its entirety in the electronic edition of the Astrophysical Journal Supplement Series.

^a F₁ corresponds to J = (N + 3/2) → (N + 1/2) and F₂ to J = (N + 1/2) → (N - 1/2).

TABLE 28
CH₂CO

REST FREQUENCY (MHz)	TRANSITION (J _{K_a,K_c})	E _u (K)	A _{ul} (s ⁻¹)	$\int T_{mb} dv$ (K km s ⁻¹)			REMARKS
				N	M	NW	
220178.2.....	11 _{1,11} → 10 _{1,10}	76	1.18 × 10 ⁻⁴	15.2	7.4	...	o SO ₂ v ₂ (M)
222119.9.....	11 _{4,7/8} → 10 _{4,6/7}	275	1.06 × 10 ⁻⁴	10.2	o CH ₃ C ₂ H (N)

NOTE.—Table 28 appears in its entirety in the electronic edition of the Astrophysical Journal Supplement Series.

TABLE 29
NH₂CN

REST FREQUENCY (MHz)	TRANSITION (J _{K_a,K_c})	E _u (K)	A _{ul} (s ⁻¹)	$\int T_{mb} dv$ (K km s ⁻¹)			REMARKS
				N	M	NW	
221361.2.....	11 _{1,10} → 10 _{1,9}	78	1.12 × 10 ⁻³	7.1	6.8	...	a CH ₃ CN v ₈ (M)
238316.0.....	12 _{1,12} → 11 _{1,11}	89	1.41 × 10 ⁻³	5.0	4.6	...	b C ₂ H ₃ CN v ₁₁ (N)

NOTE.—Table 29 appears in its entirety in the electronic edition of the Astrophysical Journal Supplement Series.

TABLE 30
HCOOH

REST FREQUENCY (MHz)	TRANSITION (J_{K_a, K_c})	E_u (K)	A_{ul} (s ⁻¹)	$\int T_{mb} dv$ (K km s ⁻¹)			REMARKS
				N	M	NW	
225512.6.....	$10_{3,7} \rightarrow 9_{3,6}$	88	1.13×10^{-4}	4.1	a C ₂ H ₃ CN/CH ₃ CHO
228544.2.....	$10_{2,8} \rightarrow 9_{2,7}$	73	1.24×10^{-4}	12.4	o C ₂ H ₃ CN

NOTE.—Table 30 appears in its entirety in the electronic edition of the Astrophysical Journal Supplement Series.

TABLE 31
HC₃N

REST FREQUENCY (MHz)	TRANSITION (J_i)	E_u (K)	A_{ul} (s ⁻¹)	$\int T_{mb} dv$ (K km s ⁻¹)			REMARKS
				N	M	NW	
218324.8.....	$24 \rightarrow 23$	131	8.23×10^{-4}	61.1	43.7	6.6	
227419.0.....	$25 \rightarrow 24$	142	9.31×10^{-4}	31.0	35.9	7.2	

NOTE.—Table 31 appears in its entirety in the electronic edition of the Astrophysical Journal Supplement Series.

TABLE 32
CH₃OH

REST FREQUENCY (MHz)	SYMMETRY	TRANSITION ($J_{K_a}^p$)	E_u (K)	A_{ul} (s ⁻¹)	$\int T_{mb} dv$ (K km s ⁻¹)			REMARKS
					N	M	NW	
218440.0.....	E	$4_2 \rightarrow 3_1$	44	4.68×10^{-5}	109.9	84.3	60.6	Not Gaussian (M,NW)
220078.6.....	E	$8_0 \rightarrow 7_1$	95	2.51×10^{-5}	48.8	28.9	...	

NOTE.—Table 32 appears in its entirety in the electronic edition of the Astrophysical Journal Supplement Series.

TABLE 33
CH₃CN

REST FREQUENCY (MHz)	TRANSITION (J_K)	E_u (K)	A_{ul} (s ⁻¹)	$\int T_{mb} dv$ (K km s ⁻¹)			REMARKS
				N	M	NW	
220323.8.....	$12_{10} \rightarrow 11_{10}$	782	2.79×10^{-4}	4.7	
220539.3.....	$12_7 \rightarrow 11_7$	419	6.04×10^{-4}	15.4	1.9	...	o CH ₃ ¹³ CN (N,M)

NOTE.—Table 33 appears in its entirety in the electronic edition of the Astrophysical Journal Supplement Series.

TABLE 34
NH₂CHO

REST FREQUENCY (MHz)	TRANSITION (J_{K_a, K_c})	E_u (K)	A_{ul} (s ⁻¹)	$\int T_{mb} dv$ (K km s ⁻¹)			REMARKS
				N	M	NW	
a-Type Transitions							
218459.6.....	$10_{1,9} \rightarrow 9_{1,8}$	61	7.47×10^{-4}	19.4	24.0	...	b HC ₃ N v ₅ ; o CH ₃ OH (N); b NH ₂ CN (M)
223453.0.....	$11_{1,11} \rightarrow 10_{1,10}$	68	8.05×10^{-4}	22.2	9.1	...	

NOTE.—Table 34 appears in its entirety in the electronic edition of the Astrophysical Journal Supplement Series.

TABLE 35
CH₃SH

REST FREQUENCY (MHz)	SYMMETRY	TRANSITION (J_K^p)	E_u (K)	A_{ul} (s ⁻¹)	$\int T_{mb} dv$ (K km s ⁻¹)			REMARKS
					N	M	NW	
227295.6.....	E	$9_0 \rightarrow 8_0$	58	2.18×10^{-5}	12.2	10.3	...	a ¹³ C ³⁴ S (N,M)
227326.3.....	A	$9_0^+ \rightarrow 8_0^+$	55	2.18×10^{-5}	9.3	

NOTE.—Table 35 appears in its entirety in the electronic edition of the Astrophysical Journal Supplement Series.

line at the frequency in question. However, if the predicted intensity of any of the lines from the other molecules is more than 25% of (but less than) that of the dominant species, this has been noted in the Remarks column as blend ("b"). In case an observed spectral line is due to an unresolved

group of transitions from a single species, we have assigned the observed integrated intensity to the transition that is predicted by the LTE model to be dominant at the rotation temperature estimated for the species. The blending transitions have been listed using the \uparrow or \downarrow signs in the intensity

TABLE 36
 CH_3NH_2

REST FREQUENCY (MHz)	SYMMETRY ^a	TRANSITION ($J_{K_a}^p$)	E_u (K)	A_{ul} (s $^{-1}$)	$\int T_{mb} dv$ (K km s $^{-1}$)			REMARKS
					N	M	NW	
219151.5.....	E	a	$8_{-2} \rightarrow 8_1$	92	2.47×10^{-5}	6.5
220826.8.....	A	a	$7_0^+ \rightarrow 6_1^+$	60	3.50×10^{-5}	5.7	...	b CH_3OCHO

NOTE.—Table 36 appears in its entirety in the electronic edition of the Astrophysical Journal Supplement Series.

^a a = asymmetric state; s = symmetric state.

TABLE 37
 $\text{CH}_3\text{C}_2\text{H}$

REST FREQUENCY (MHz)	TRANSITION (J_K)	E_u (K)	A_{ul} (s $^{-1}$)	$\int T_{mb} dv$ (K km s $^{-1}$)			REMARKS
				N	M	NW	
222014.5.....	$13_6 \rightarrow 12_6$	334	2.71×10^{-5}	5.0	b $\text{CH}_2\text{CO}/\text{H}38\beta$ (N)
222061.0.....	$13_5 \rightarrow 12_5$	255	2.94×10^{-5}	6.4	1.7	...	Blended region (N)

NOTE.—Table 37 appears in its entirety in the electronic edition of the Astrophysical Journal Supplement Series.

TABLE 38
 CH_3CHO

REST FREQUENCY (MHz)	SYMMETRY	TRANSITION (J_{K_a, K_c}^p)	E_u (K)	A_{ul} (s $^{-1}$)	$\int T_{mb} dv$ (K km s $^{-1}$)			REMARKS
					N	M	NW	
<i>a</i> -Type Transitions								
223650.1.....	E	$12_{-1,12} \rightarrow 11_{-1,11}$	72	3.92×10^{-4}	8.2	\downarrow
223660.6.....	A	$12_{1,12}^+ \rightarrow 11_{1,11}^+$	72	3.92×10^{-4}	6.1	6.7

NOTE.—Table 38 appears in its entirety in the electronic edition of the Astrophysical Journal Supplement Series.

TABLE 39
 $\text{c-C}_2\text{H}_4\text{O}$

REST FREQUENCY (MHz)	TRANSITION (J_{K_a, K_c})	E_u (K)	A_{ul} (s $^{-1}$)	$\int T_{mb} dv$ (K km s $^{-1}$)			REMARKS
				N	M	NW	
219512.8.....	$6_{3,4} \rightarrow 5_{2,3}$	40	1.04×10^{-4}	5.5	b $\text{C}_2\text{H}_3\text{CN} \nu_{11}$; o $\text{C}_2\text{H}_5\text{CN}$
235106.1.....	$8_{0/1,8} \rightarrow 7_{1/0,7}$	52	2.33×10^{-4}	2.6	

NOTE.—Table 39 appears in its entirety in the electronic edition of the Astrophysical Journal Supplement Series.

TABLE 40
 $\text{C}_2\text{H}_3\text{CN}$

REST FREQUENCY (MHz)	TRANSITION (J_{K_a, K_c})	E_u (K)	A_{ul}^a (s $^{-1}$)	$\int T_{mb} dv$ (K km s $^{-1}$)			REMARKS
				N	M	NW	
<i>a</i> -Type Transitions							
218398.6.....	$23_{7,16/17} \rightarrow 22_{7,15/16}$	232	7.84×10^{-4}	14.1	4.2	...	
218402.4.....	$23_{6,18/17} \rightarrow 22_{6,17/16}$	204	8.05×10^{-4}	\uparrow	\uparrow	...	

NOTE.—Table 40 appears in its entirety in the electronic edition of the Astrophysical Journal Supplement Series.

^a In case of K -doublets, the A_{ul} values listed refer to the individual transitions.

columns, indicating blend with the previous or following transition, respectively. Furthermore, some species have pairs of related transitions, doublets, with only very small separation in rest frequency. If the separation is less than

1 MHz, and their E_u and A_{ul} are equal, the transition nomenclature has been abbreviated using the slash (/) sign. Examples of this can, e.g., be found in the CH₃OCHO (K-doublets) and CH₃OH (+/- parity) tables.

TABLE 41
CH₃OCHO

REST FREQUENCY (MHz)	SYMMETRY	TRANSITION (J_{K_a, K_c}^L)	E_u (K)	A_{ul} (s ⁻¹)	$\int T_{mb} dv$ (K km s ⁻¹)			REMARKS
					N	M	NW	
<i>a</i> -Type Transitions								
220166.8.....	E	17 _{2,15} → 16 _{4,12}	103	1.52 × 10 ⁻⁴	16.5	b SO ₂ v ₂ (N)
220190.2.....	A	17 _{4,13} → 16 _{4,12}	103	1.52 × 10 ⁻⁴	17.7	

NOTE.—Table 41 appears in its entirety in the electronic edition of the Astrophysical Journal Supplement Series.

TABLE 42
C₂H₅OH

REST FREQUENCY (MHz)	TRANSITION (J_{K_a, K_c})	E_u (K)	A_{ul} (s ⁻¹)	$\int T_{mb} dv$ (K km s ⁻¹)			REMARKS
				N	M	NW	
C ₂ H ₅ OH in the <i>trans</i> substate							
218554.5.....	21 _{5,16} → 21 _{4,17}	226	5.93 × 10 ⁻⁵	4.8	
218654.0.....	7 _{2,5} → 6 _{1,6}	29	2.22 × 10 ⁻⁵	2.8	1.3	...	

NOTE.—Table 42 appears in its entirety in the electronic edition of the Astrophysical Journal Supplement Series.

TABLE 43
CH₃OCH₃

REST FREQUENCY ^a (MHz)	TRANSITION ^b (J_{K_a, K_c})	E_u (K)	A_{ul}^a (s ⁻¹)	$\int T_{mb} dv$ (K km s ⁻¹)			REMARKS
				N	M	NW	
218492.4.....	23 _{3,21} → 23 _{2,22}	264	3.36 × 10 ⁻⁵	11.2	o H ₂ CO (N)
220847.6.....	24 _{4,20} → 23 _{5,19}	297	1.26 × 10 ⁻⁵	4.0	b C ₂ H ₅ CN (N)

NOTE.—Table 43 appears in its entirety in the electronic edition of the Astrophysical Journal Supplement Series.

^a The rest frequencies and A_{ul} values listed always refer to the subcomponent with highest statistical weight, EE, unless otherwise is stated.

^b For most transitions, the splitting of CH₃OCH₃ into its four torsional substates AA, EE, EA, and AE, has not been resolved, and for brevity we list only J_{K_a, K_c} in these cases.

TABLE 44
C₂H₅CN

REST FREQUENCY (MHz)	TRANSITION (J_{K_a, K_c})	E_u (K)	A_{ul} (s ⁻¹)	$\int T_{mb} dv$ (K km s ⁻¹)			REMARKS
				N	M	NW	
<i>a</i> -Type Transitions							
218390.0.....	24 _{3,21} → 23 _{3,20}	140	8.66 × 10 ⁻⁴	14.0	
219505.6.....	24 _{2,22} → 23 _{2,21}	136	8.87 × 10 ⁻⁴	29.9	8.6	...	Not Gaussian (N)

NOTE.—Table 44 appears in its entirety in the electronic edition of the Astrophysical Journal Supplement Series.

TABLE 45
RECOMBINATION LINES

REST FREQUENCY (MHz)	TRANSITION	$\int T_{mb} dv$ (K km s ⁻¹)			REMARKS
		N	M	NW	
222011.8.....	H38β	...	7.6	...	b CH ₃ C ₂ H (M)
231900.9.....	H30α	10.0	19.7	...	b ³³ SO ₂ (M); not Gaussian (N)

NOTE.—Table 45 appears in its entirety in the electronic edition of the Astrophysical Journal Supplement Series.

TABLE 46
UNIDENTIFIED LINES

OBSERVED FREQUENCY ^a (MHz)	$\int T_{\text{mb}} dv$ (K km s ⁻¹)			
	N	M	NW	REMARKS
219216	18.4	
219318	26.0	

NOTES.—Table 46 appears in its entirety in the electronic edition of the Astrophysical Journal Supplement Series. In case the U-line is common to N and M, the observed frequency listed is valid for N, and the frequency for M is noted in the Remarks column, if different. Additional notes appear in the electronic edition of the table.

^a Assuming $V_{\text{LSR}} = +62$ km s⁻¹ for all three positions.

Because of the high line widths in Sgr B2, the lines are frequently overlapping with each other in the spectra, so that the individual lines are only partly resolved. If a Gaussian has been fitted to a spectral line feature that is intermixed with another line to such a high degree that the line parameters are believed to be poorly determined, e.g., if the assigned line is located in the wing of a stronger line, this has been noted as overlap ("o") in the Remarks column. For some lines with complicated shapes, e.g., emission from multiple velocity components, extended line wings, or intermixed emission and absorption, multiple Gaussians had to be fitted to these lines to account correctly for their total integrated intensity. These lines have been marked as "not Gaussian" in the Remarks column in the tables. In some cases it has been difficult to distinguish intermixed individual lines from complex velocity structure.

For a few of the complex molecules, the transitions have been subdivided into groups depending on the selection rule obeyed for the transition in question: *a*-, *b*-, or *c*-type. These groups usually have very different *A*-coefficients and therefore occupy separate regions in the rotation diagrams (see Turner 1991). This will be discussed in detail in Paper II.

Absorption lines have been indicated in the tables by negative integrated intensities.

4.2. Explanation of the Spectra

The spectra are presented in Figure 1 on a uniform frequency (540 MHz per spectra, with a 20 MHz overlap between consecutive spectra) and intensity scale for each of the N, M, and NW sources. The only exceptions are the 218.30–219.02 and the 262.98–263.55 GHz bands, i.e., the first and the last spectra, for which a wider frequency range was used. The main-beam brightness temperature scale is used, and the rest frequency scale was calculated for $V_{\text{LSR}} = +62$ km s⁻¹ for all three sources. The continuum levels have been removed from the spectra.

All suggested identifications are displayed in the spectra with markers consisting of a molecule label and a pointer indicating the observed frequency given by the Gaussian fit to the line. Lines that were ambiguously identified have been marked with all plausible identifications in the spectra, and unidentified lines are labeled with a U followed by the observed frequency in MHz. There is always one single molecule identification marker per transition, even for non-Gaussian lines where several line components were fitted, in which case the marker indicates the main component.

The CO($J = 2 \rightarrow 1$) and $^{13}\text{CO}(J = 2 \rightarrow 1)$ lines at 230.54 and 220.40 GHz are distorted by emission in the reference beam and therefore are not useful in any of the sources. In the spectra around 222.66 GHz, there is contamination

from the CO($J = 2 \rightarrow 1$) line present in the upper (image) sideband, and therefore no lines have been assigned in that band.

5. RESULTS AND DISCUSSION

Speaking in general terms, the Sgr B2(N) position is by far richer in emission lines than Sgr B2(M). Most of these lines emanate from complex carbon-bearing molecules. The M position, on the other hand, usually emits more or equally strongly in simple (diatomic and triatomic) and inorganic species. It is also notable that most sulfur-bearing molecules peak strongly toward M (see discussion about line flux below). In comparison, the NW position is relatively poor in spectral line emission.

In total, we detected 1730, 660, and 110 lines toward N, M, and NW, respectively. The resulting spectral-line density averaged over the covered band is 38, 15, and two lines per GHz. The lines originate from 42 different molecules and 36 isotopomers. Among the species detected toward Sgr B2(N) is the recently identified $\text{c-C}_2\text{H}_4\text{O}$, ethylene oxide (Dickens et al. 1997, including data from the present survey).

Among all detected lines, 337 (19%), 51 (8%), and eight (7%) are still unidentified toward the N, M, and NW positions, respectively. Twenty-two of the U-lines are common to N and M (within 5 MHz from each other), and U247563 occurs both in M and NW. At least nine of the U-lines seen in N are unblended and 1 K or stronger. Six of the U-lines were also seen in the line surveys of Orion by Sutton et al. (1985), Blake et al. (1986), and Greaves & White (1991). We believe that many of the weaker unidentified lines, especially, can be attributed to unlisted transitions of several well-known molecules. This was clearly demonstrated when spectral-line data for $\text{C}_2\text{H}_3\text{CN}$ in its two lowest vibrational states v_{11} and v_{15} recently became available (JPL catalog; Poynter & Pickett 1985), and we found about 100 coincidences with previously unassigned line features. Since $\text{C}_2\text{H}_5\text{CN}$ has vibrational modes similar to $\text{C}_2\text{H}_3\text{CN}$, many of our U-lines will probably be eliminated when appropriate spectroscopic data for this molecule become available. Also, ^{13}C -isotopomers of some of the complex molecules may be identified.

The average line widths toward N, M, and NW were found to be 13, 17, and 14 km s⁻¹, respectively. In particular toward the NW source, many of the lines have two or more distinct emission components, separated by 12–15 km s⁻¹, but also in N and M some molecules have asymmetric line profiles or line wings. A discussion of line widths and emission velocities will follow in Paper II.

The dual beam switch observation mode used gives reliable continuum levels during stable atmospheric condi-

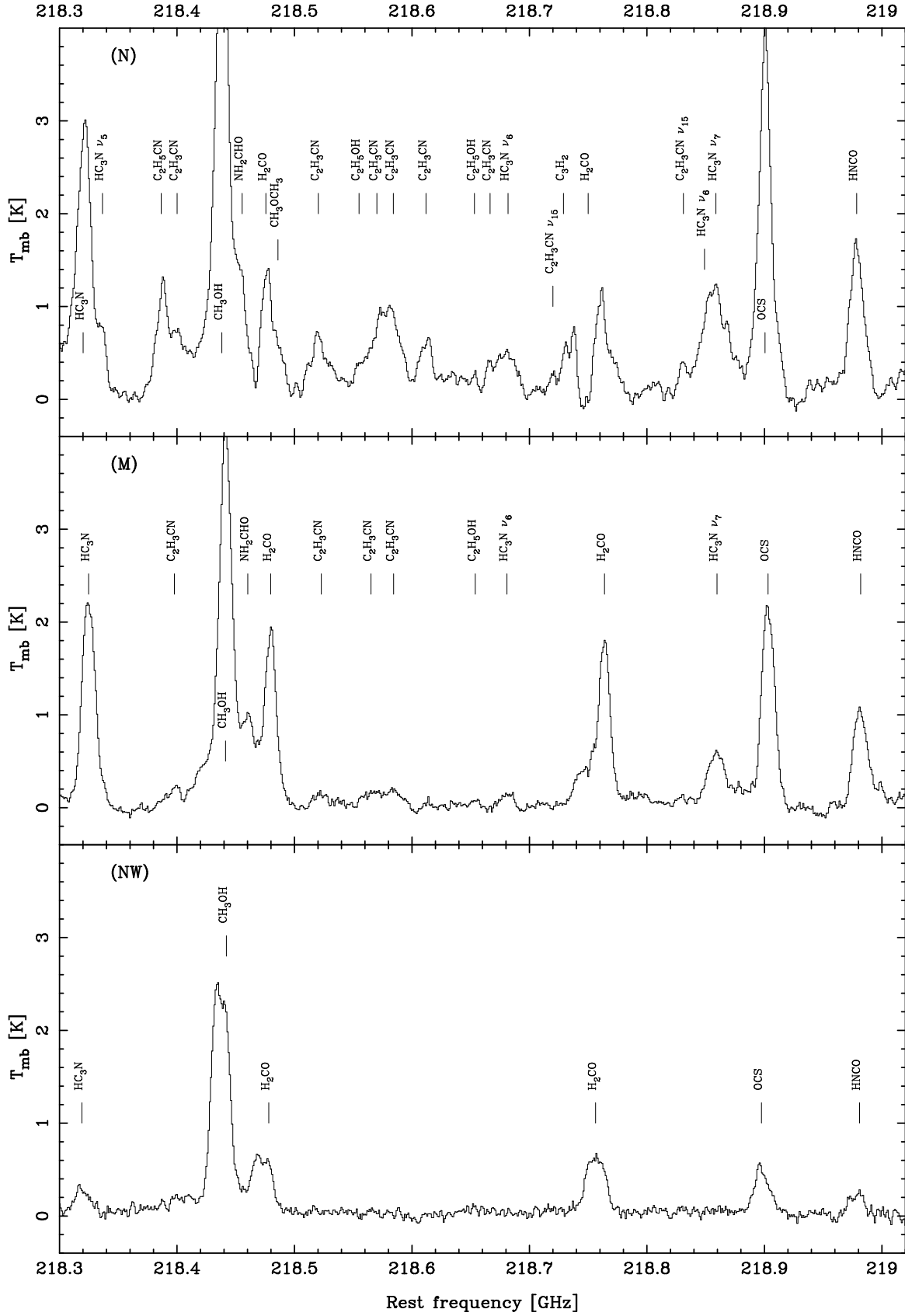


FIG. 1.—In this figure, all spectra together with suggested line identifications are shown in 540 MHz bands, except for the first (218.30–219.02 GHz) and last (262.98–263.55 GHz) spectra, which have wider frequency ranges. The continuum levels have been removed from all spectra for uniformity, and the average levels removed are 1.8 K, 1.7 K, and 0.3 K (T_{mb}) toward N, M, and NW, respectively. The rest frequency scale assumes $V_{\text{LSR}} = +62 \text{ km s}^{-1}$, and the intensity is given in terms of the main-beam brightness temperature scale.

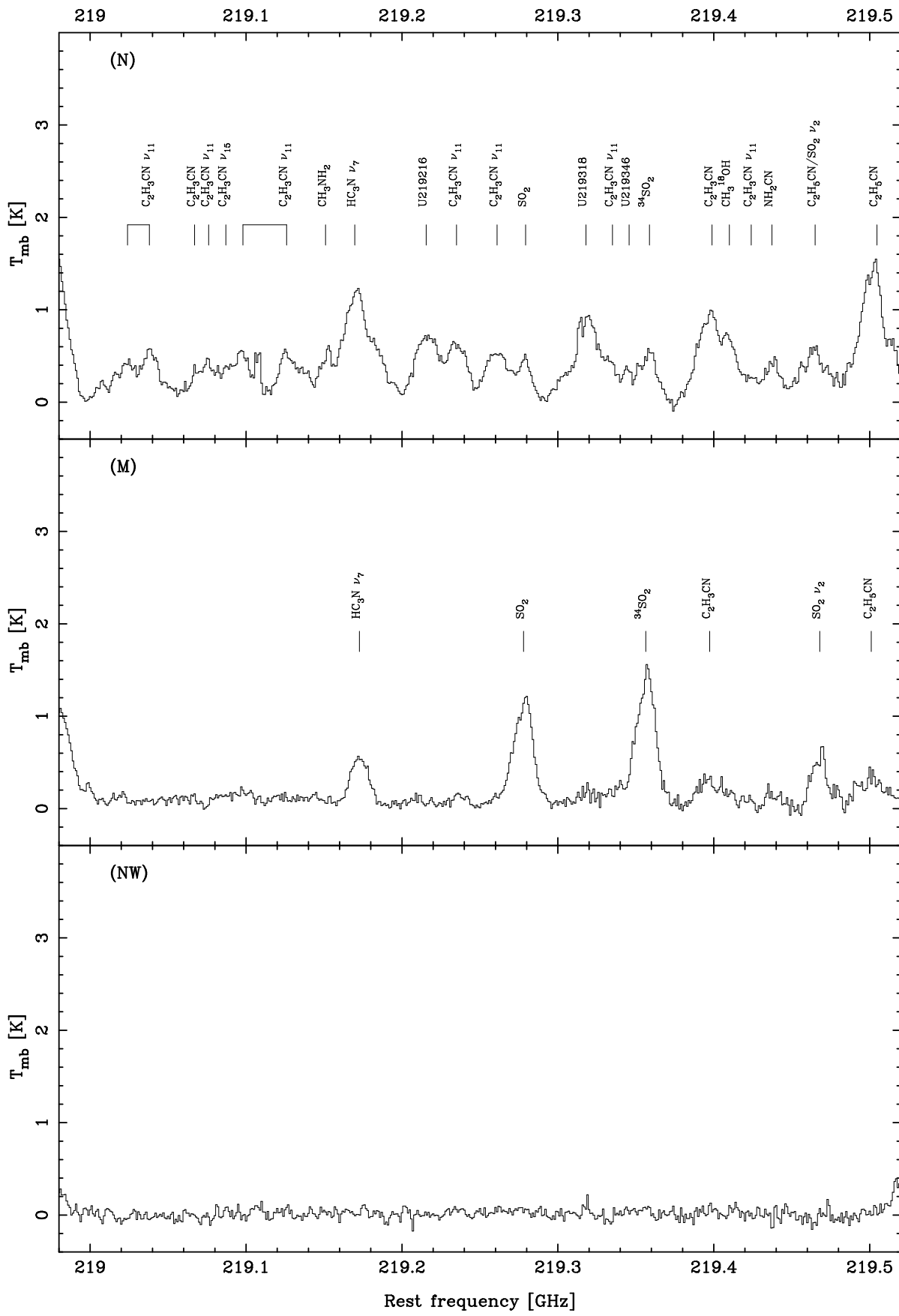


FIG. 1.—Continued

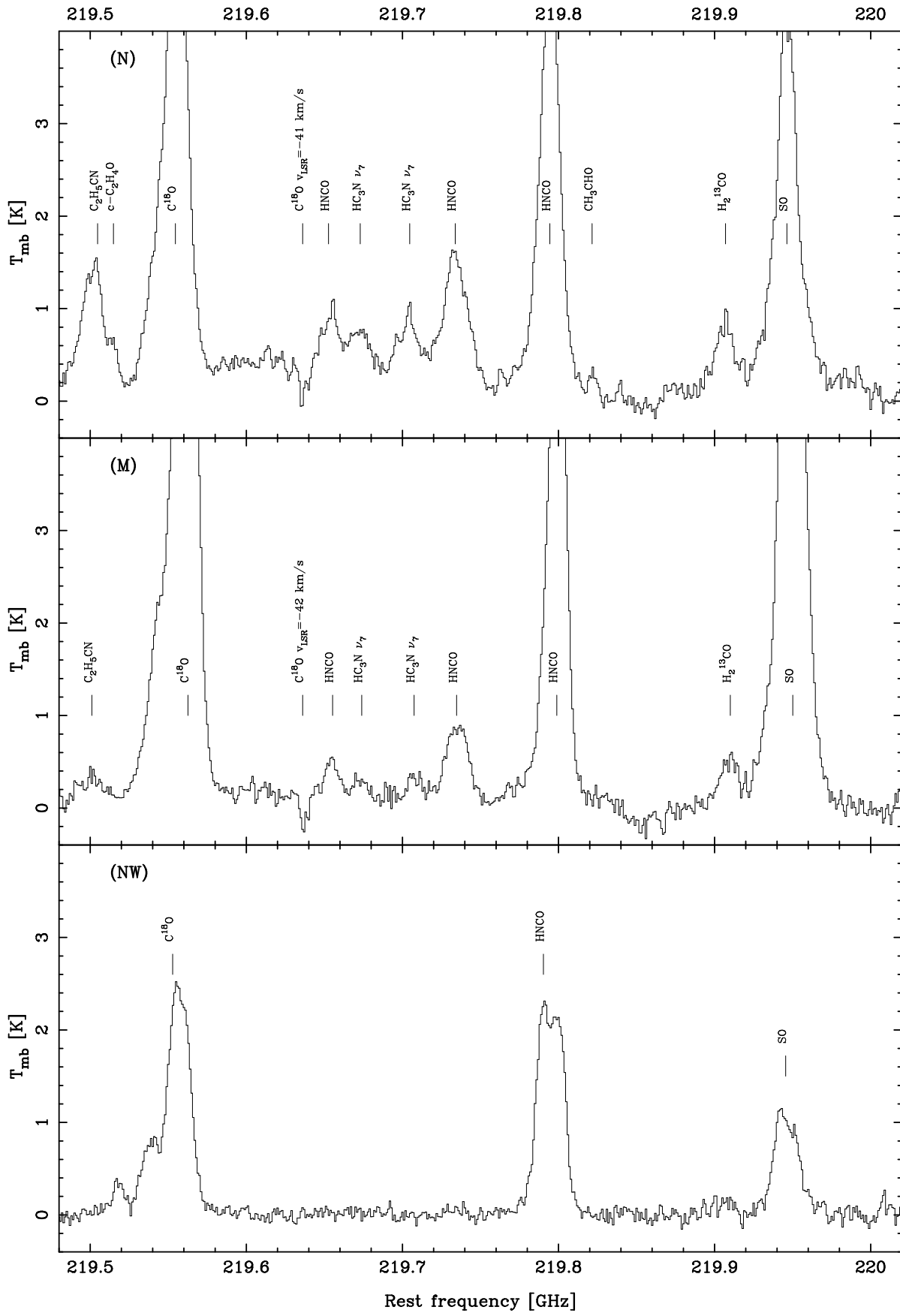


FIG. 1.—Continued

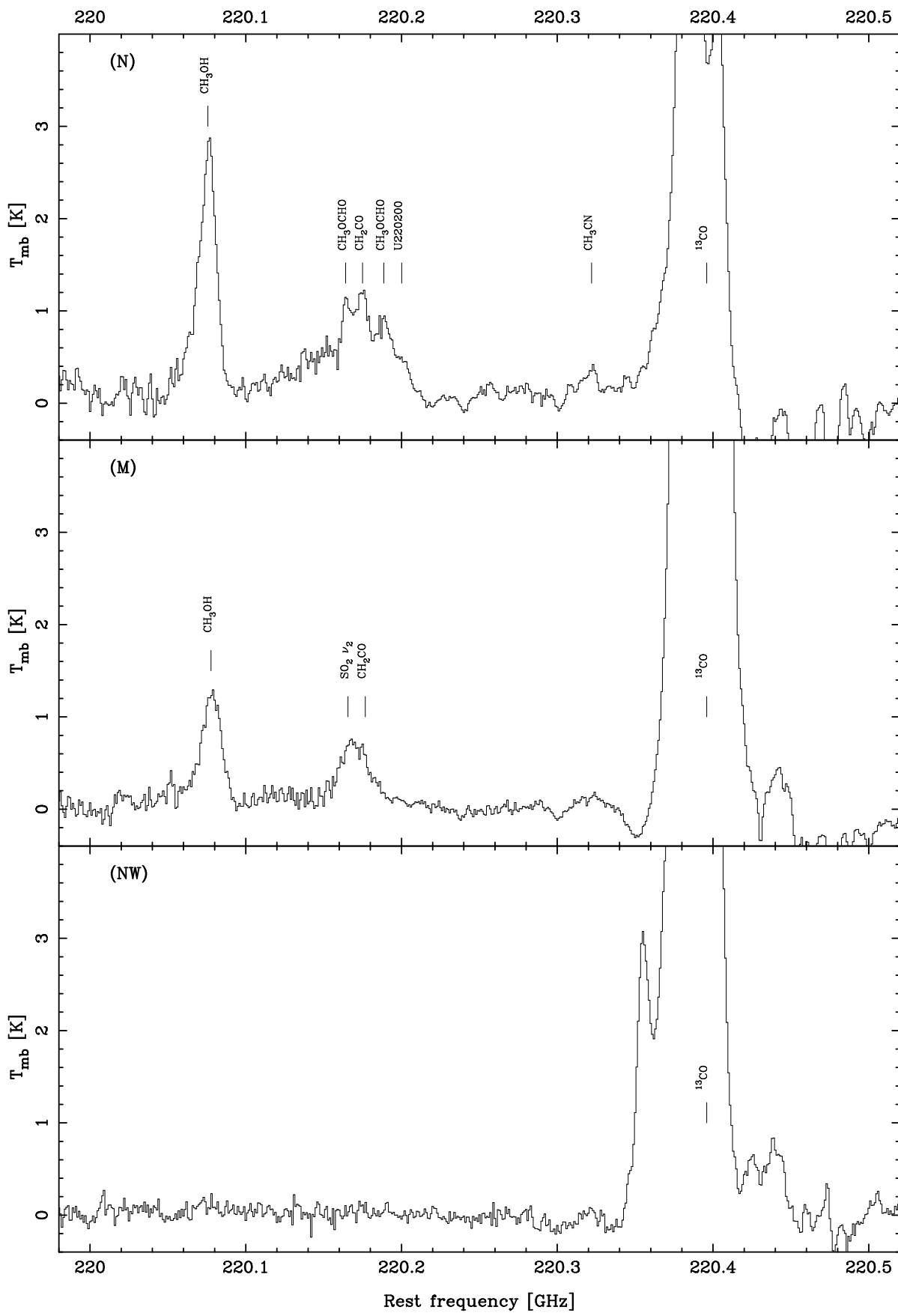


FIG. 1.—Continued

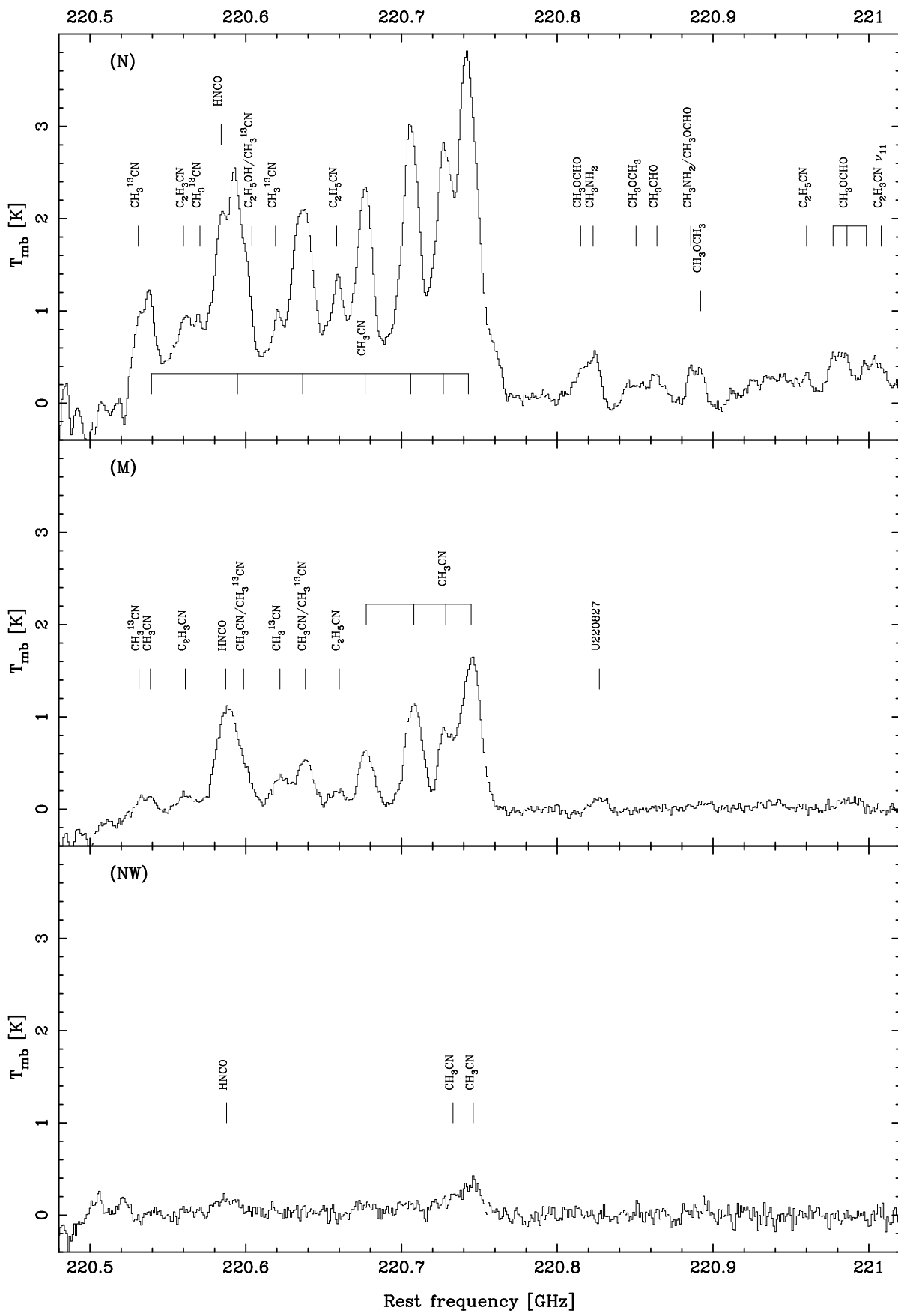


FIG. 1.—Continued

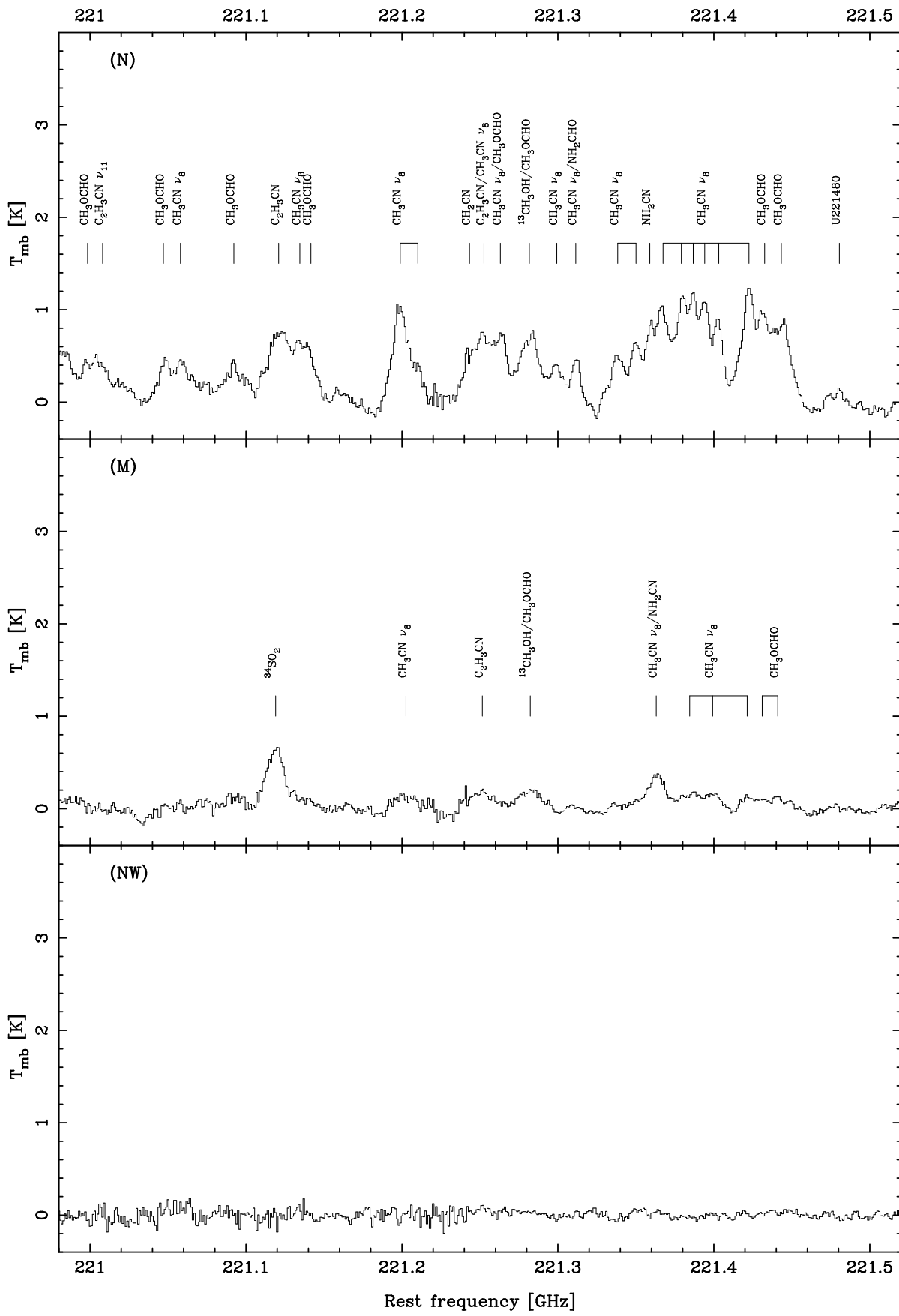


FIG. 1.—Continued

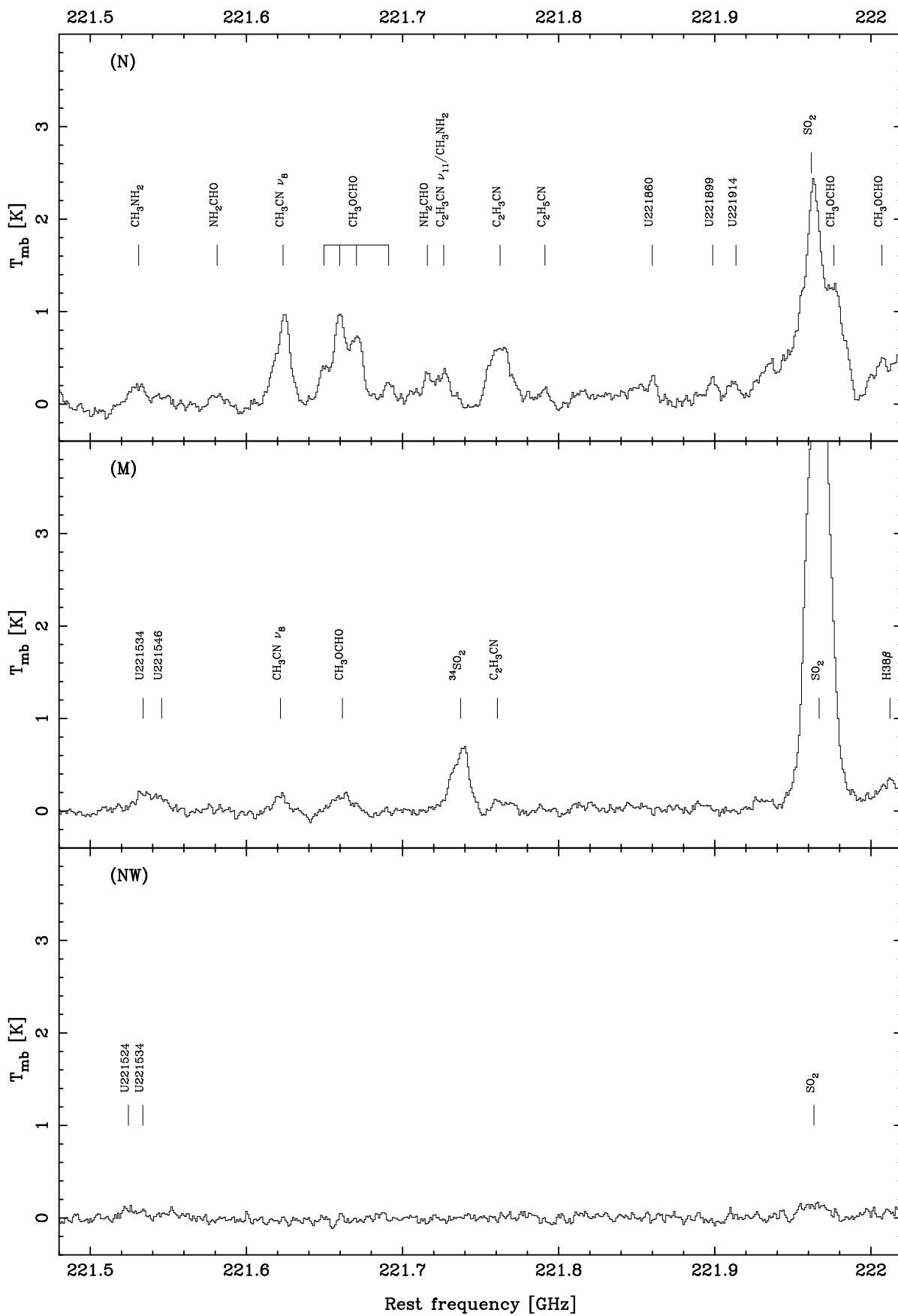


FIG. 1.—Continued

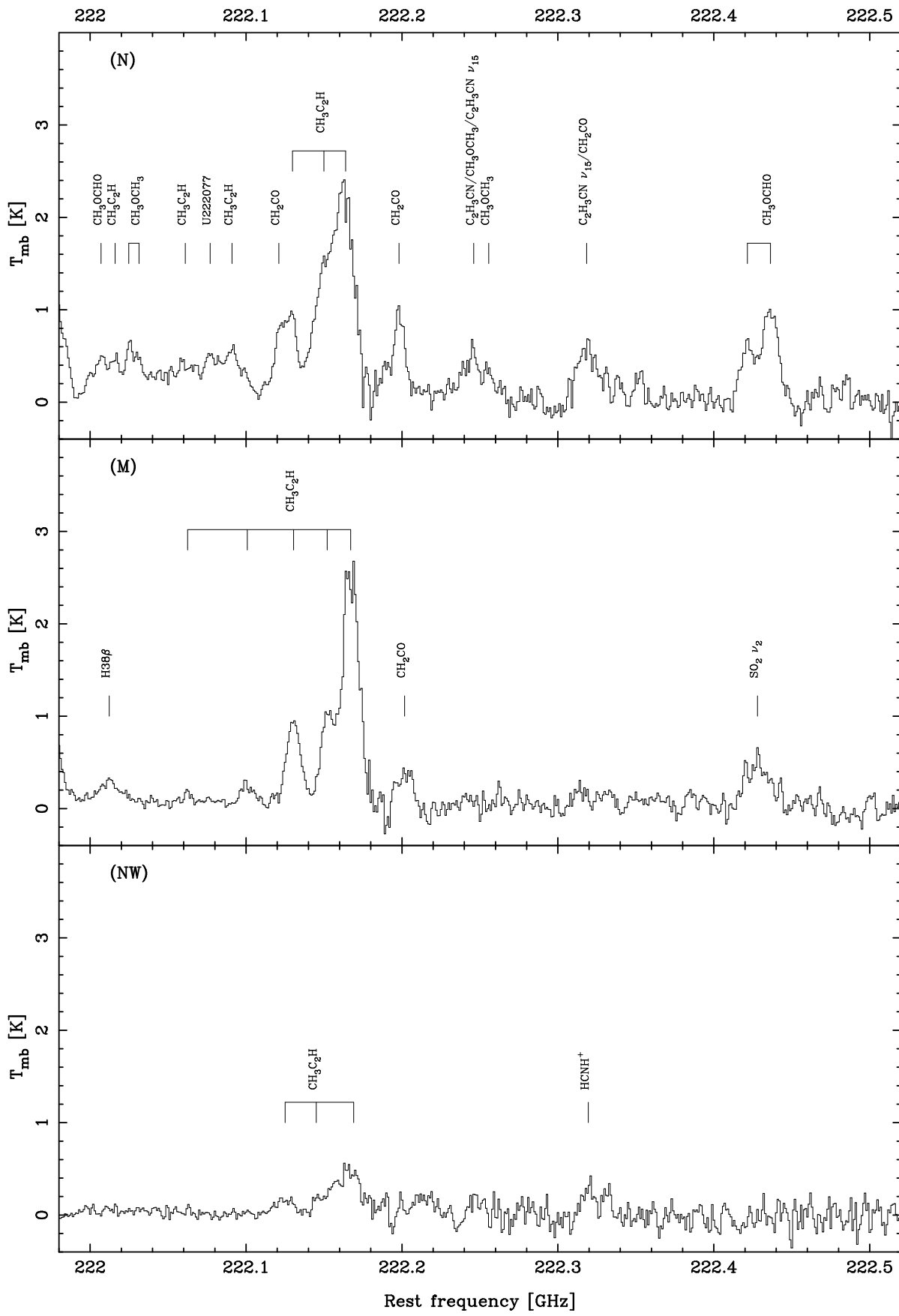


FIG. 1.—Continued

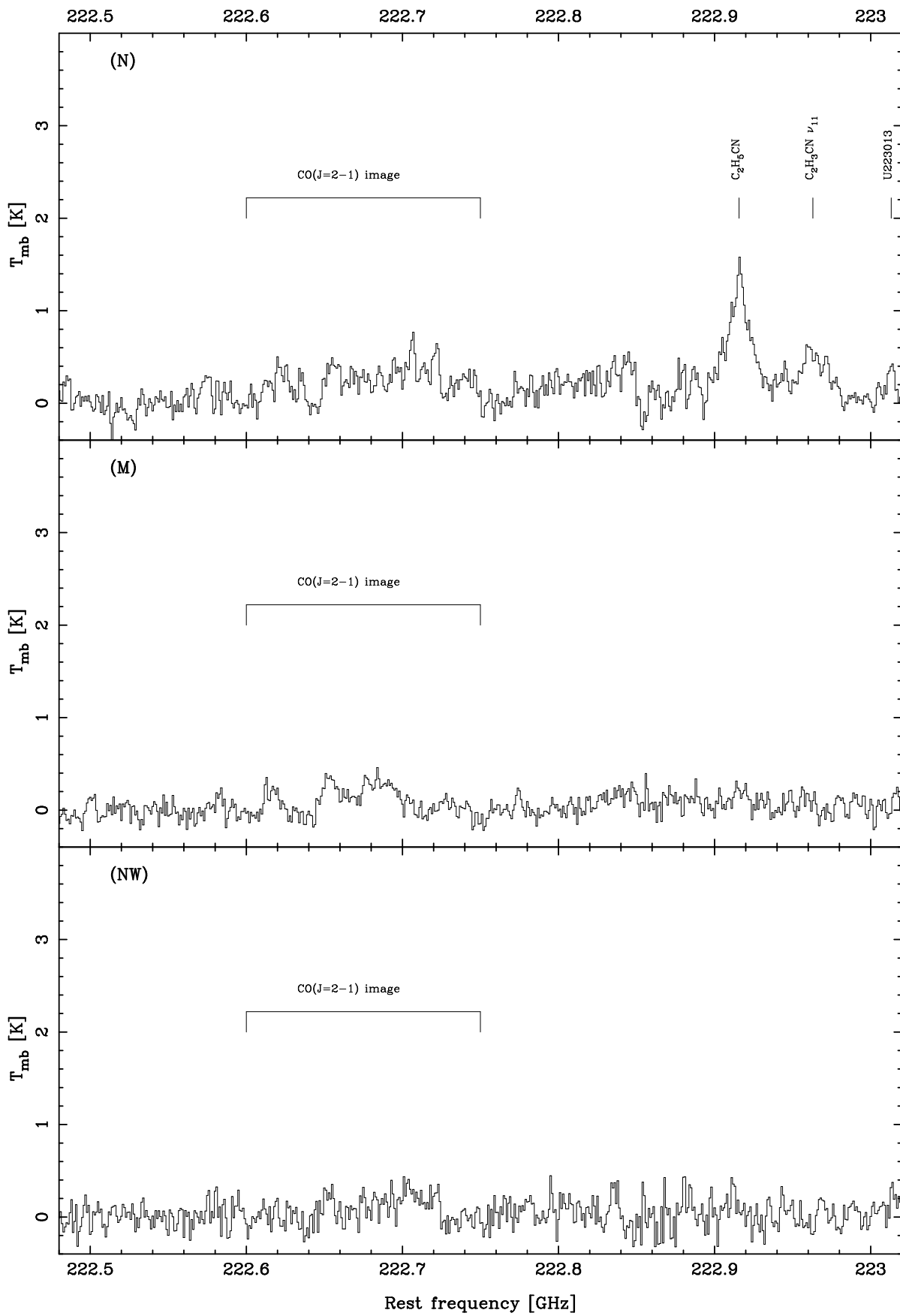


FIG. 1.—Continued

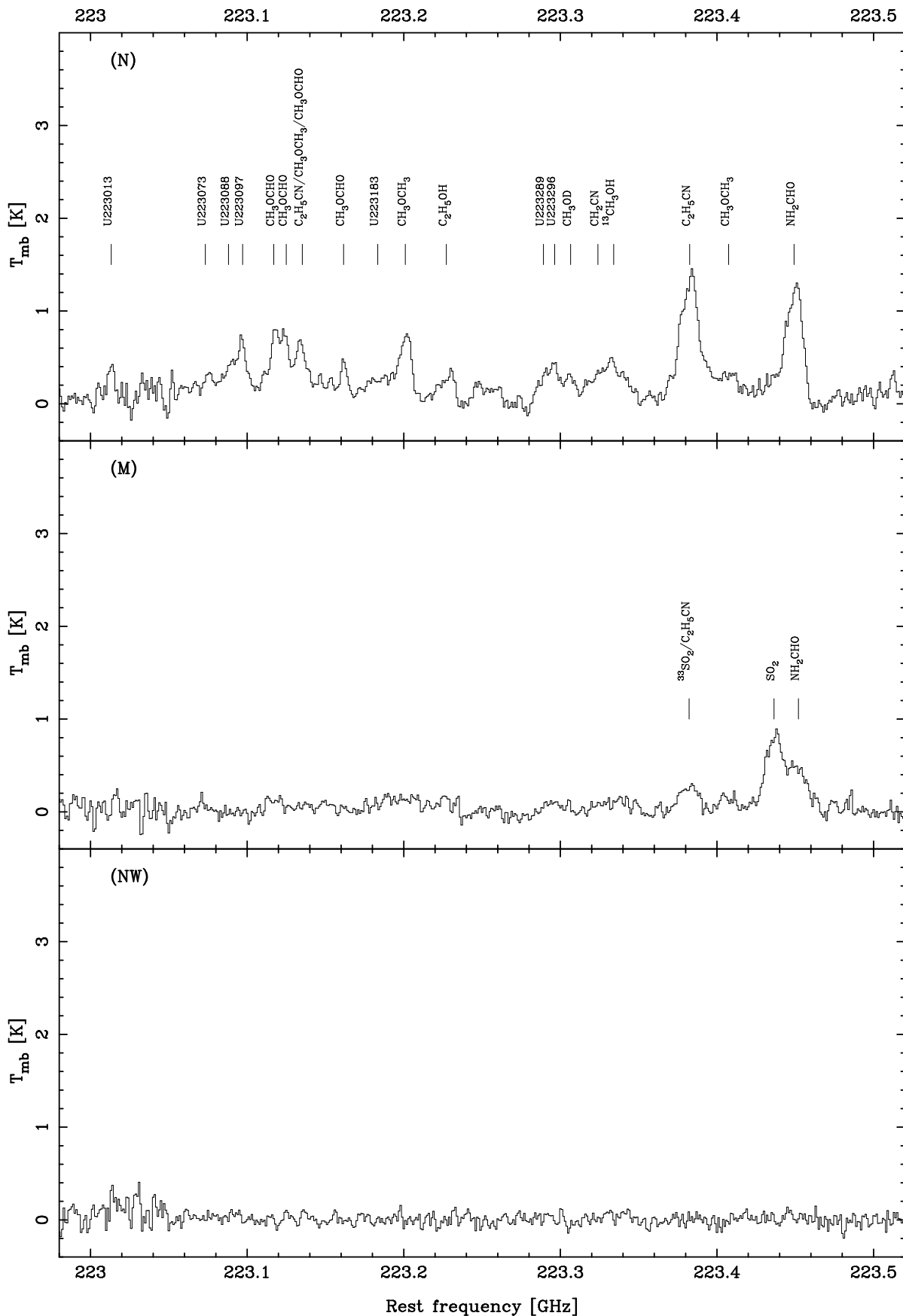


FIG. 1.—Continued

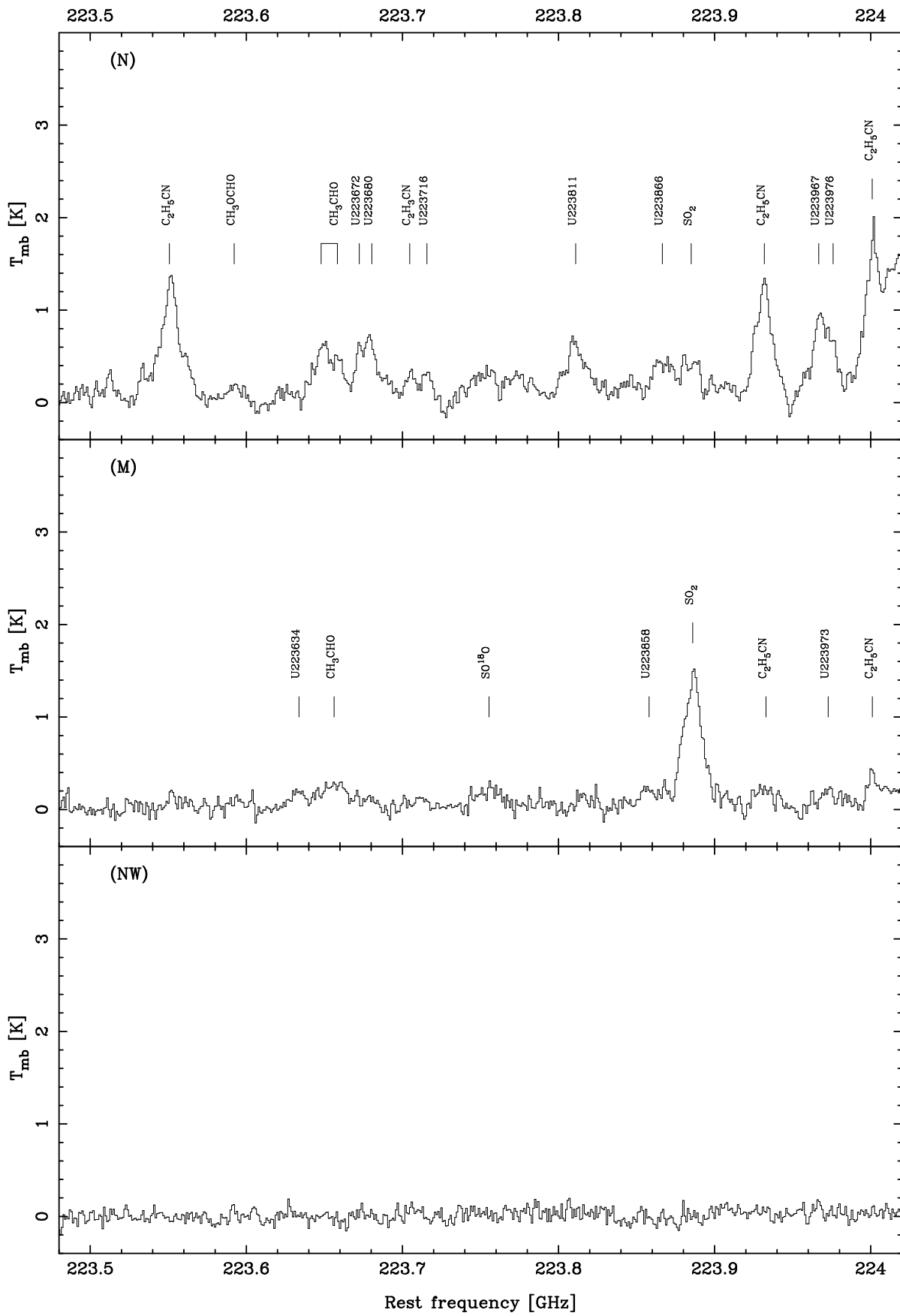


FIG. 1.—Continued

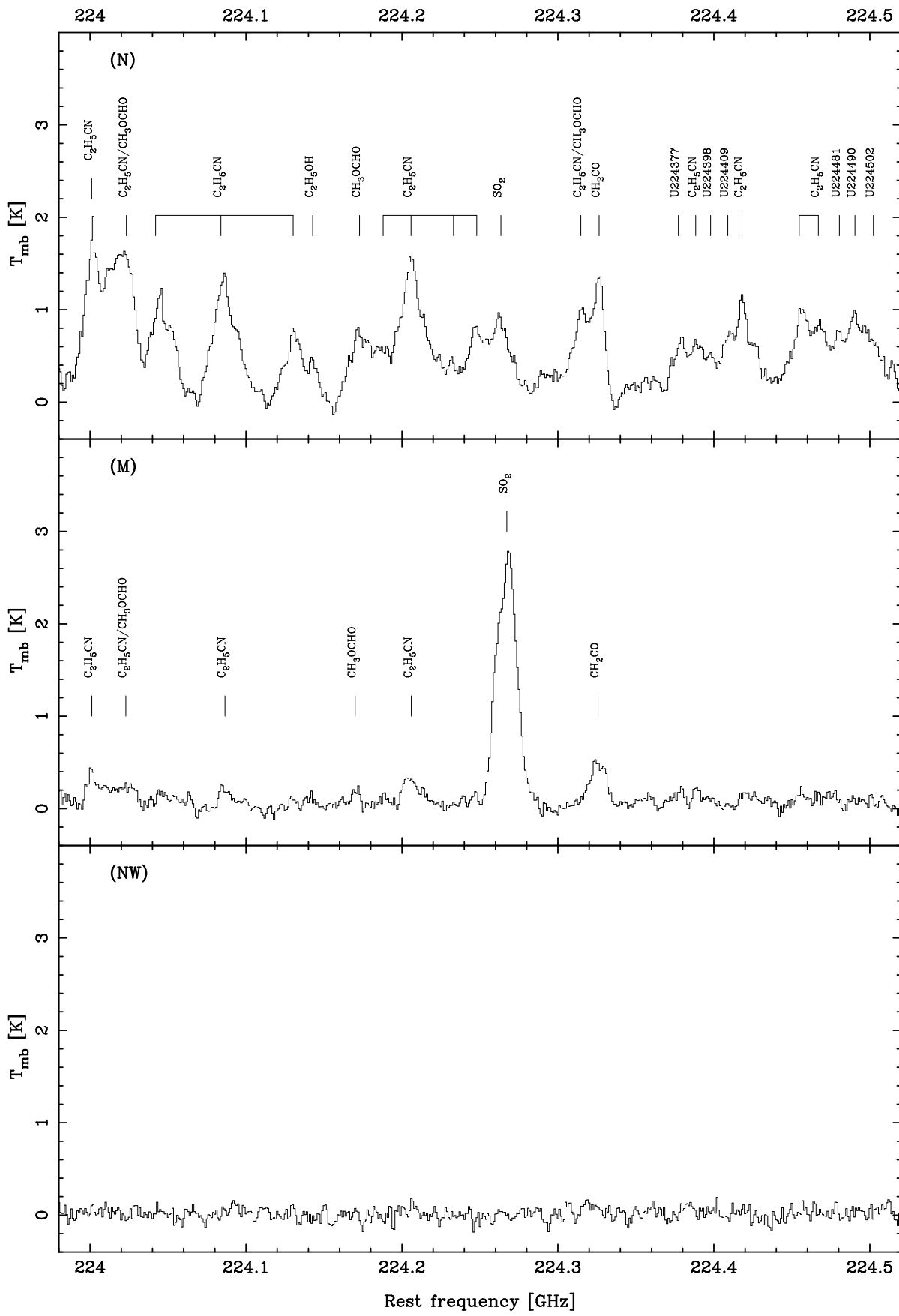


FIG. 1.—Continued

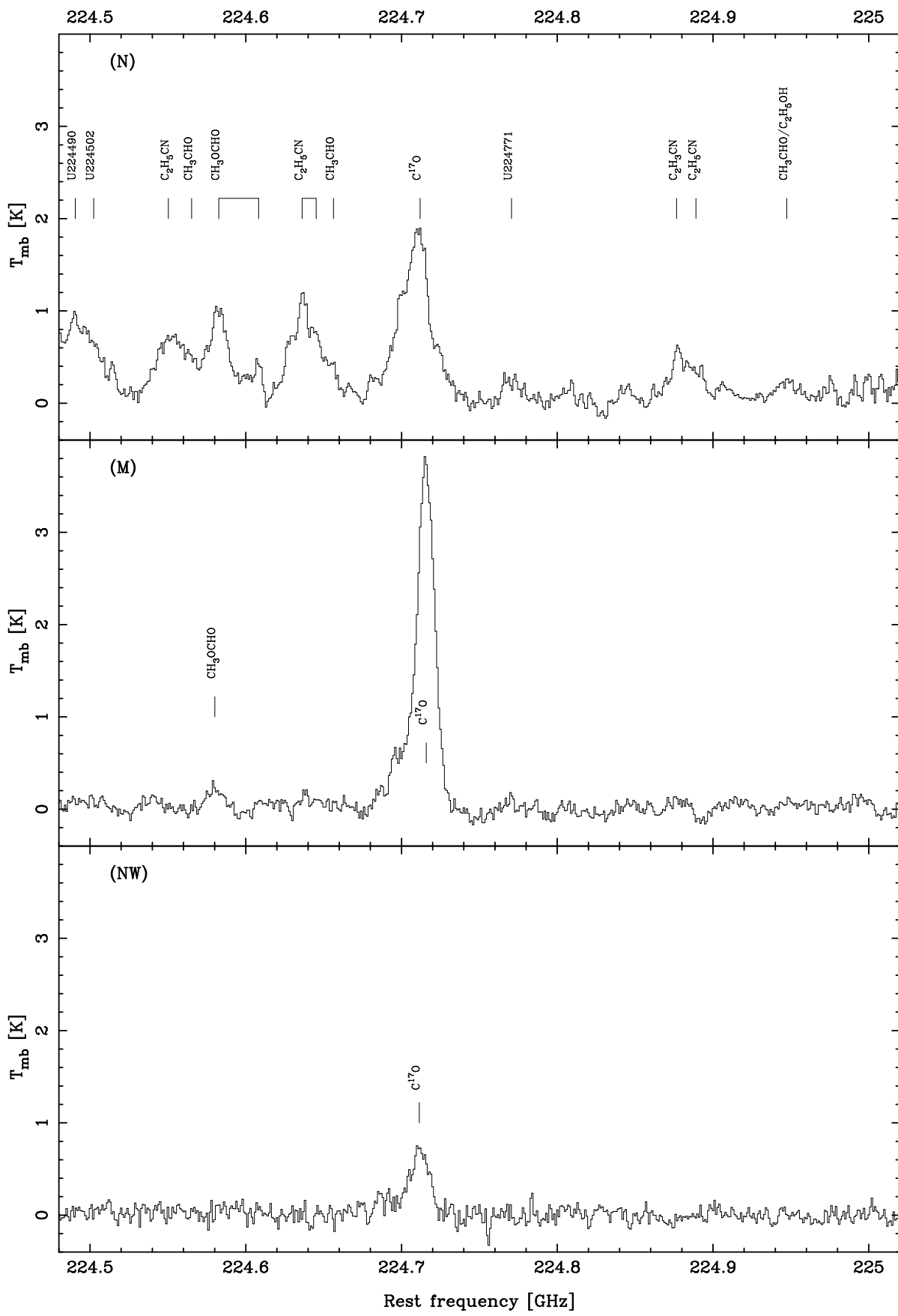


FIG. 1.—Continued

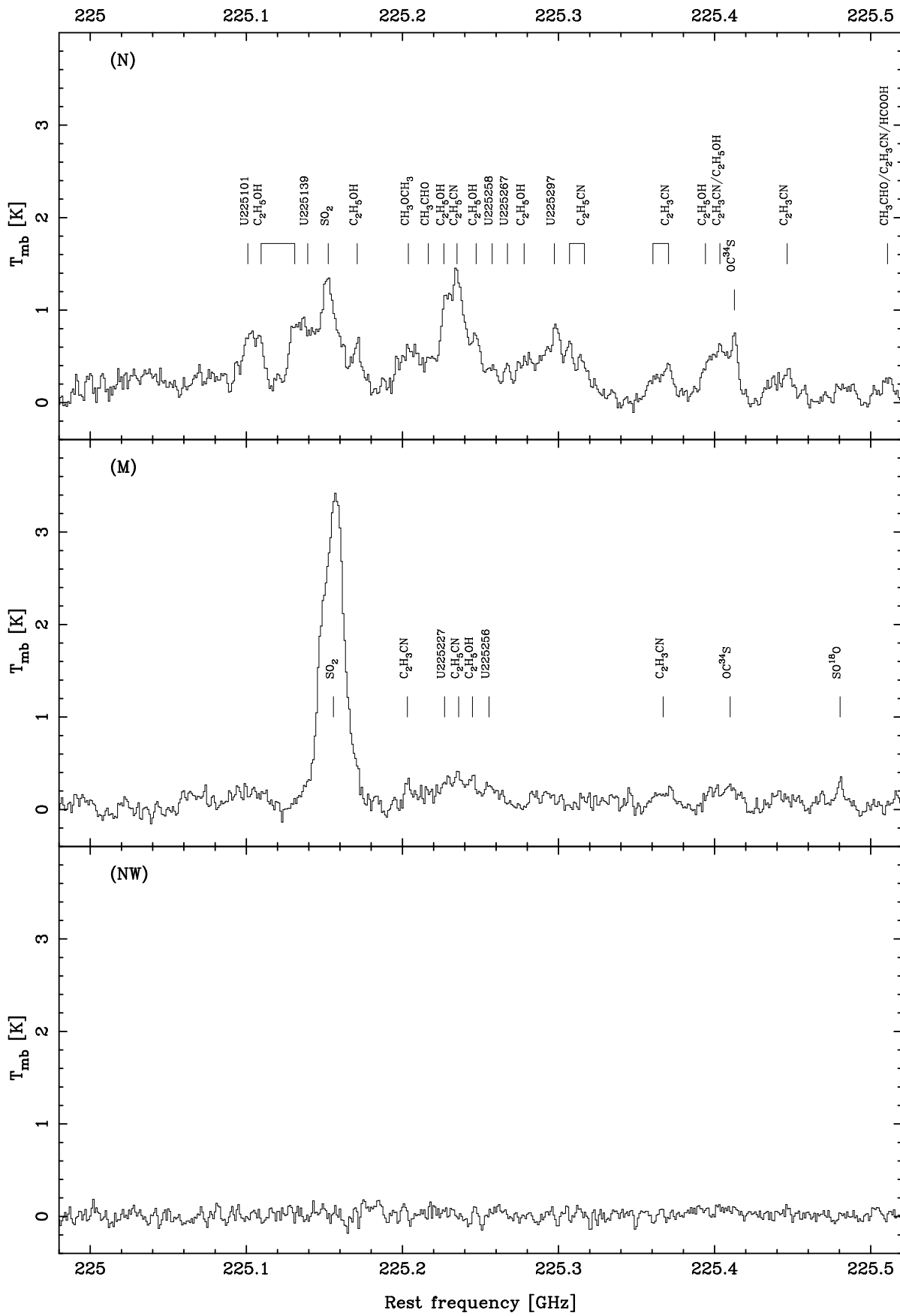


FIG. 1.—Continued

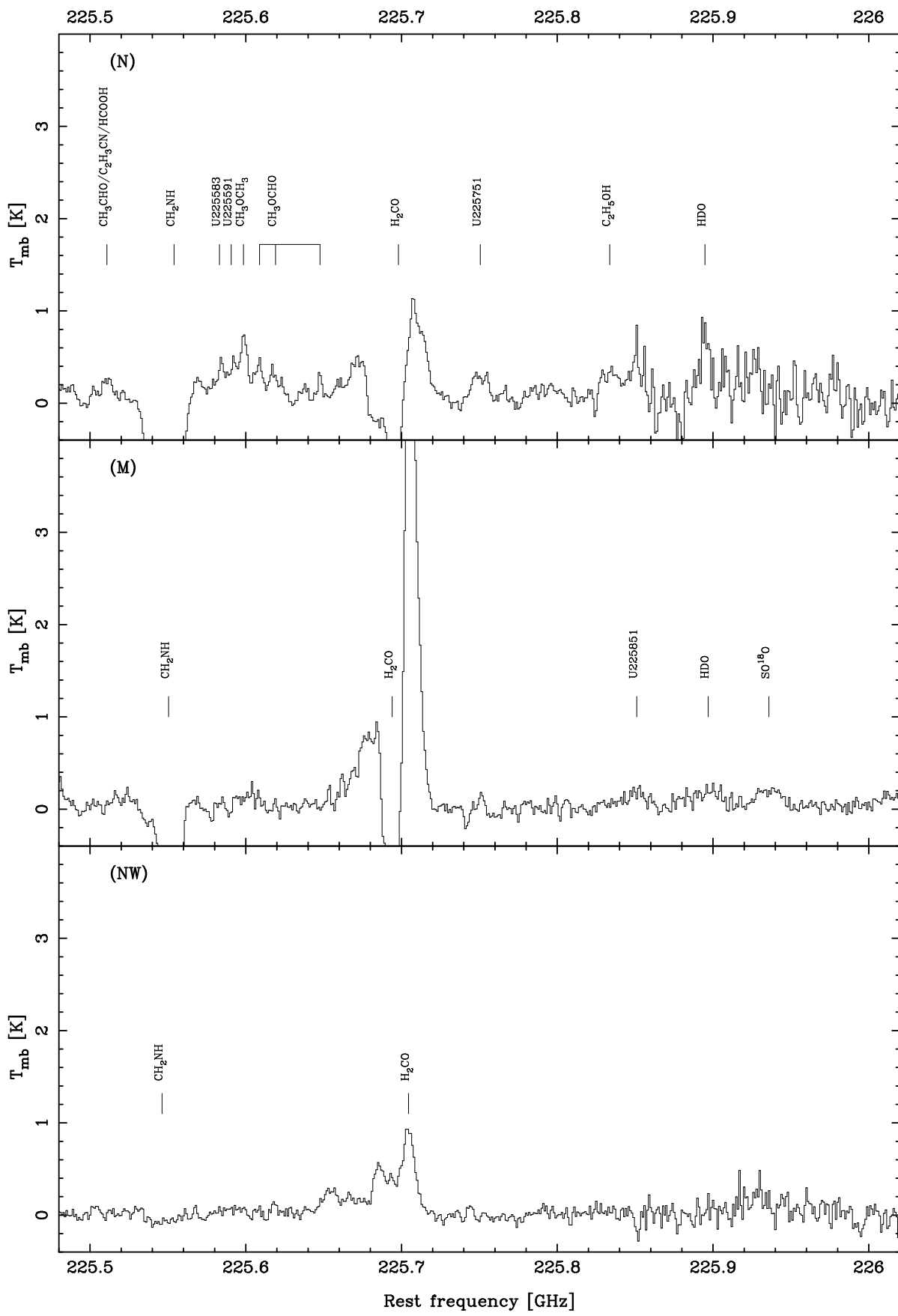


FIG. 1.—Continued

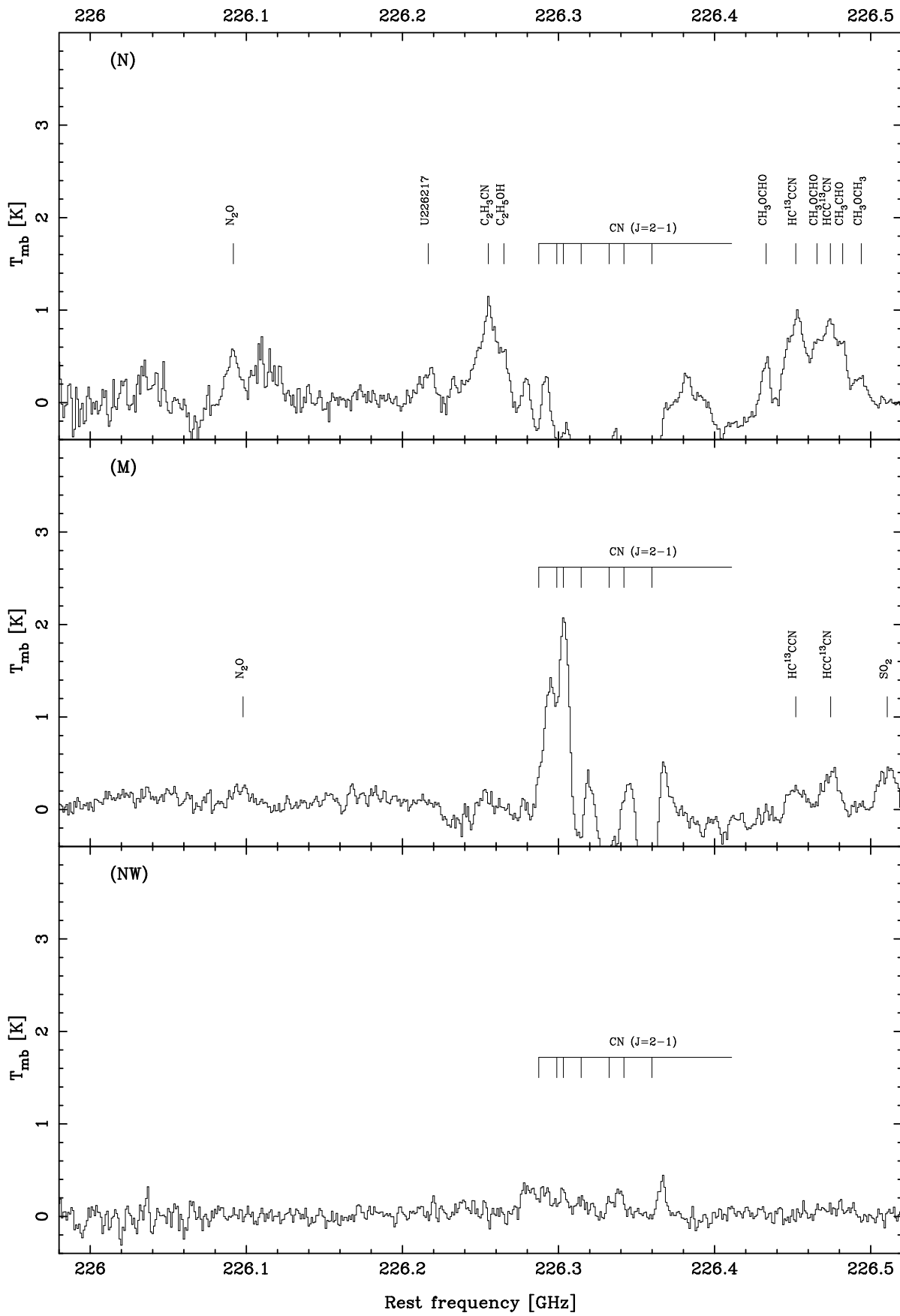


FIG. 1.—Continued

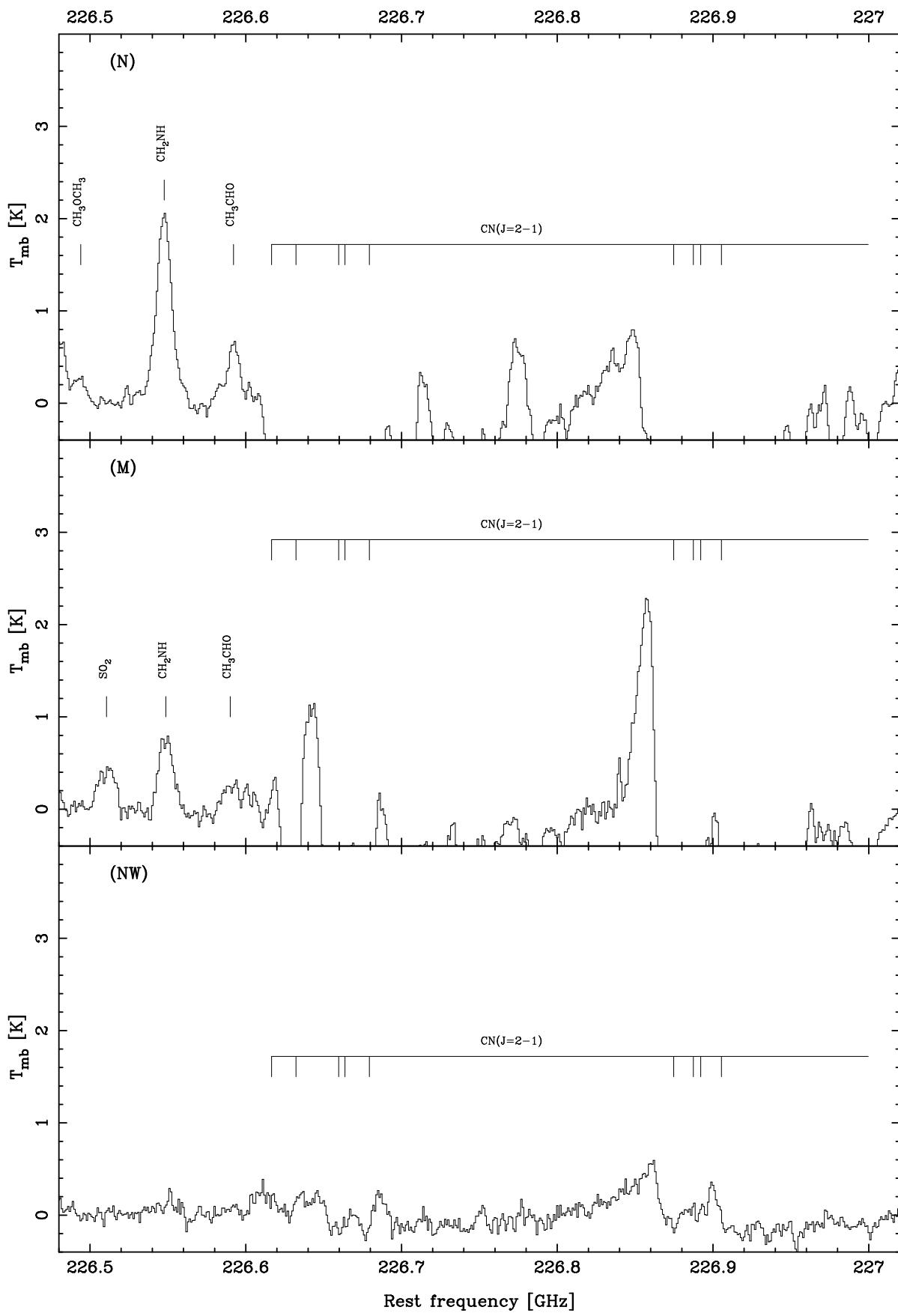


FIG. 1.—Continued

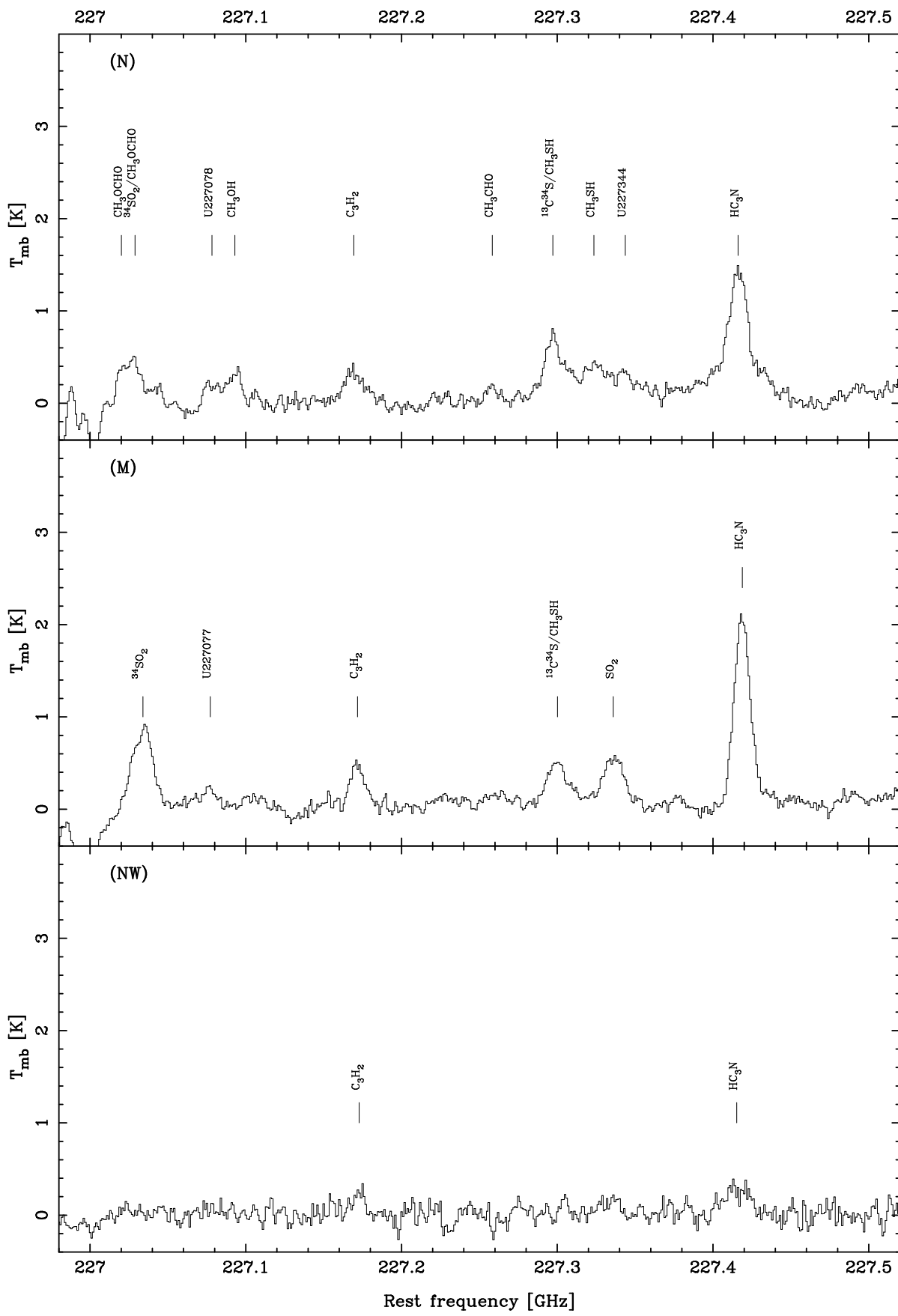


FIG. 1.—Continued

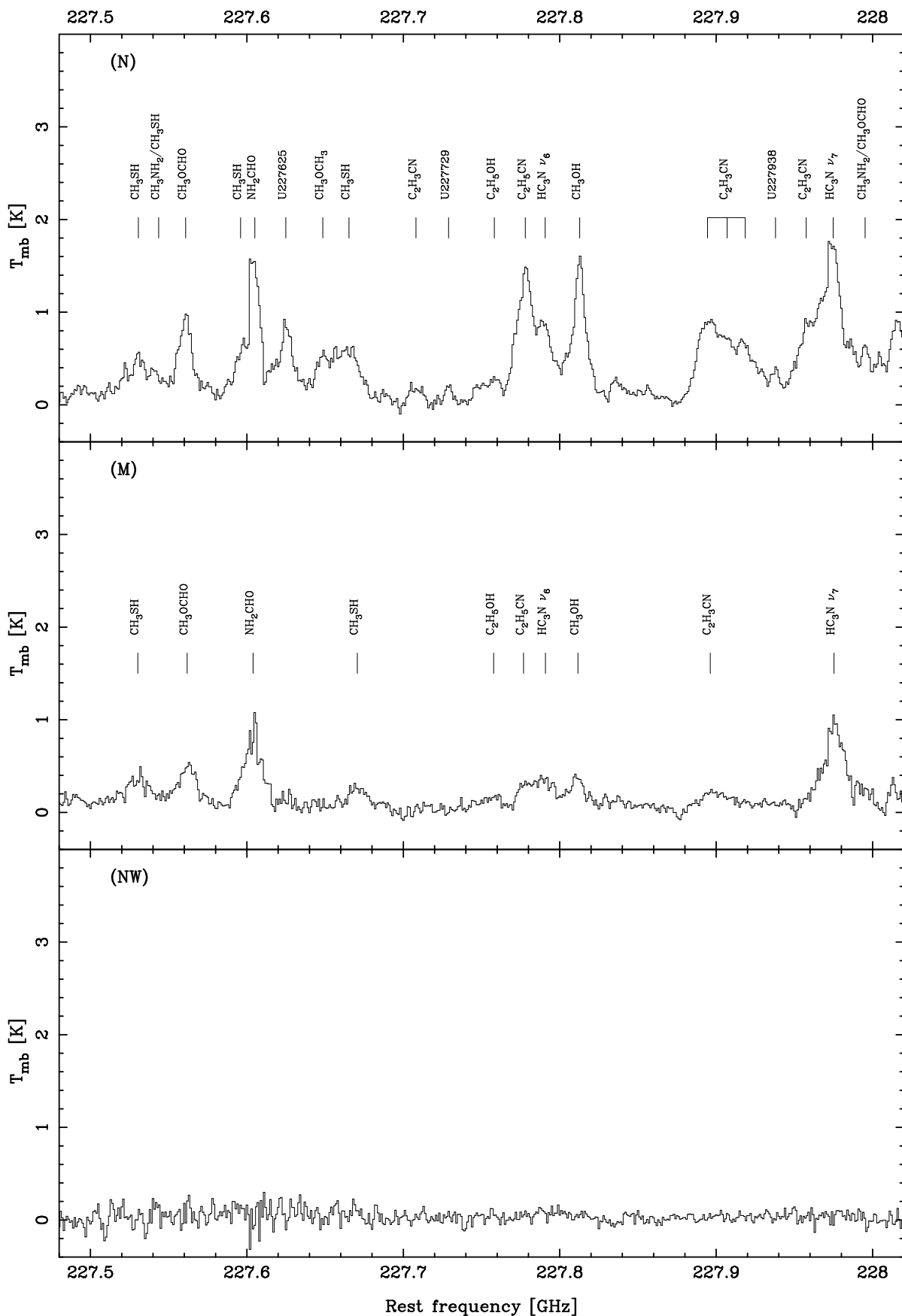


FIG. 1.—Continued

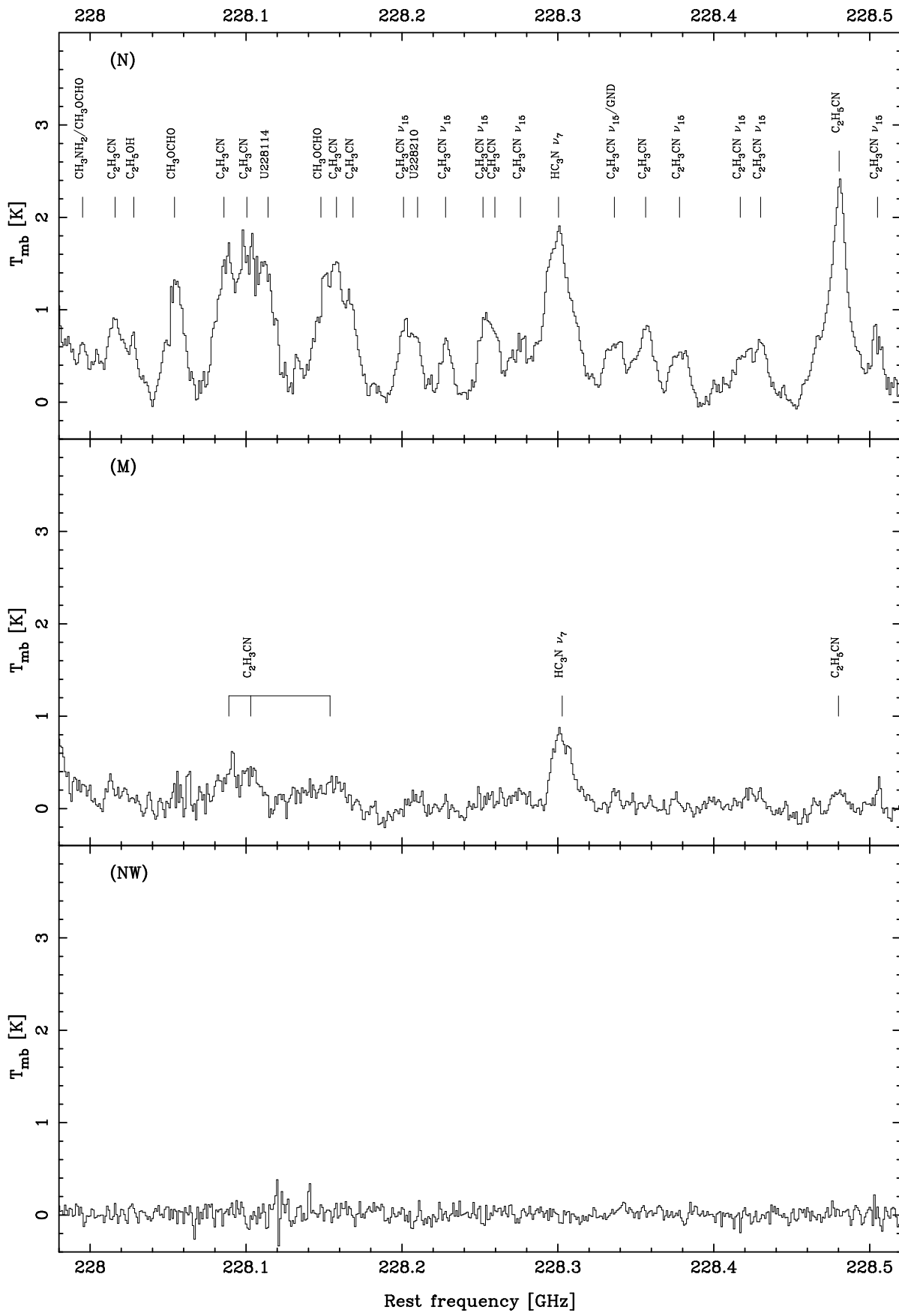


FIG. 1.—Continued

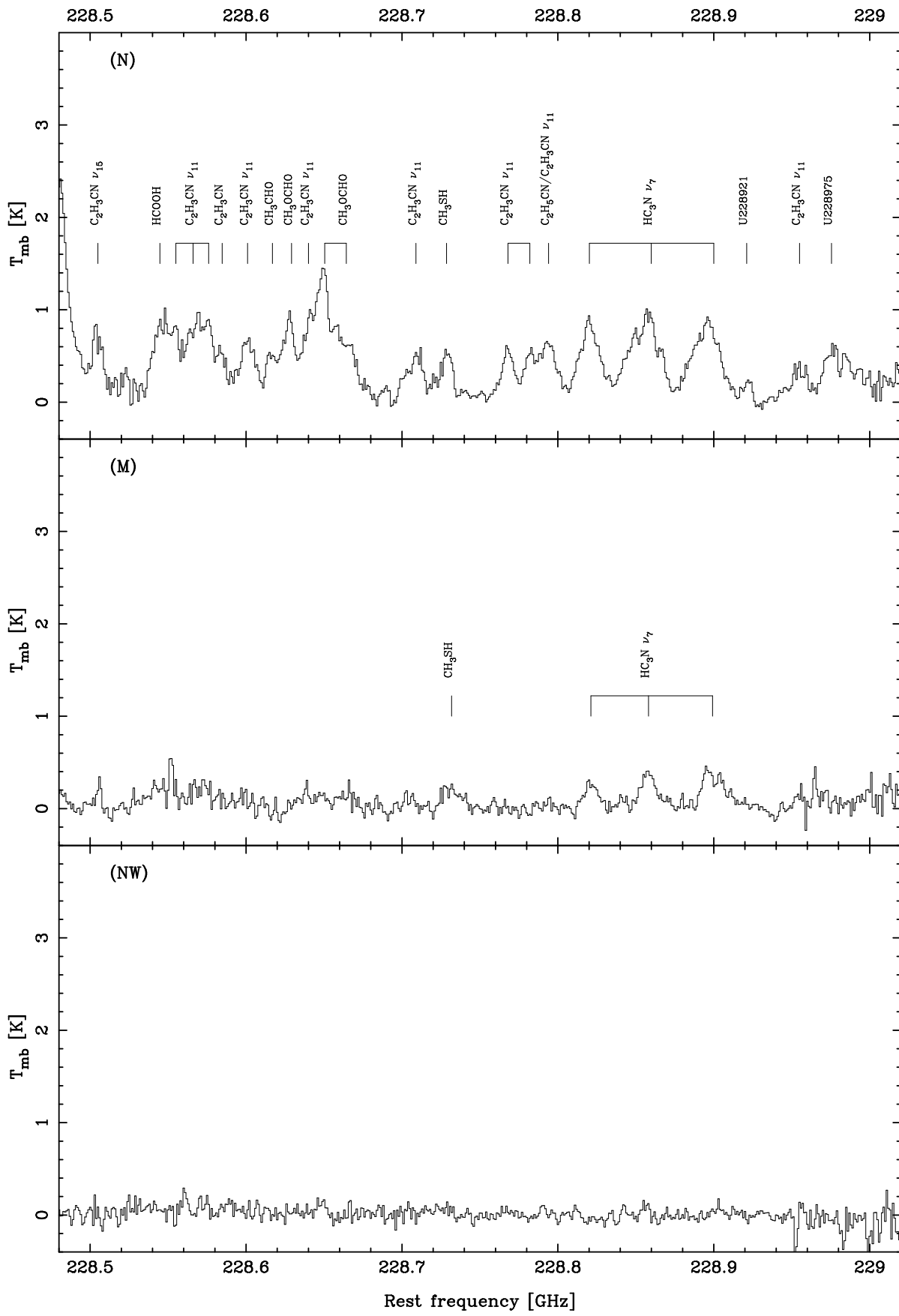


FIG. 1.—Continued

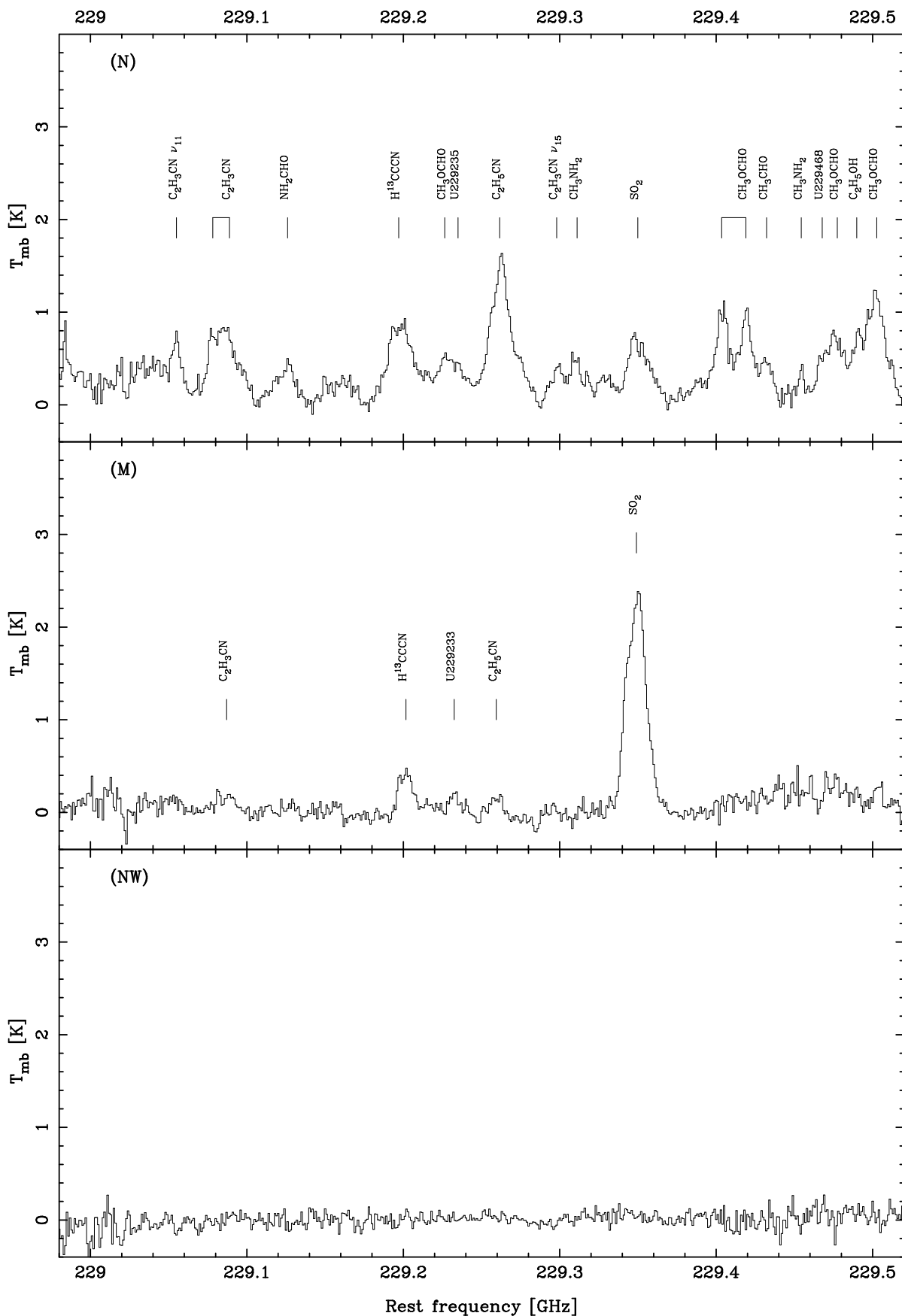


FIG. 1.—Continued

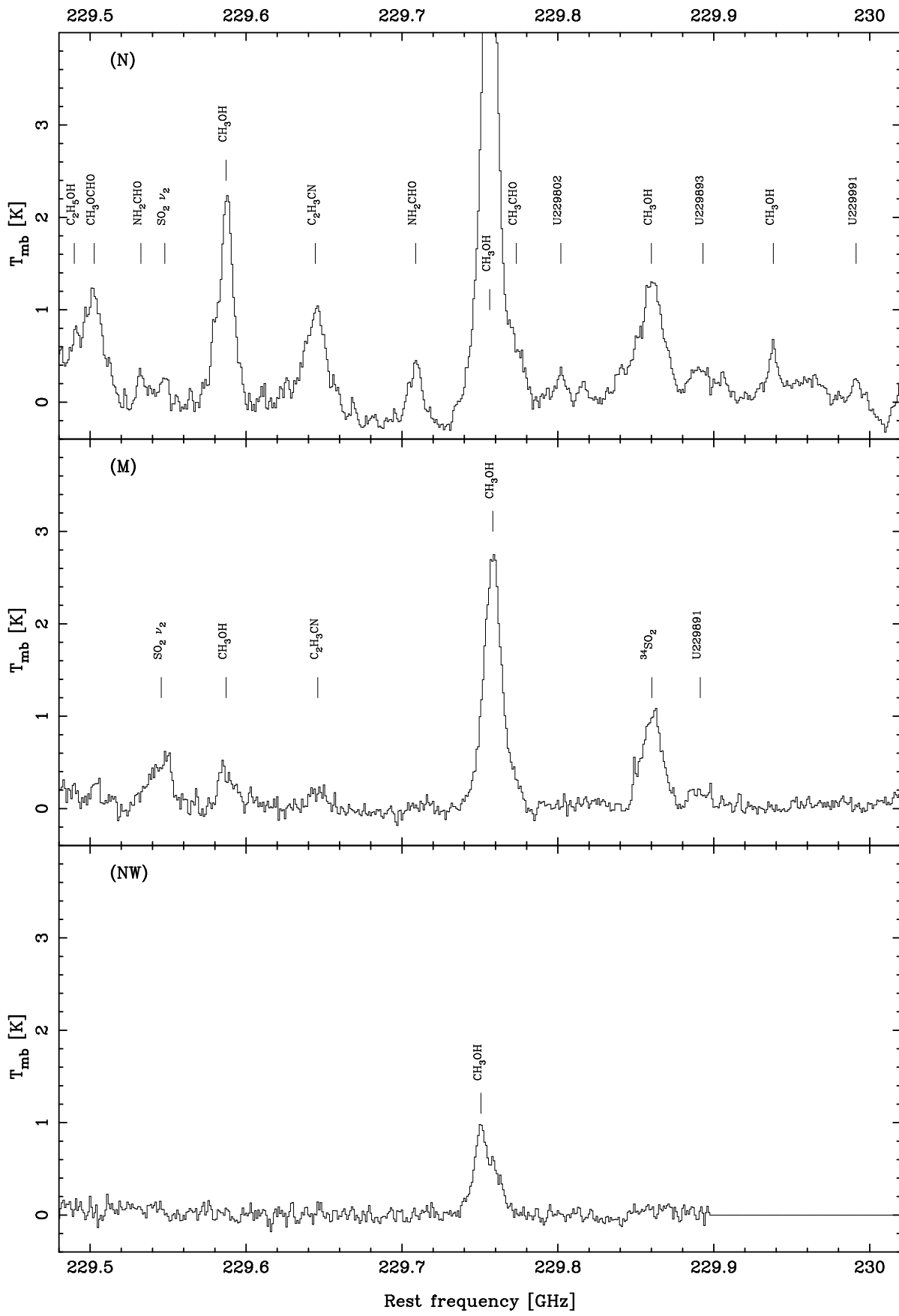


FIG. 1.—Continued

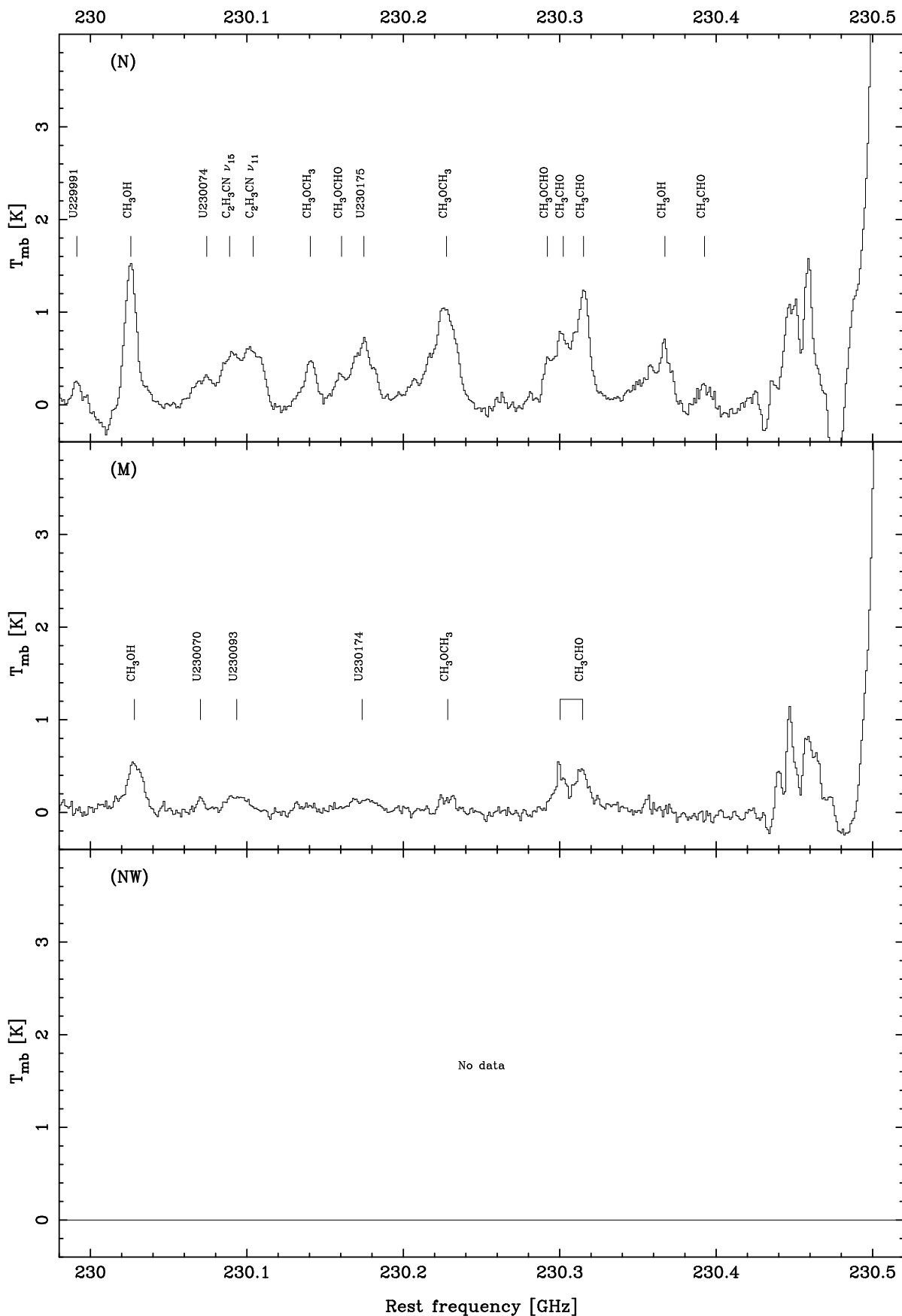


FIG. 1.—Continued

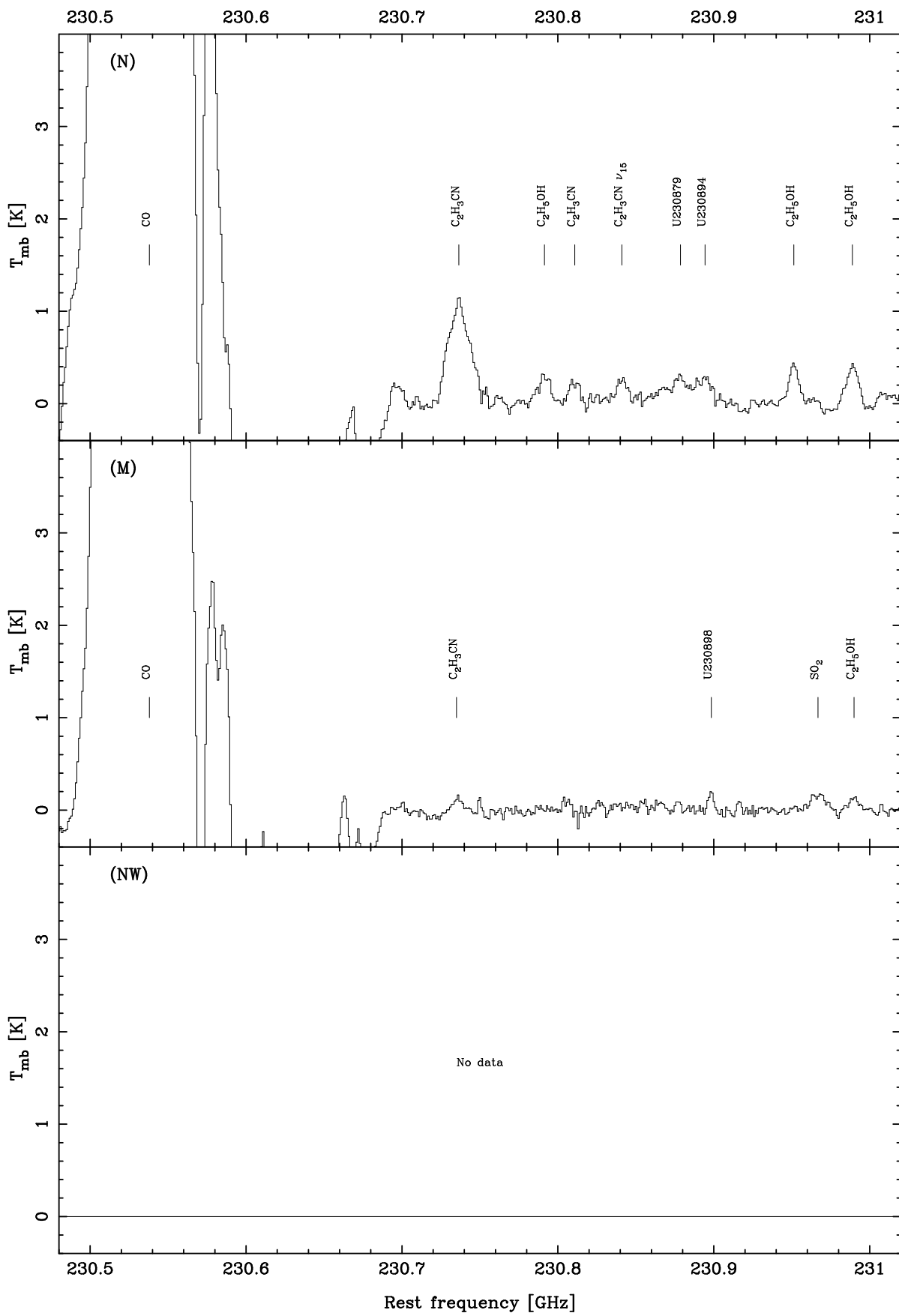


FIG. 1.—Continued

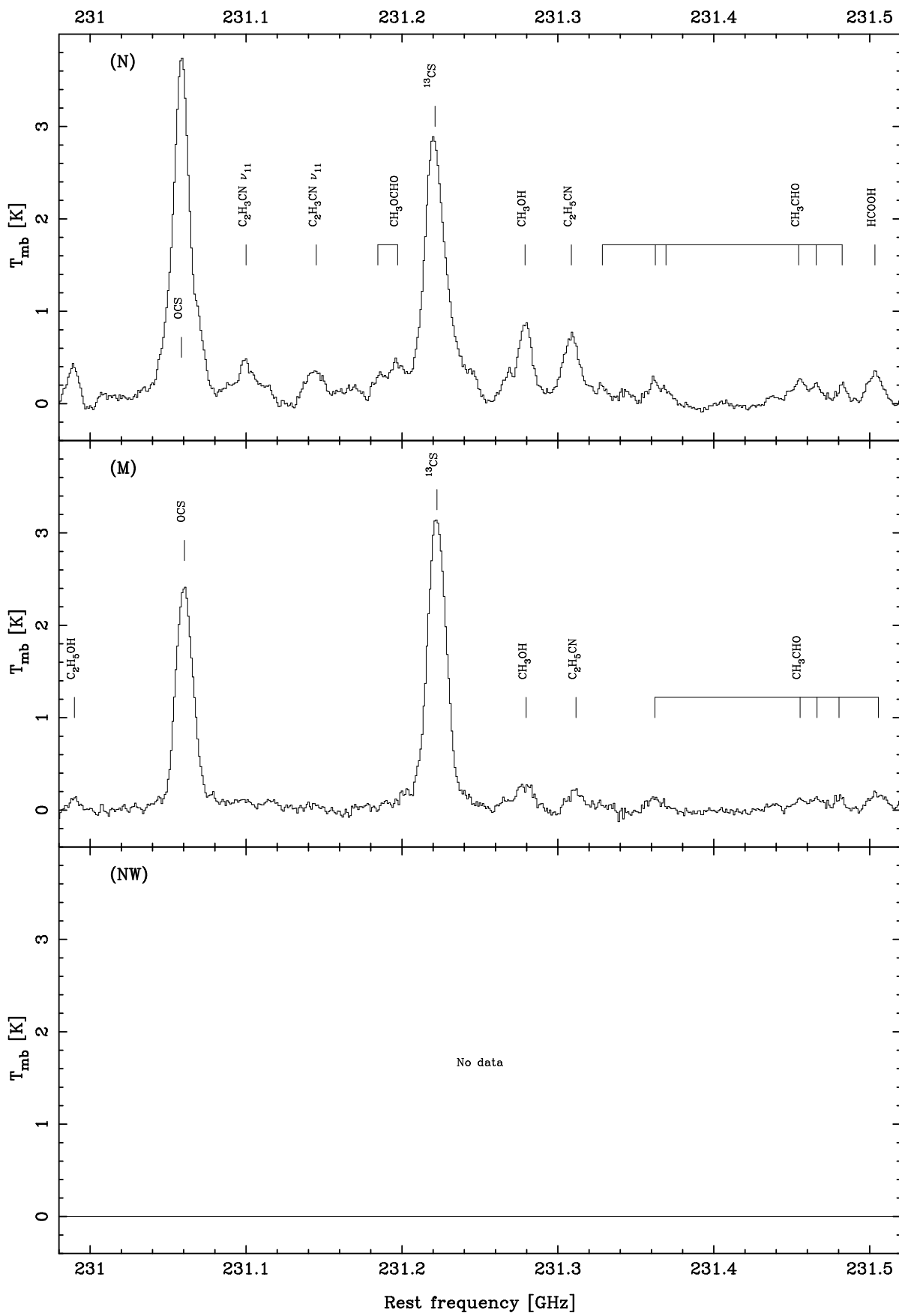


FIG. 1.—Continued

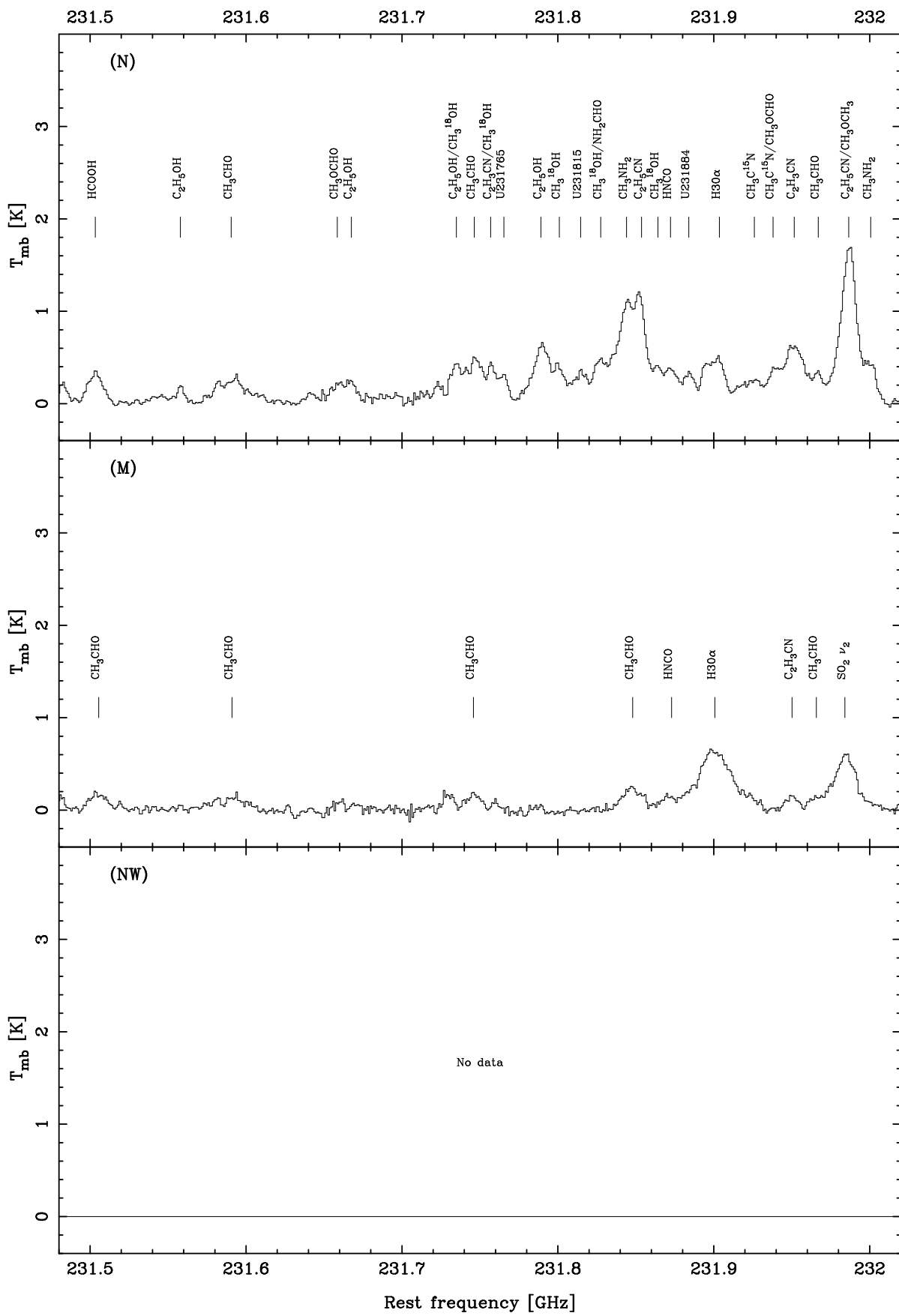


FIG. 1.—Continued

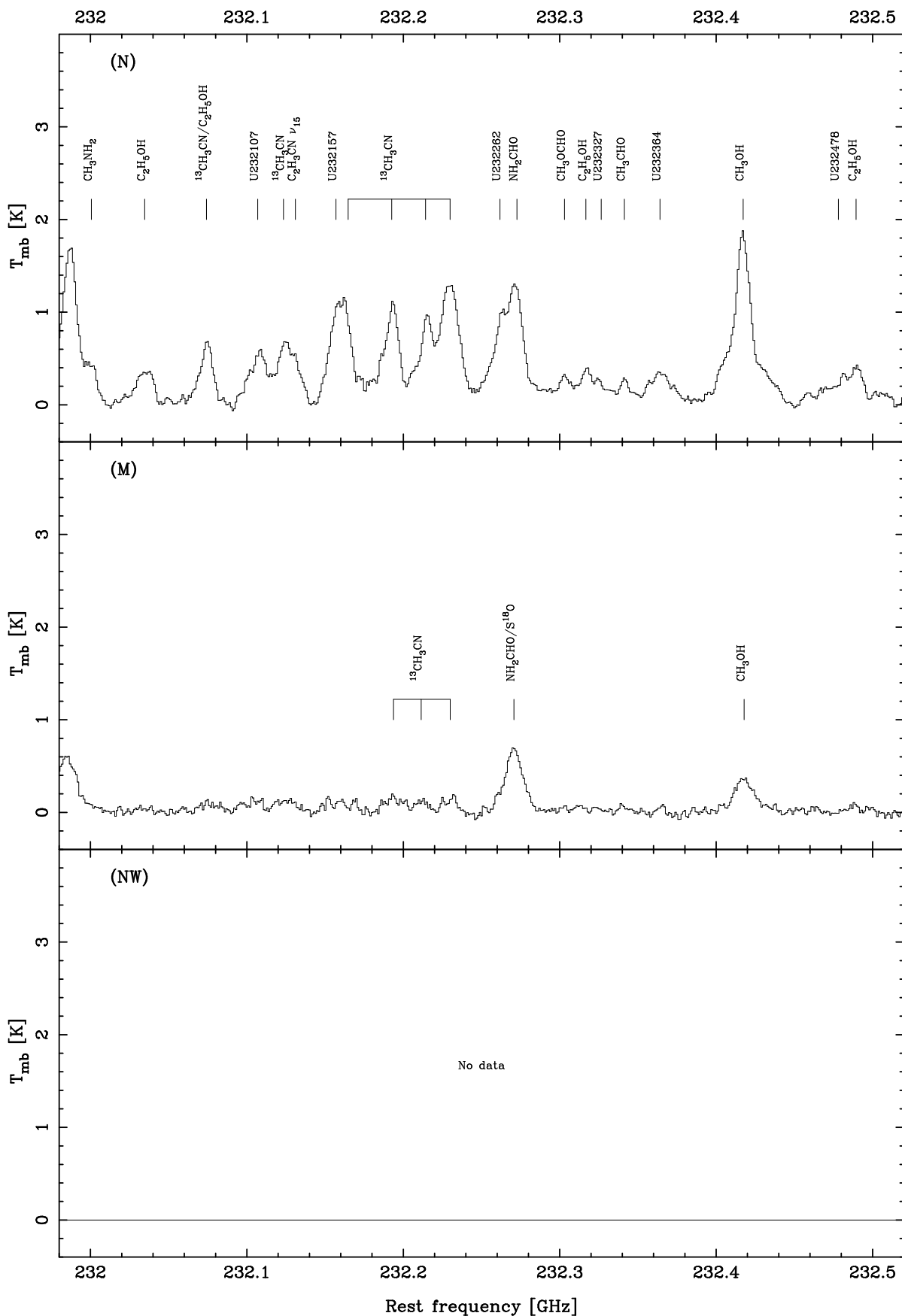


FIG. 1.—Continued

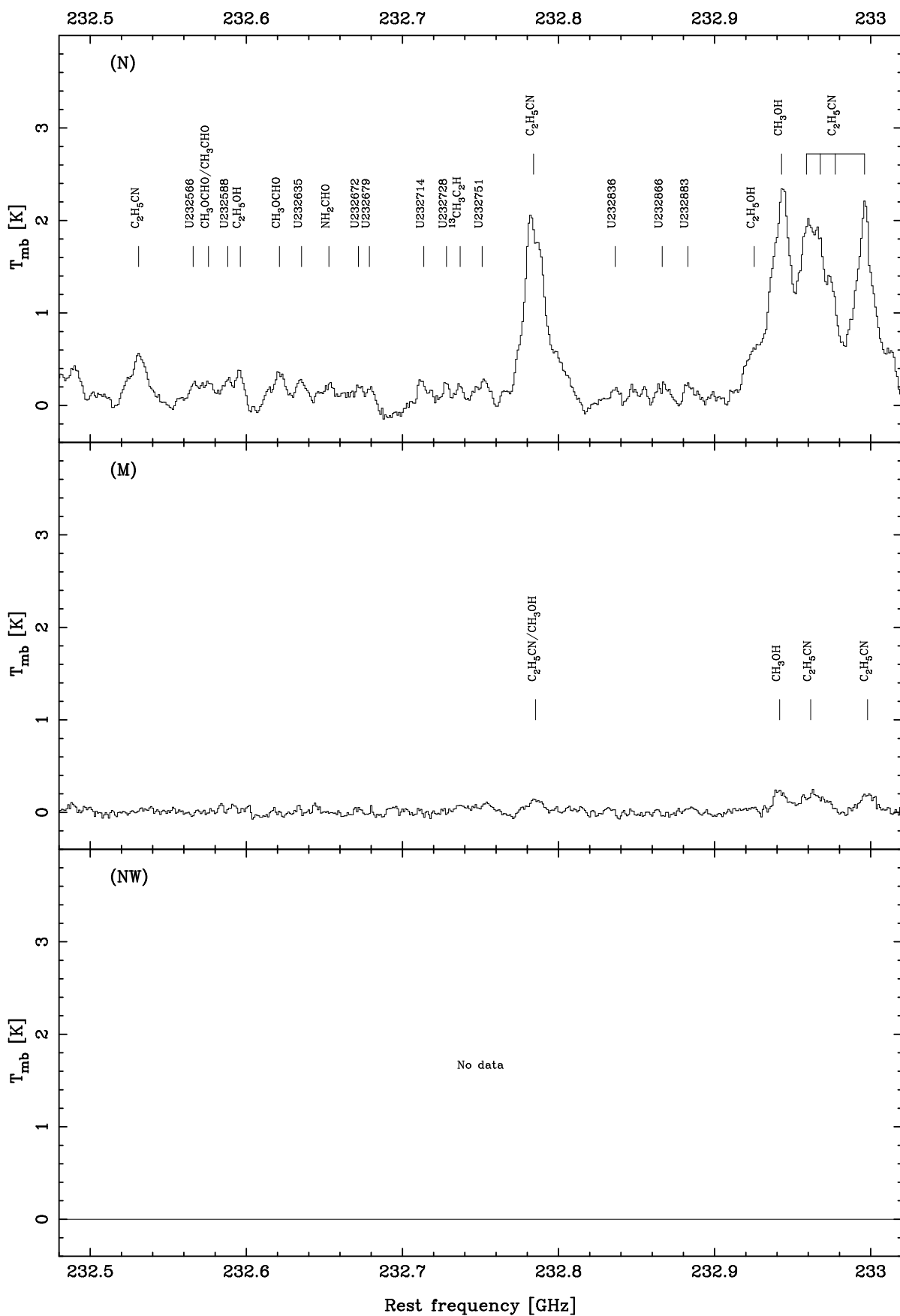


FIG. 1.—Continued

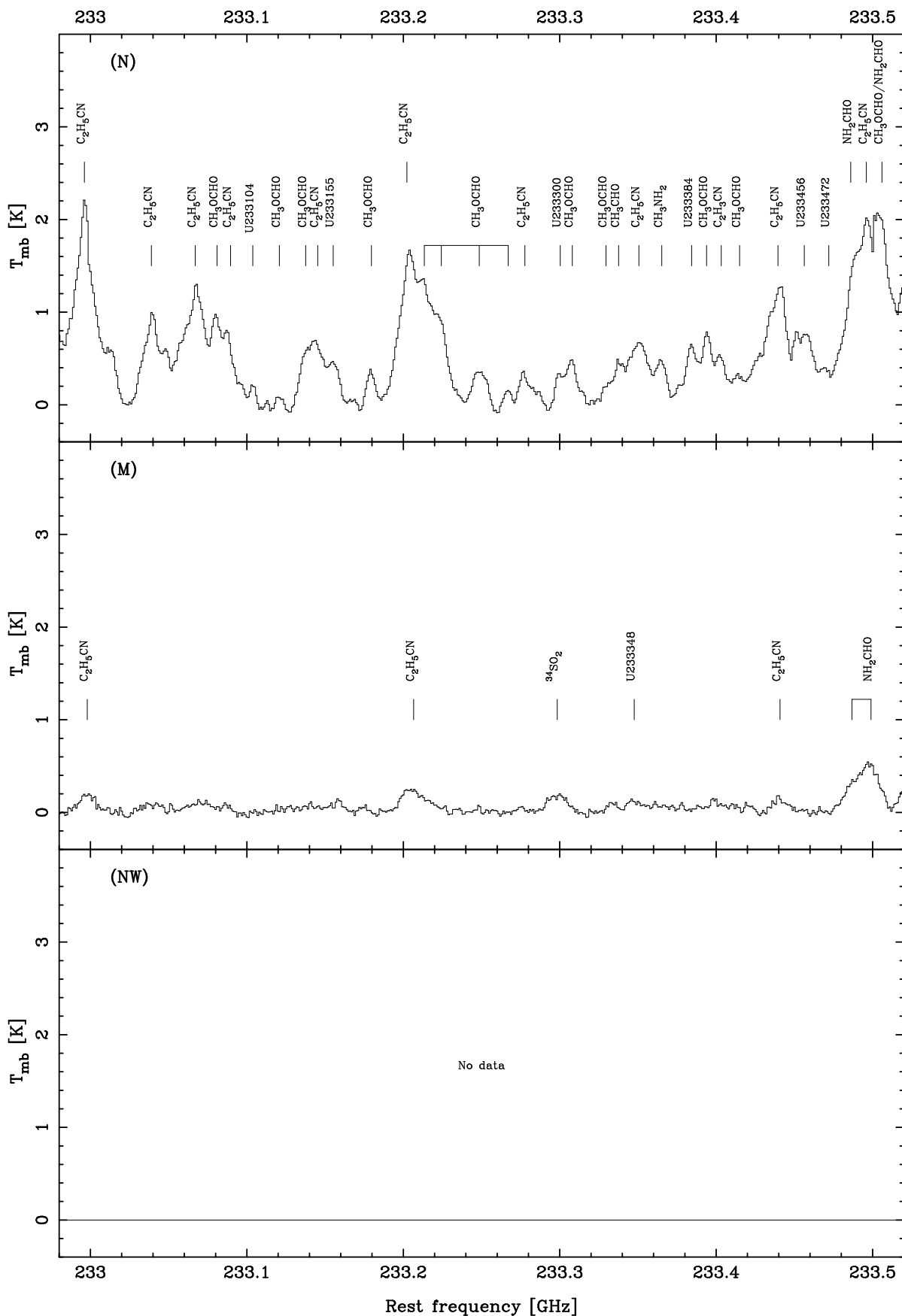


FIG. 1.—Continued

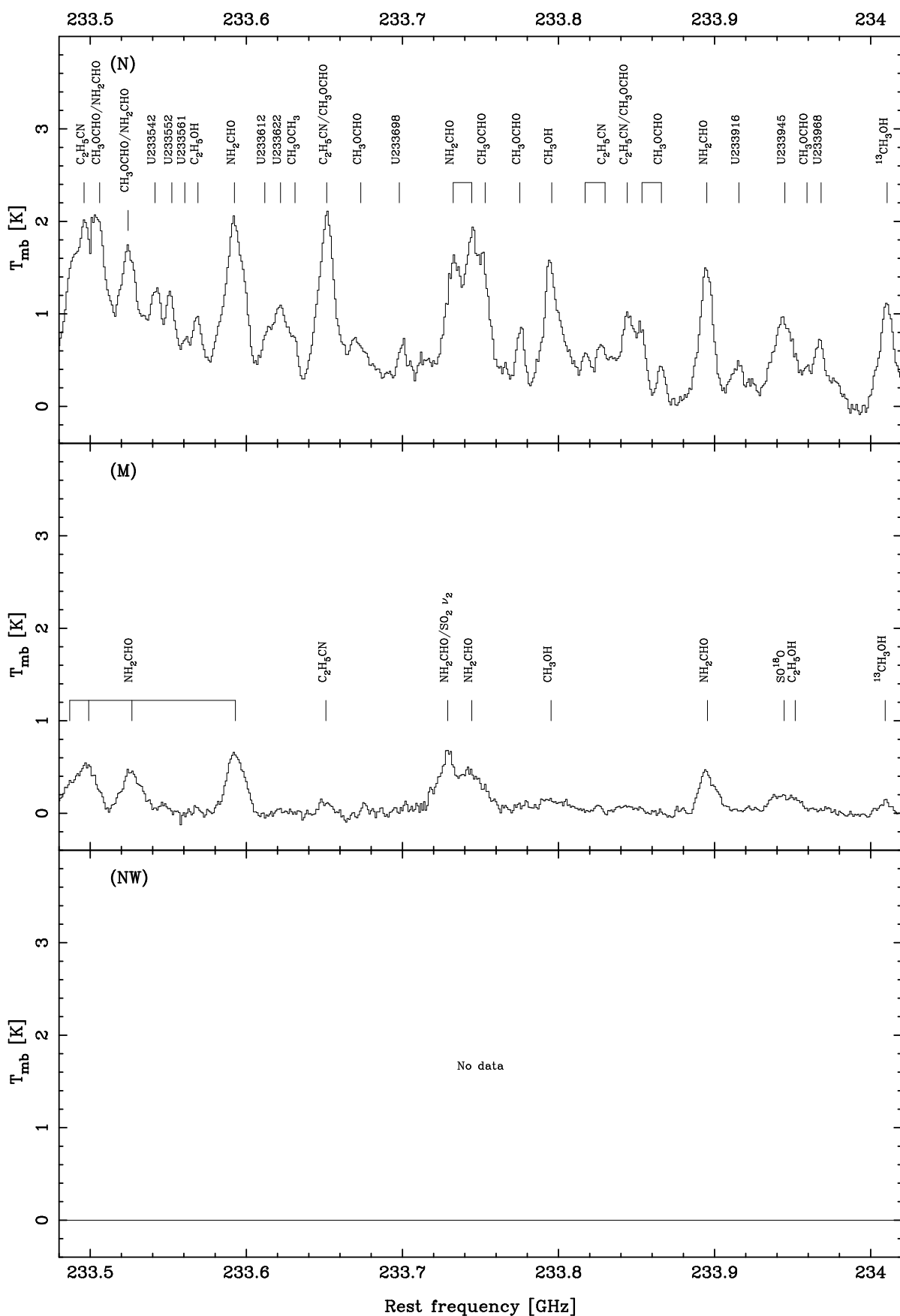


FIG. 1.—Continued

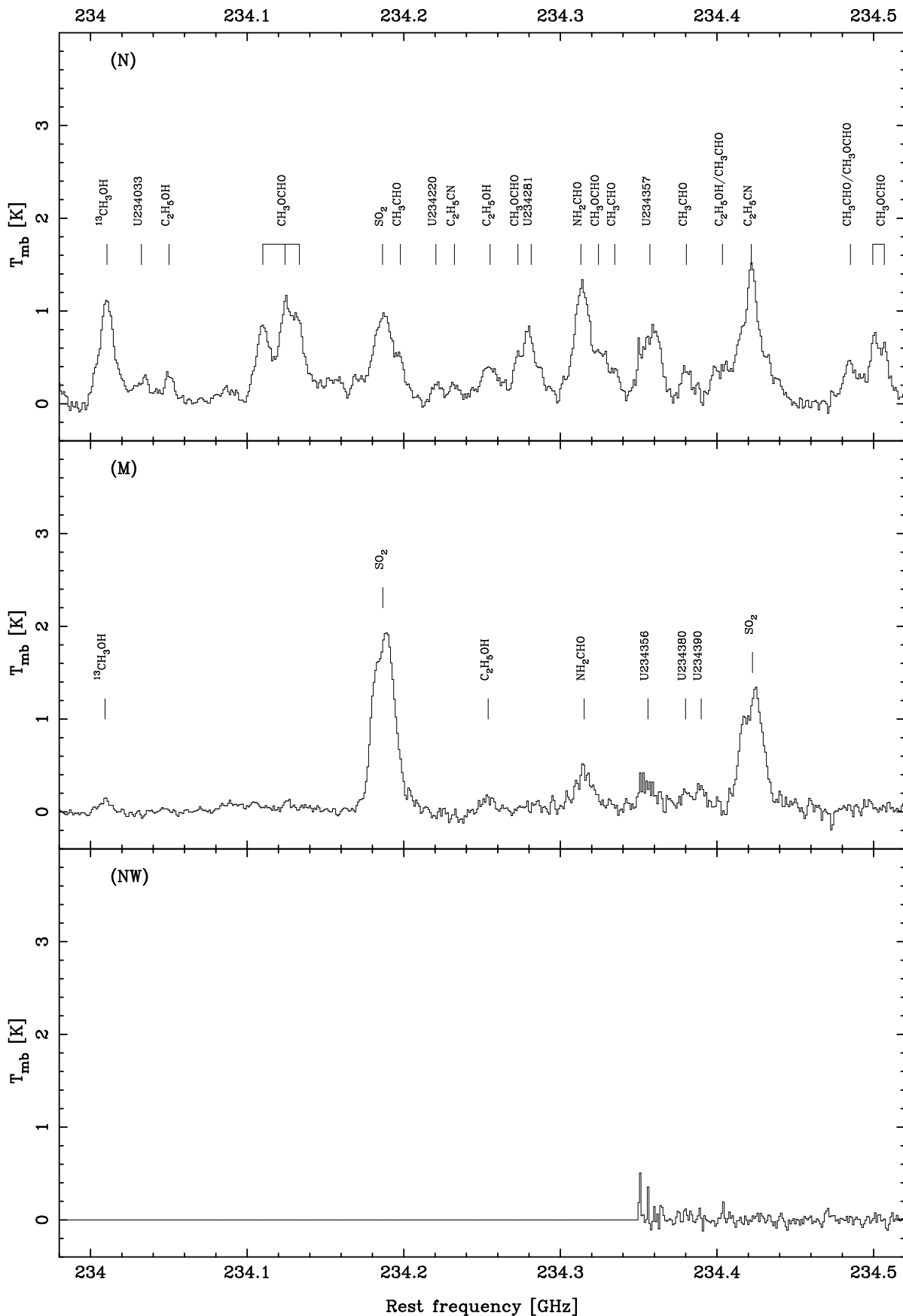


FIG. 1.—Continued

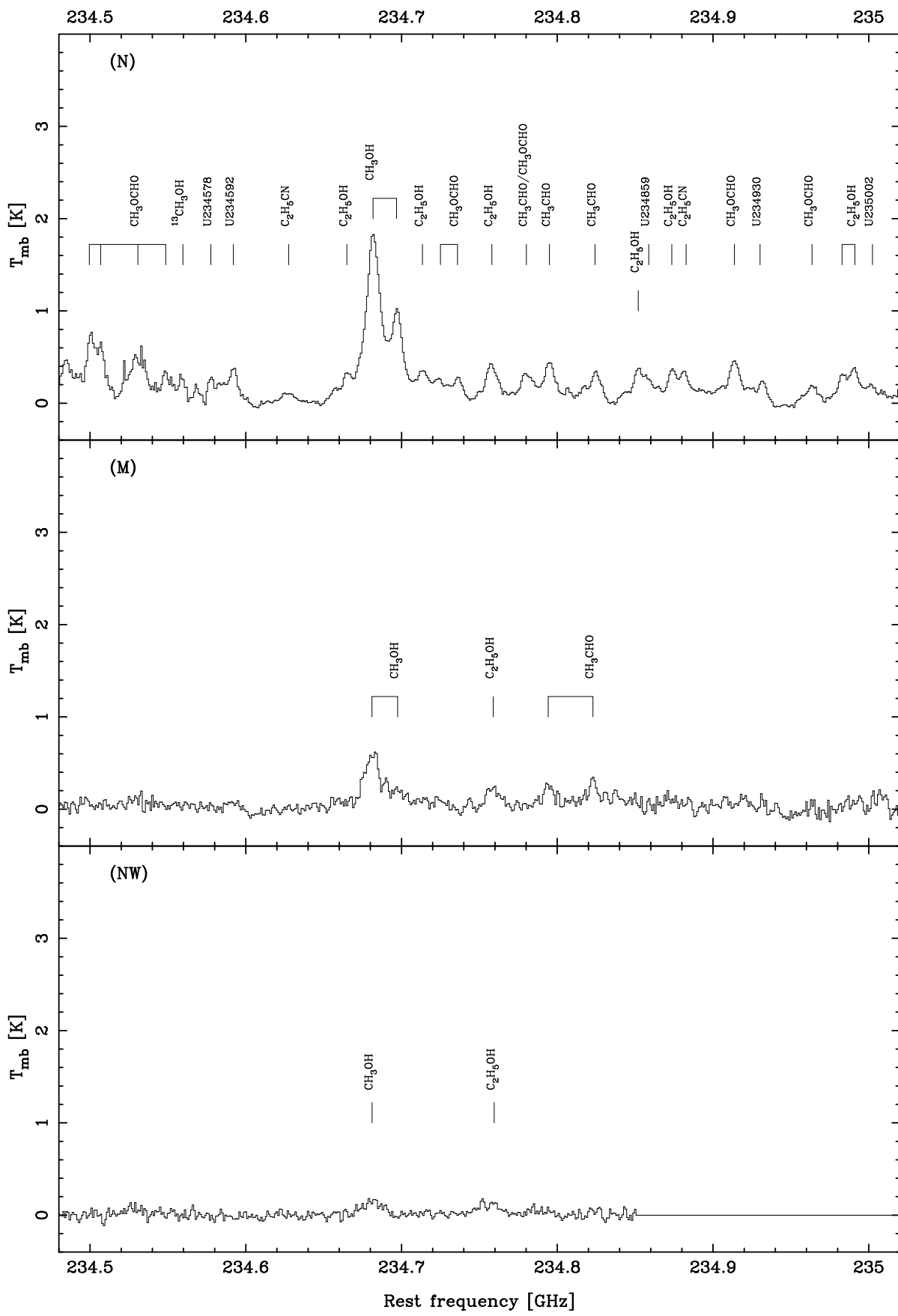


FIG. 1.—Continued

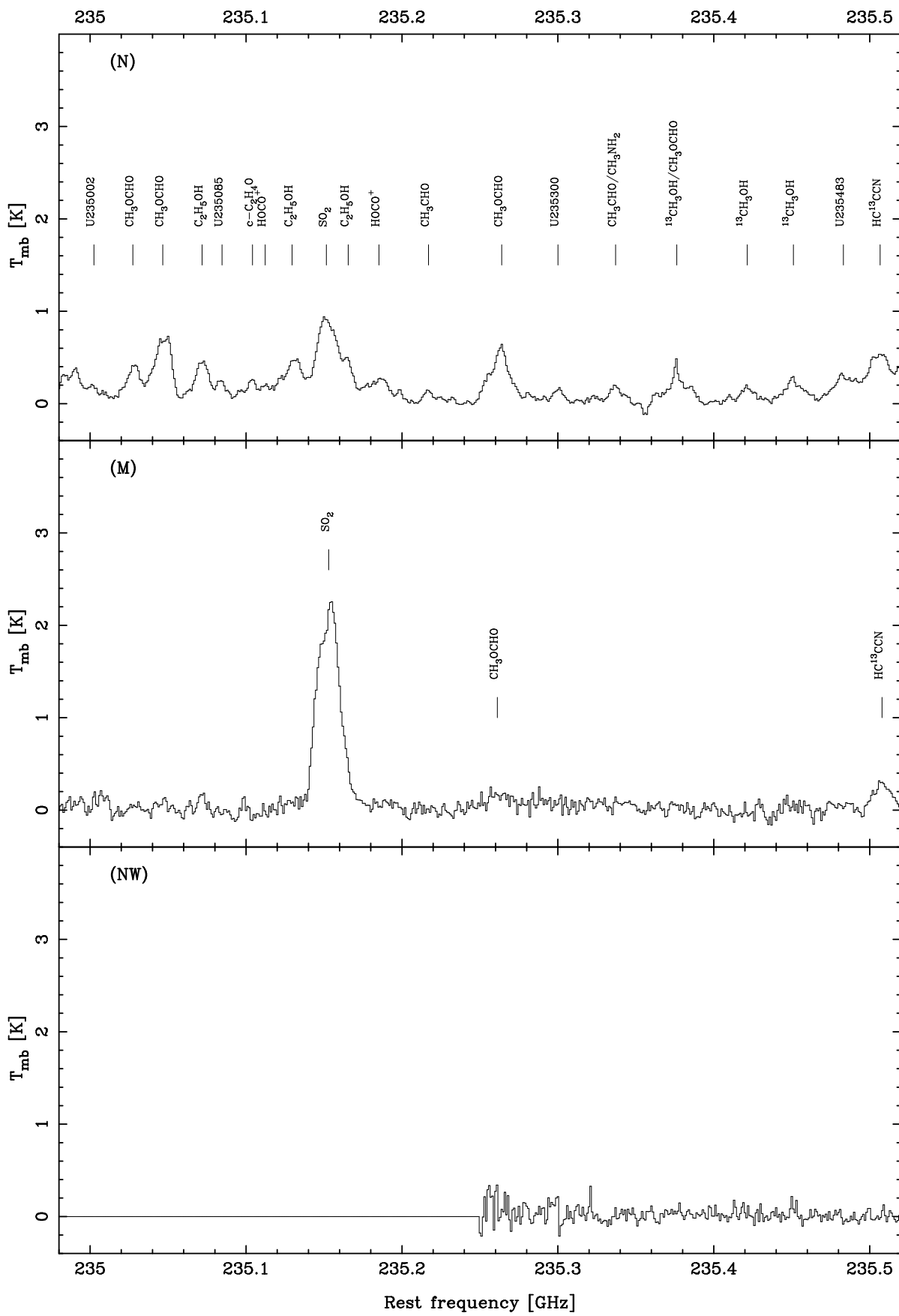


FIG. 1.—Continued

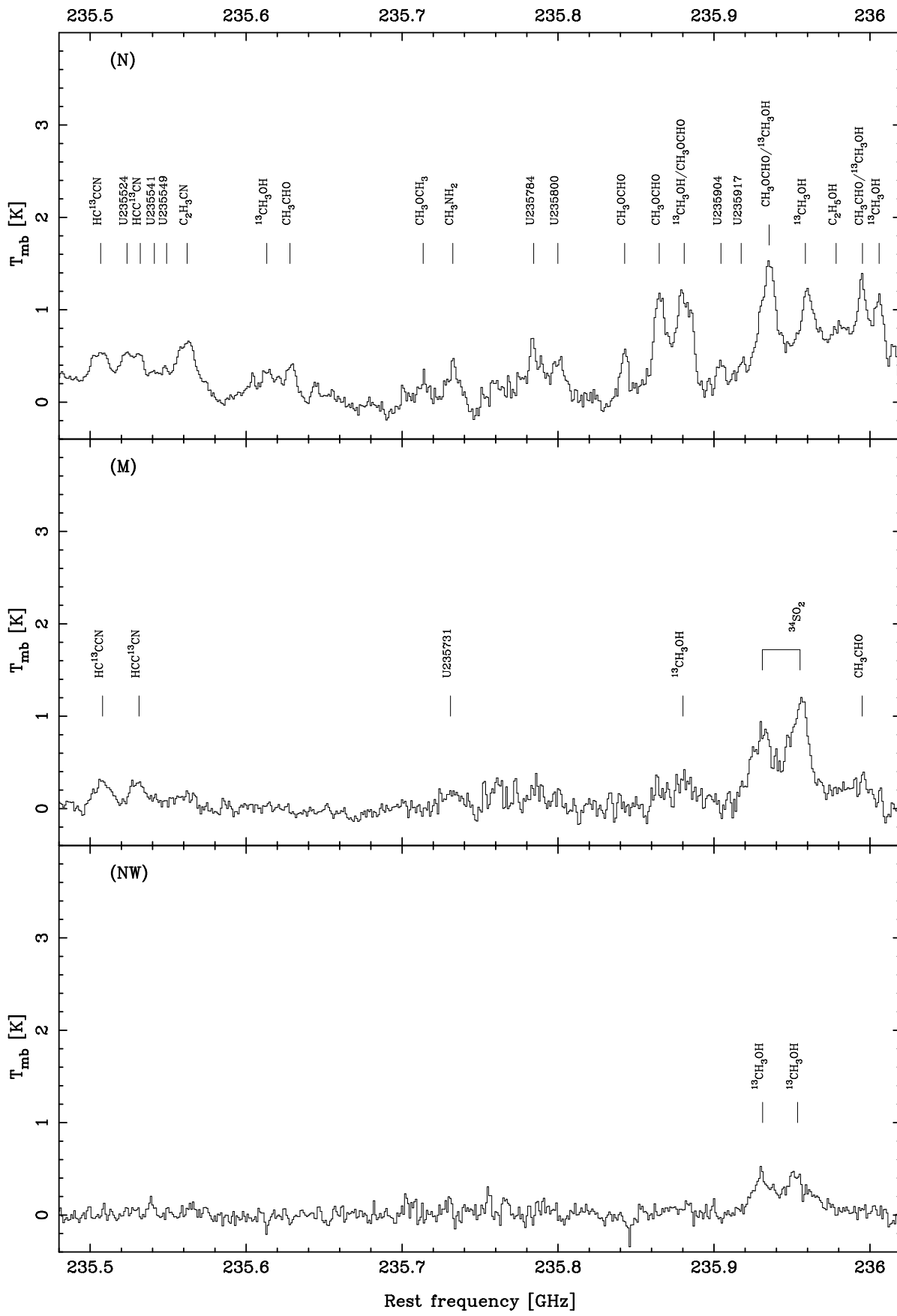


FIG. 1.—Continued

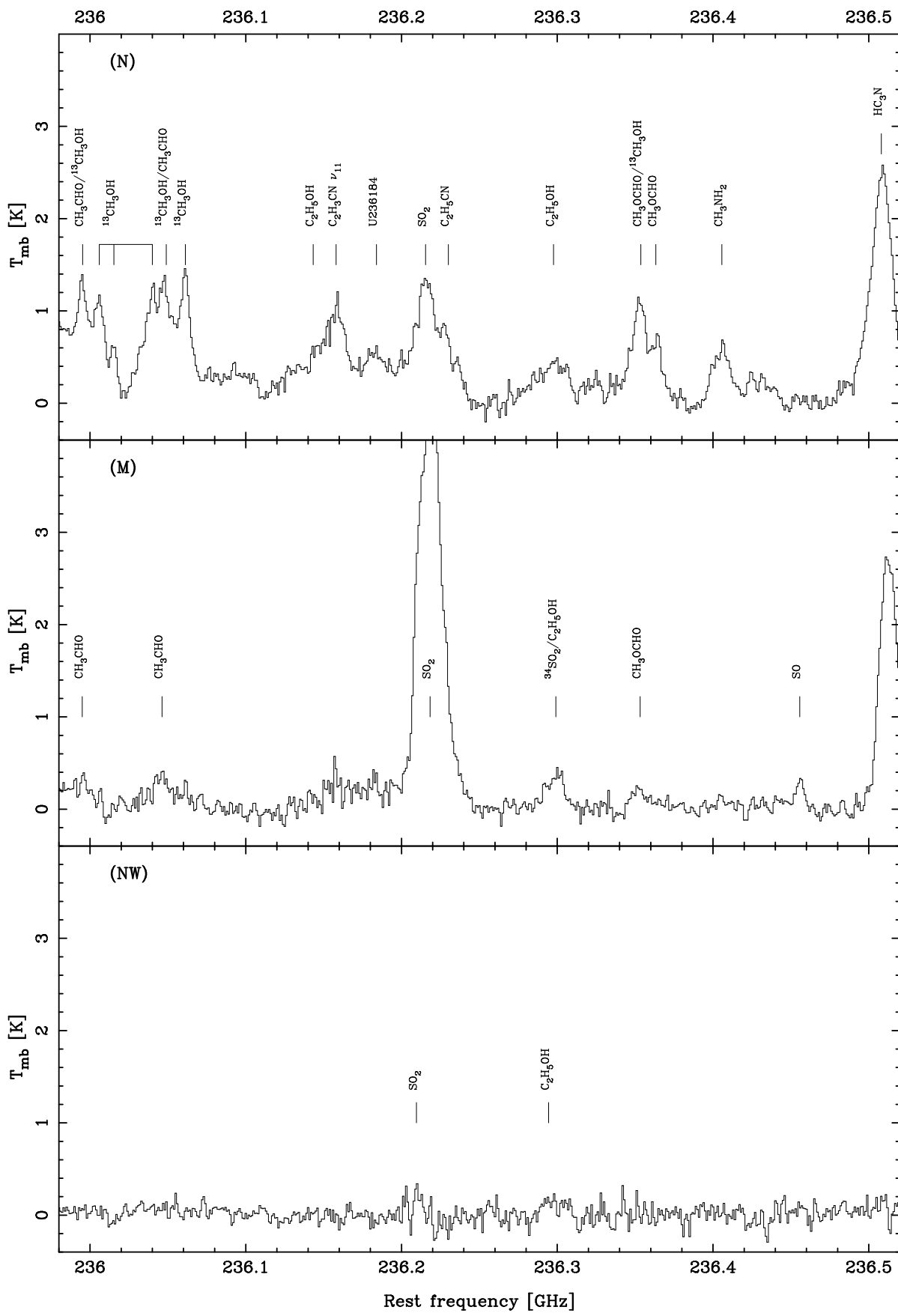


FIG. 1.—Continued

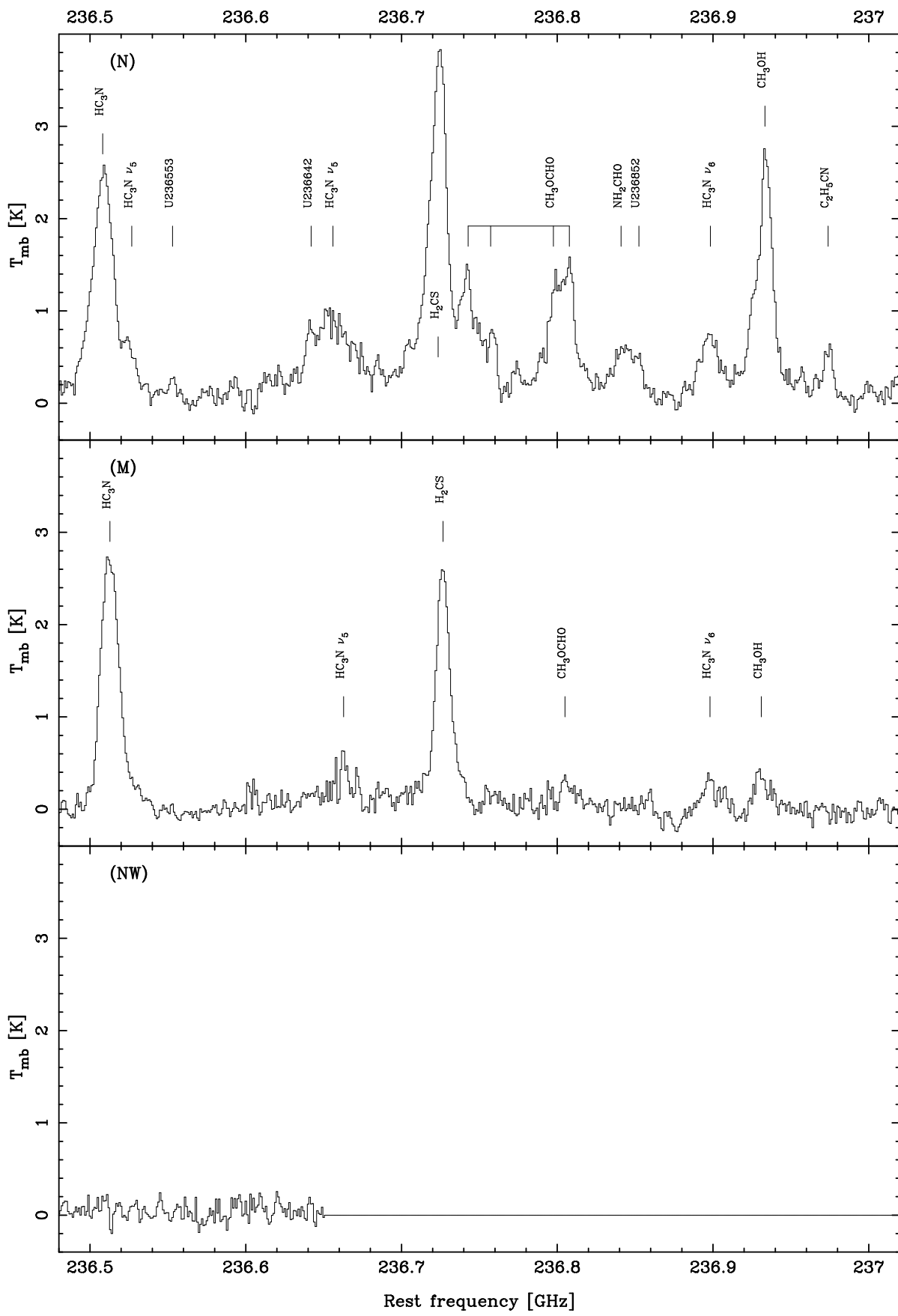


FIG. 1.—Continued

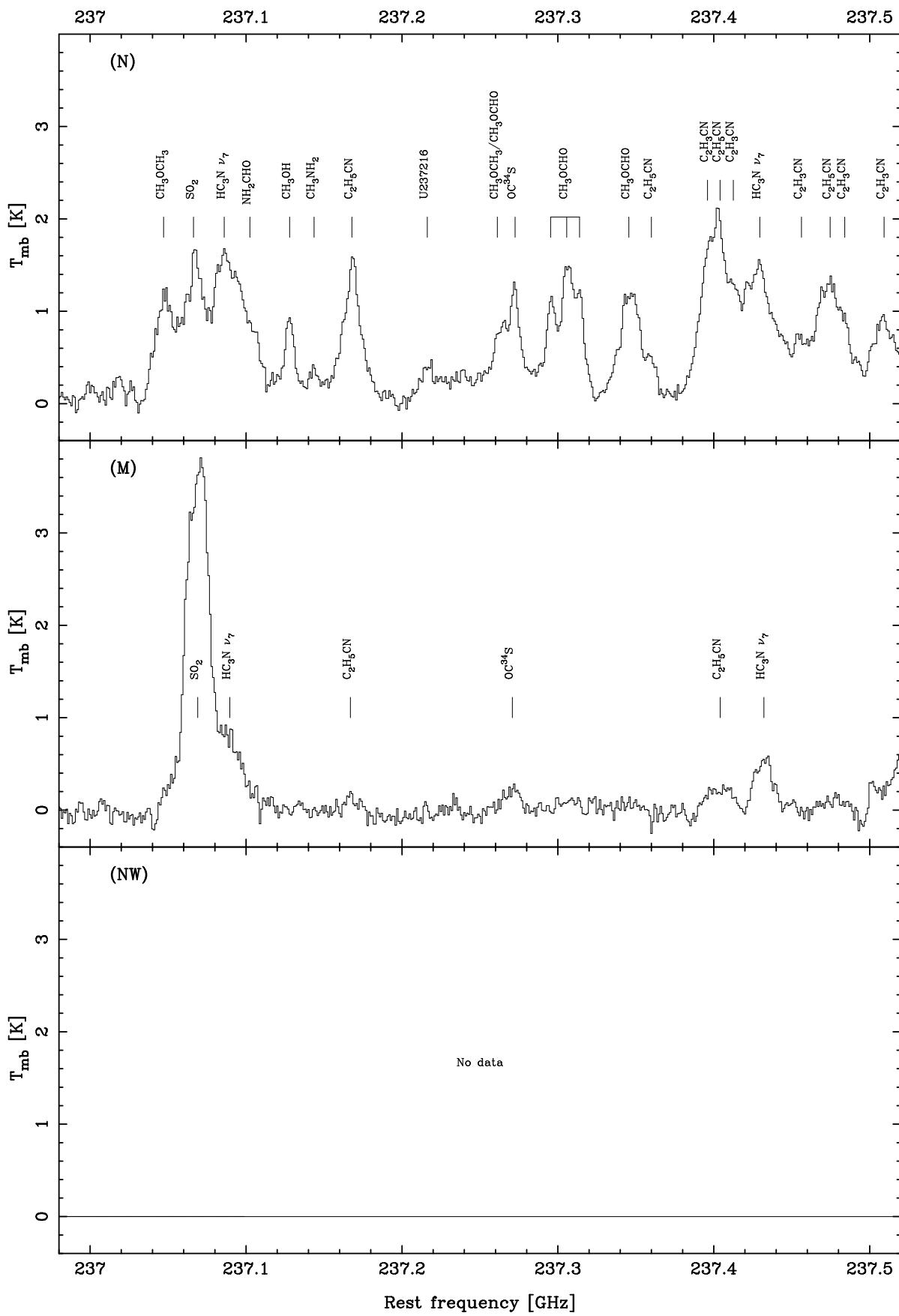


FIG. 1.—Continued

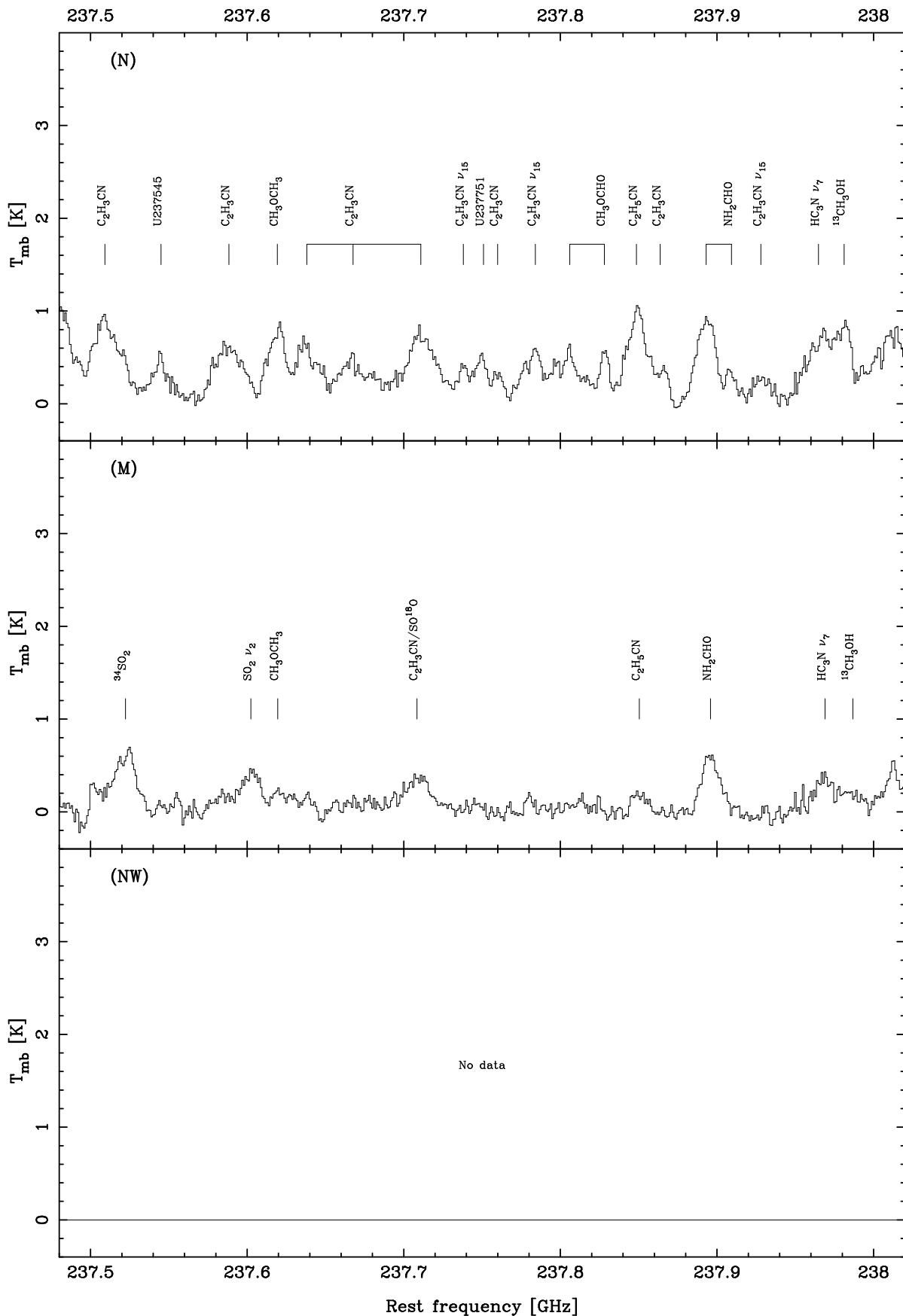


FIG. 1.—Continued

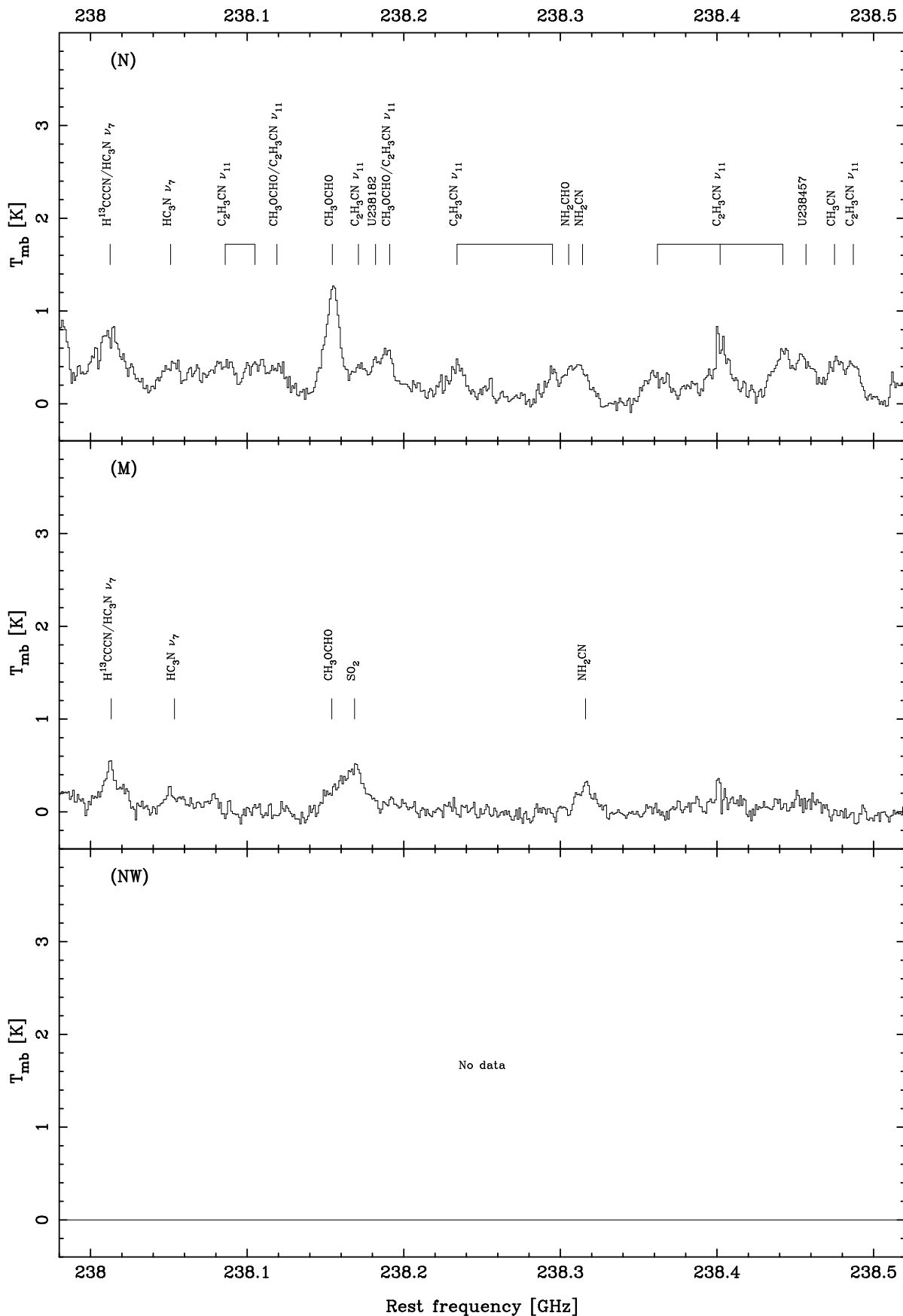


FIG. 1.—Continued

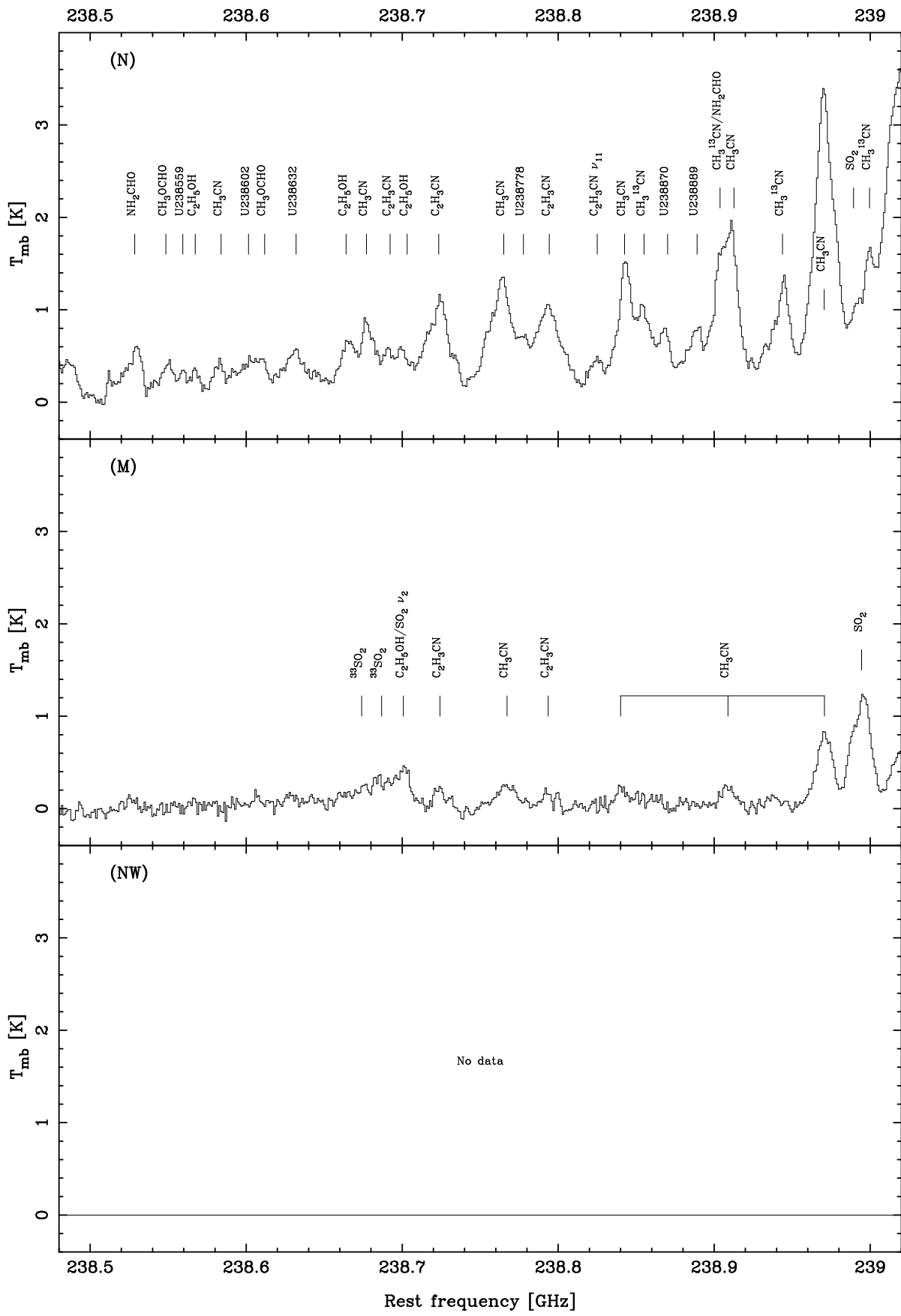


FIG. 1.—*Continued*

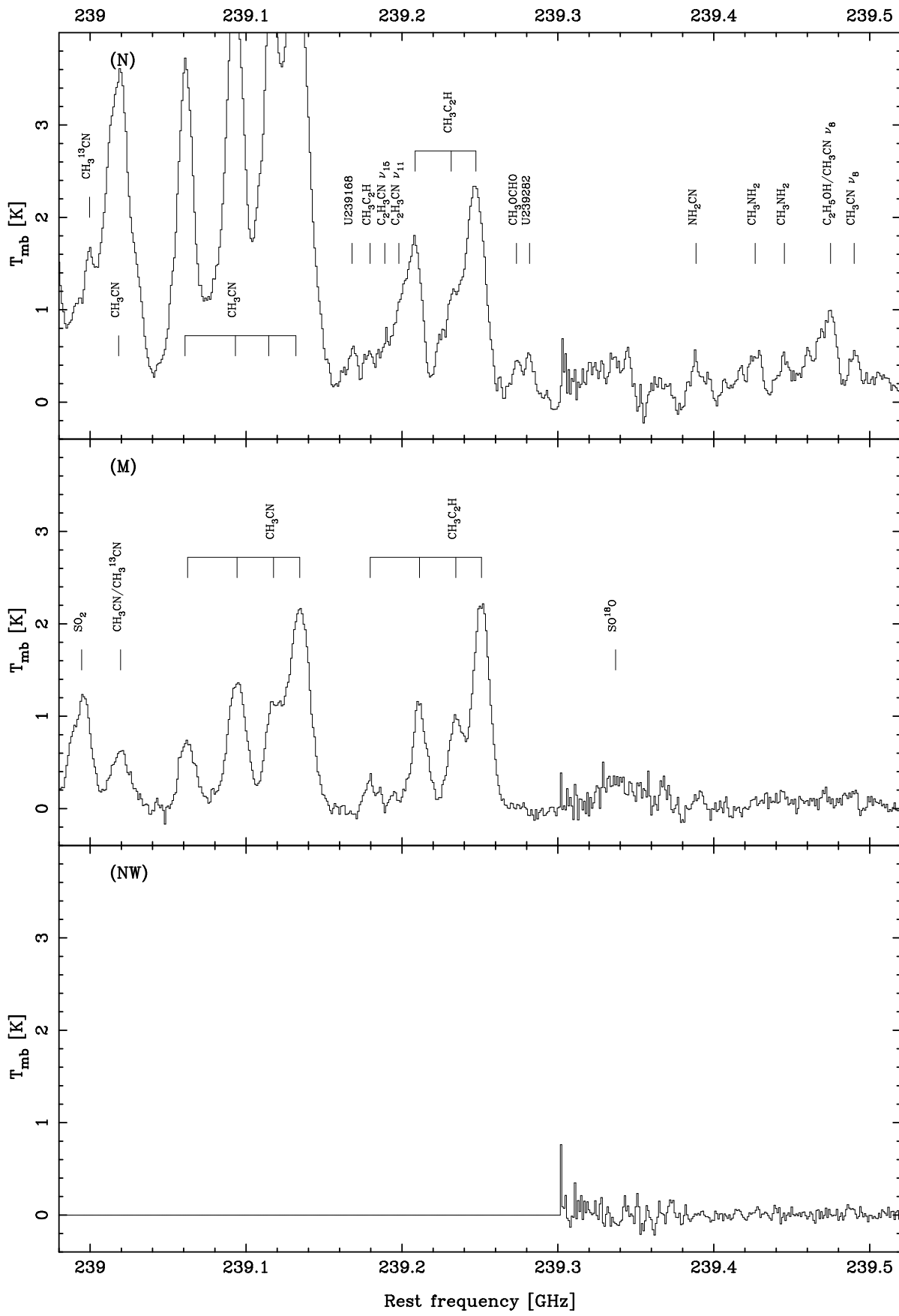


FIG. 1.—Continued

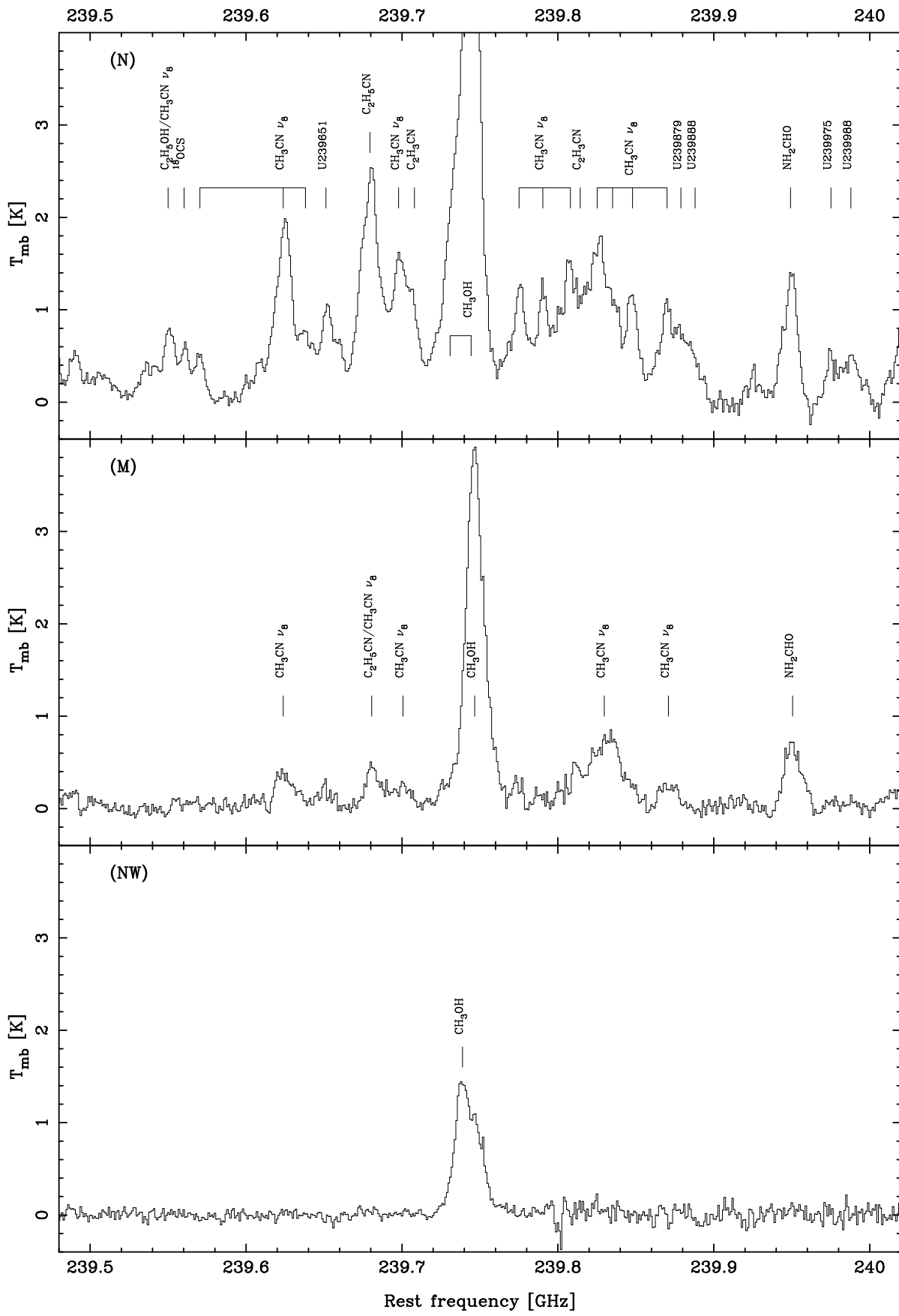


FIG. 1.—Continued

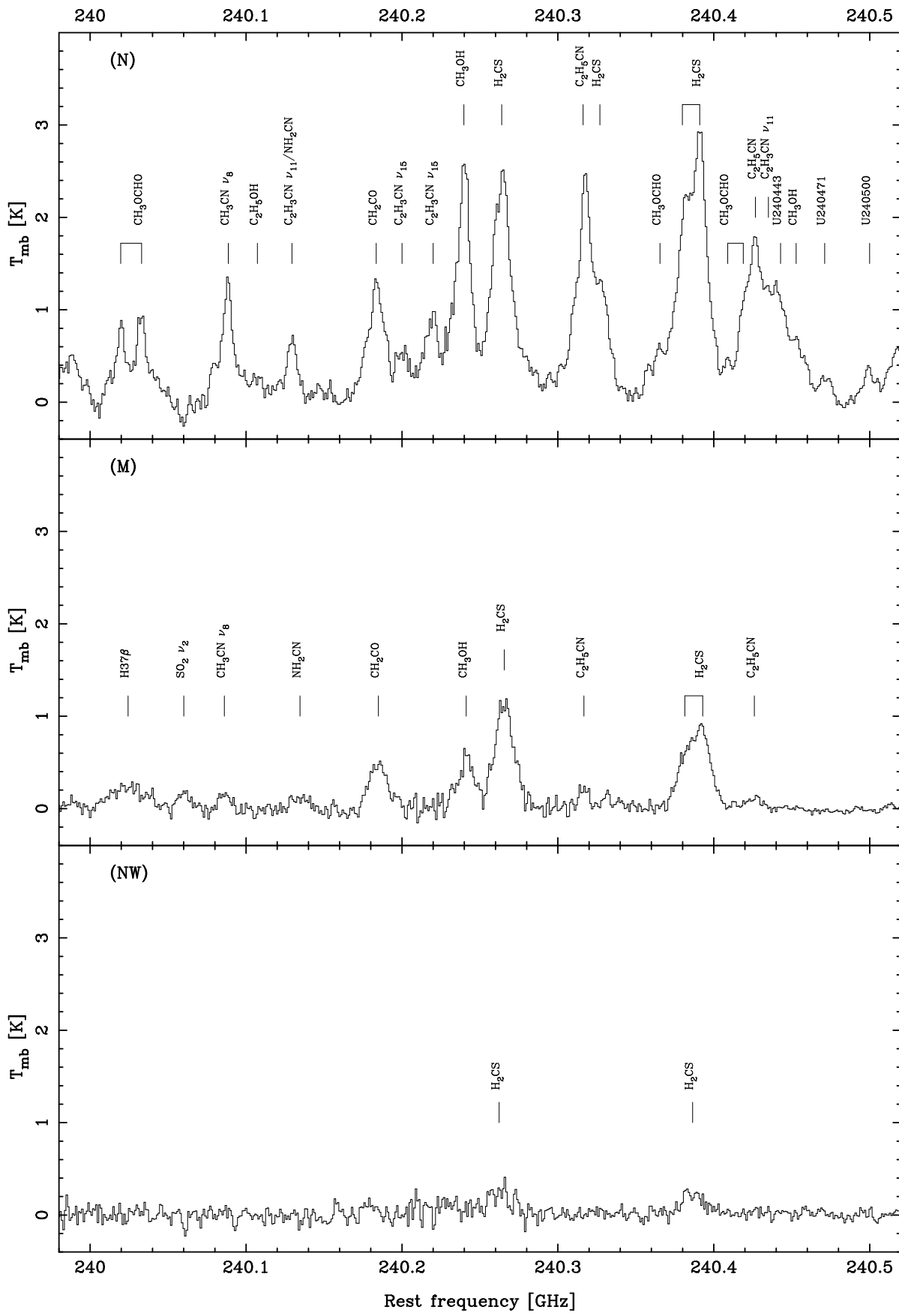


FIG. 1.—Continued

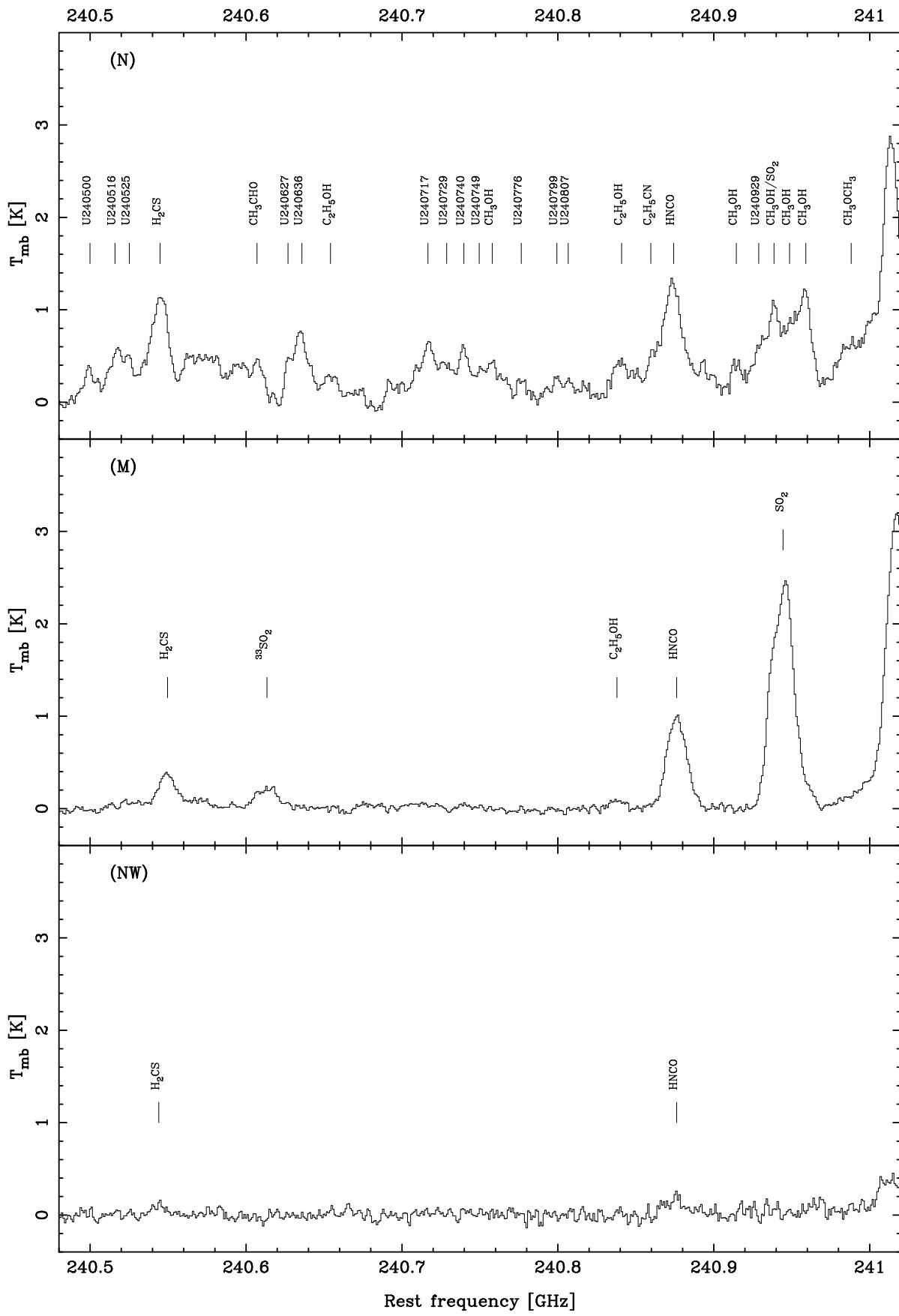


FIG. 1.—Continued

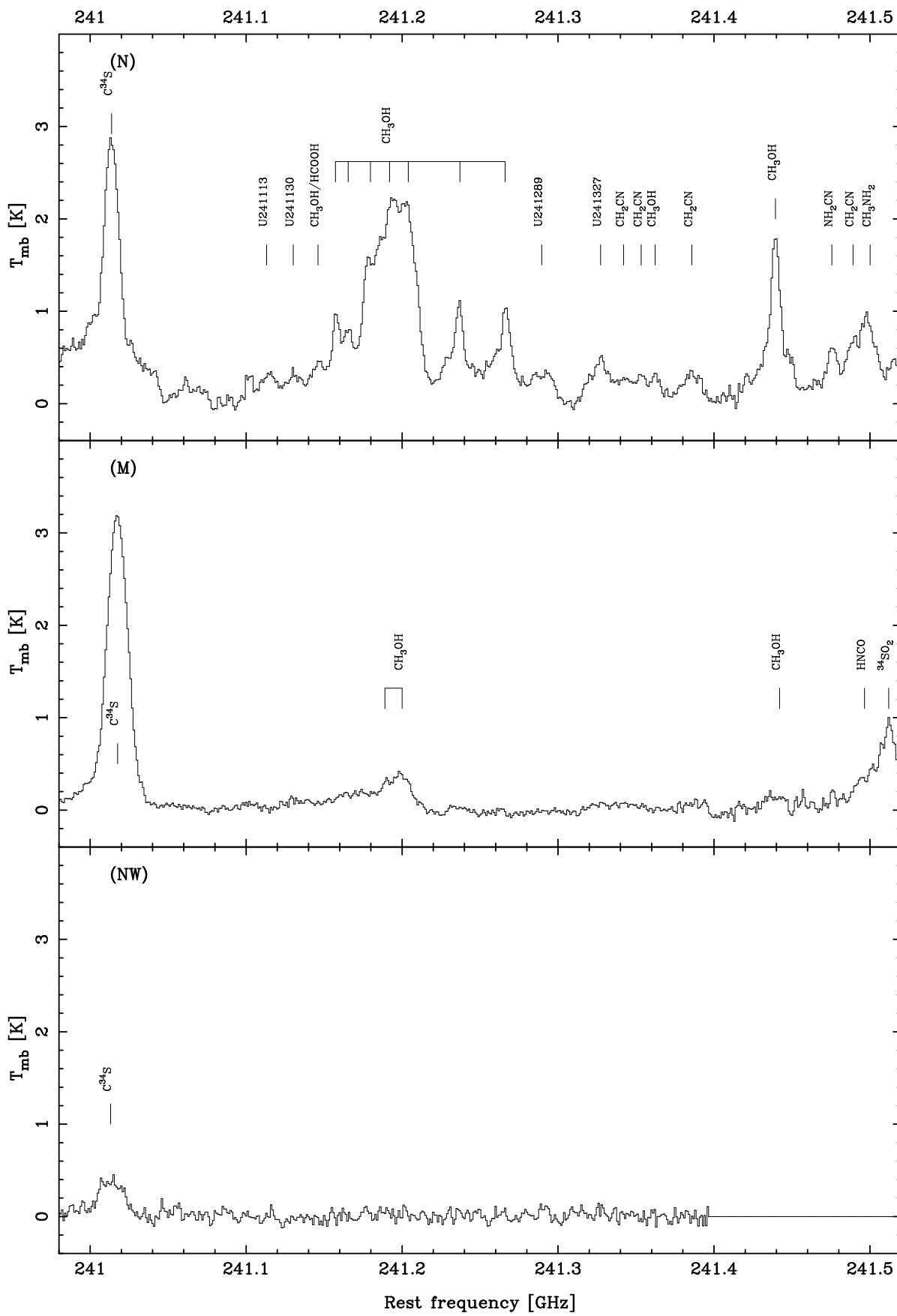


FIG. 1.—Continued

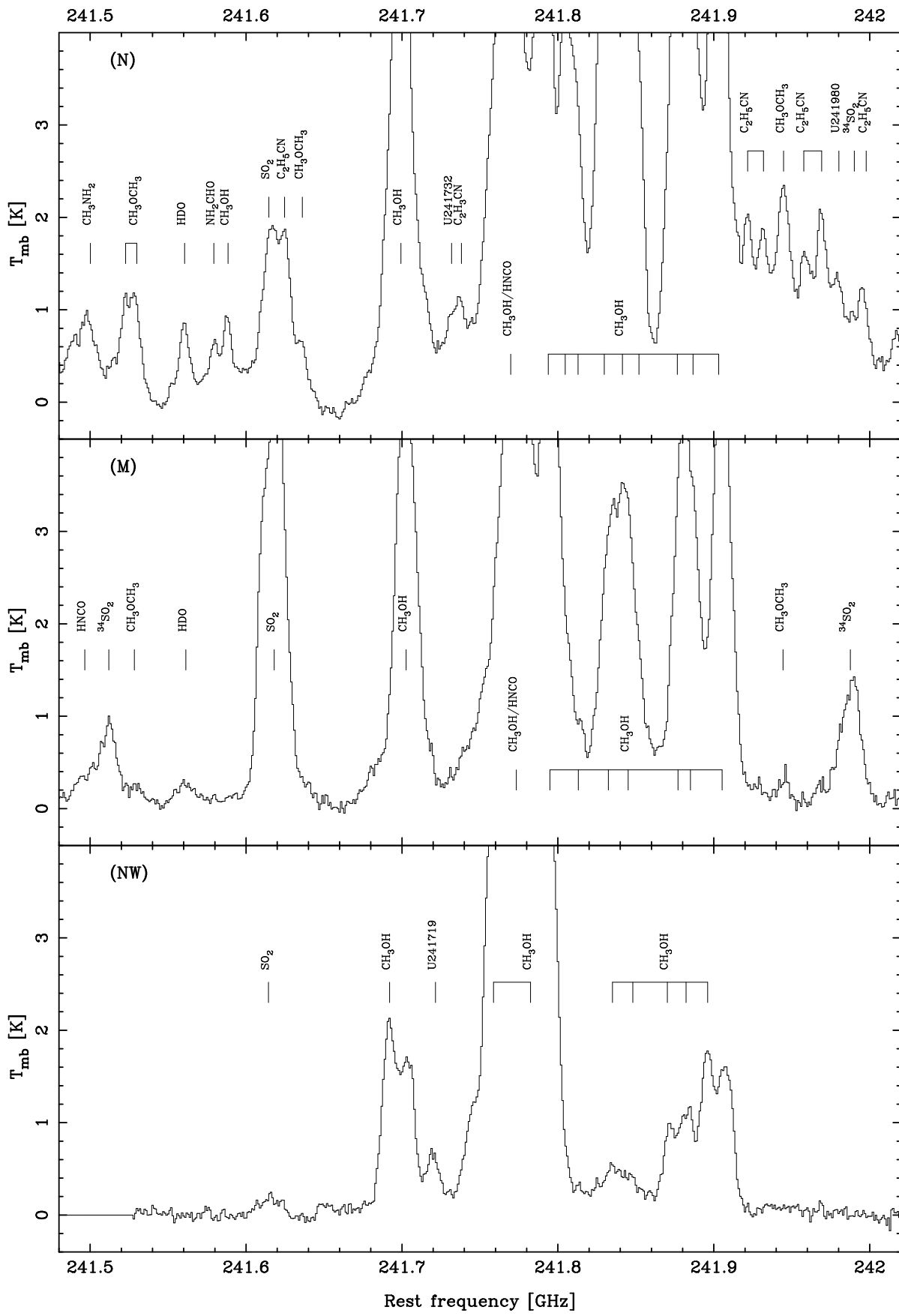


FIG. 1.—Continued

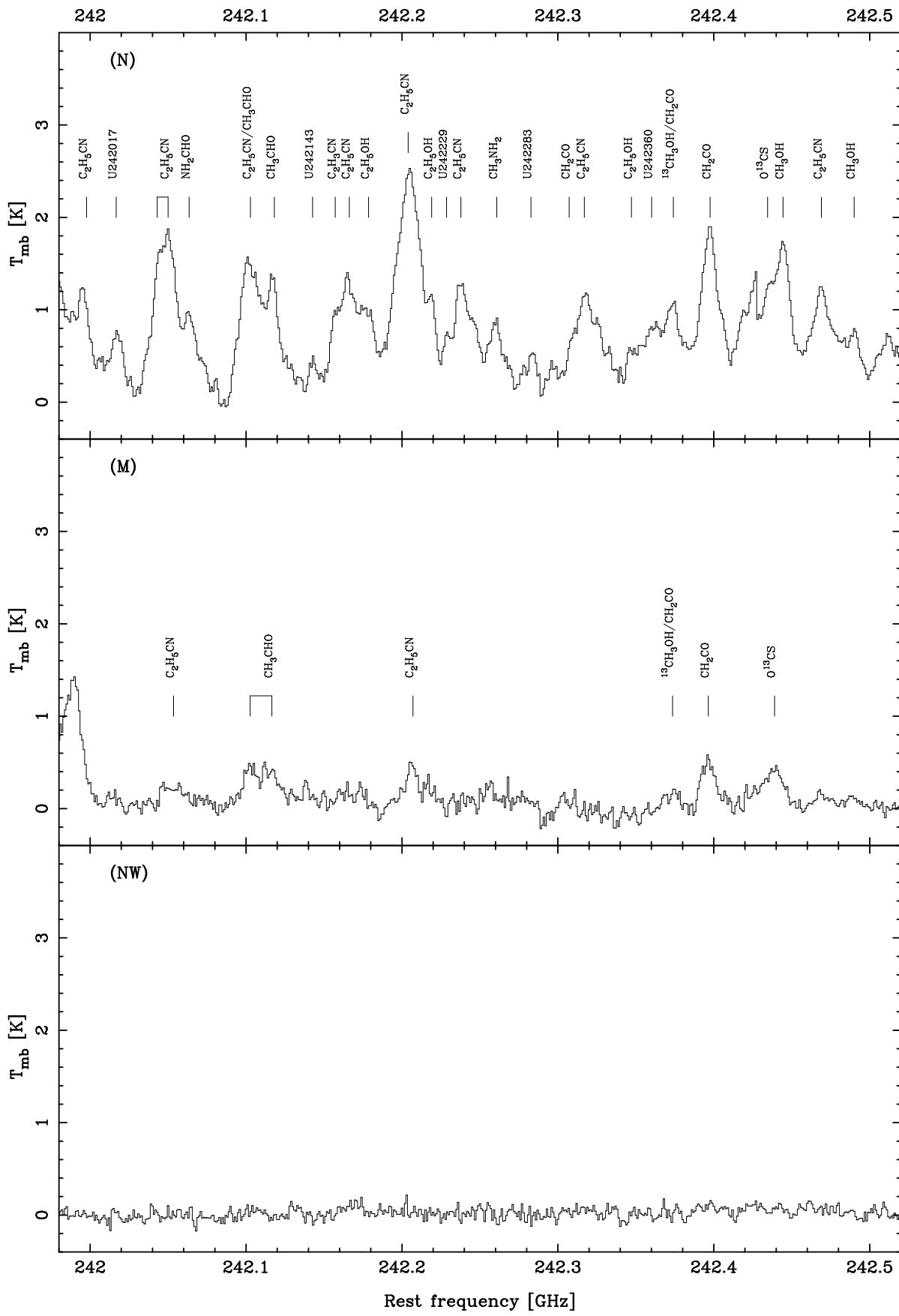


FIG. 1.—Continued

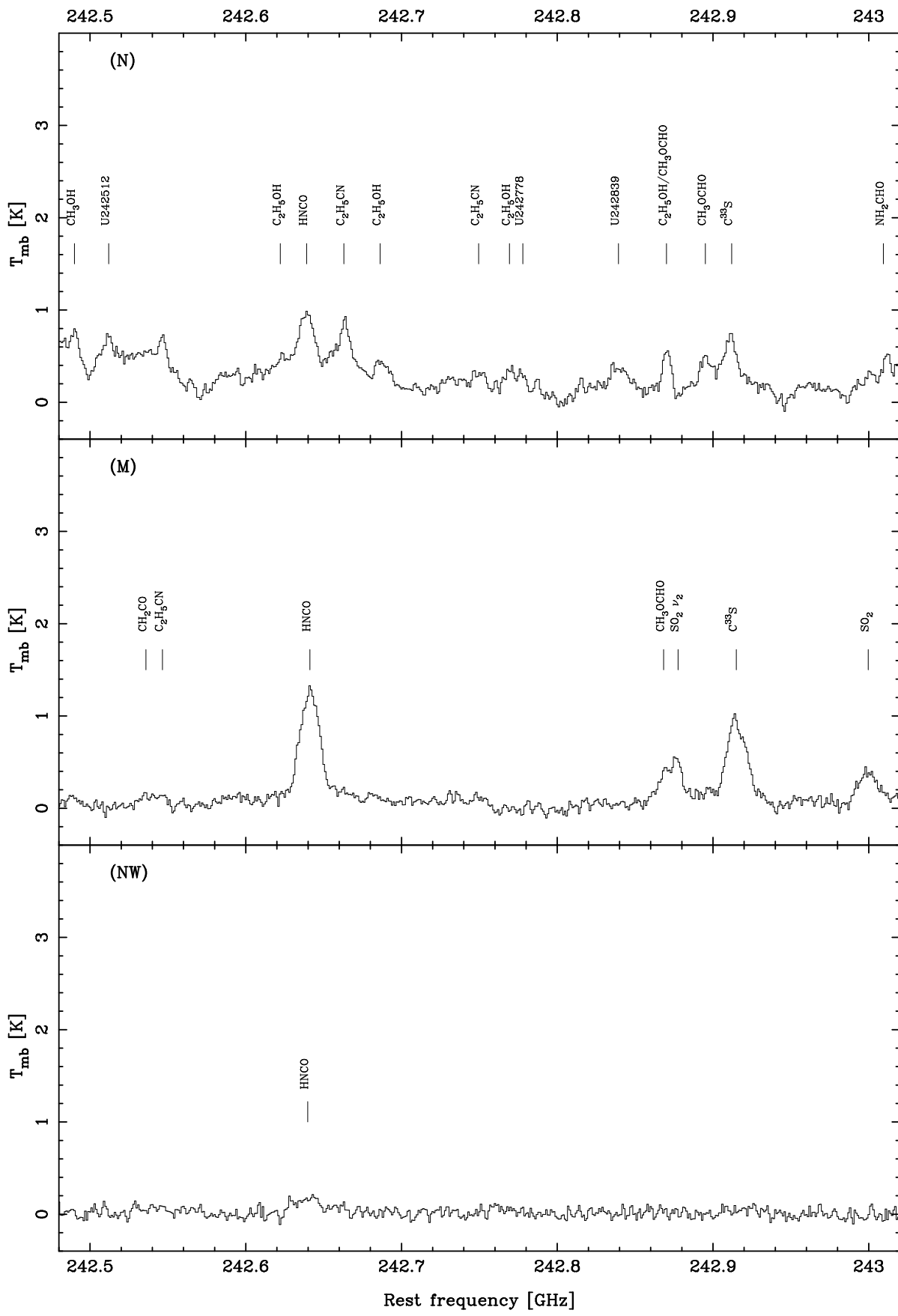


FIG. 1.—Continued

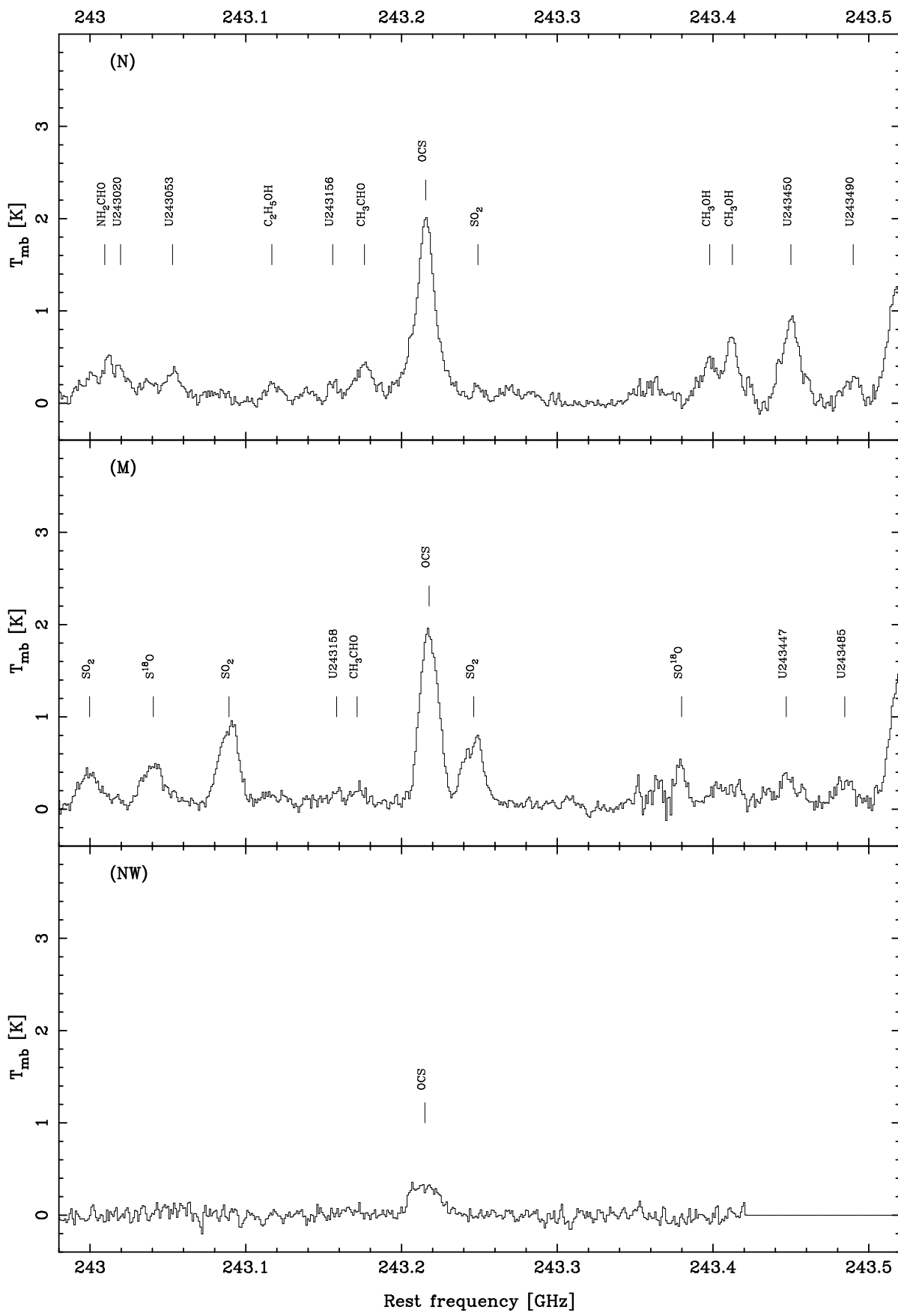


FIG. 1.—Continued

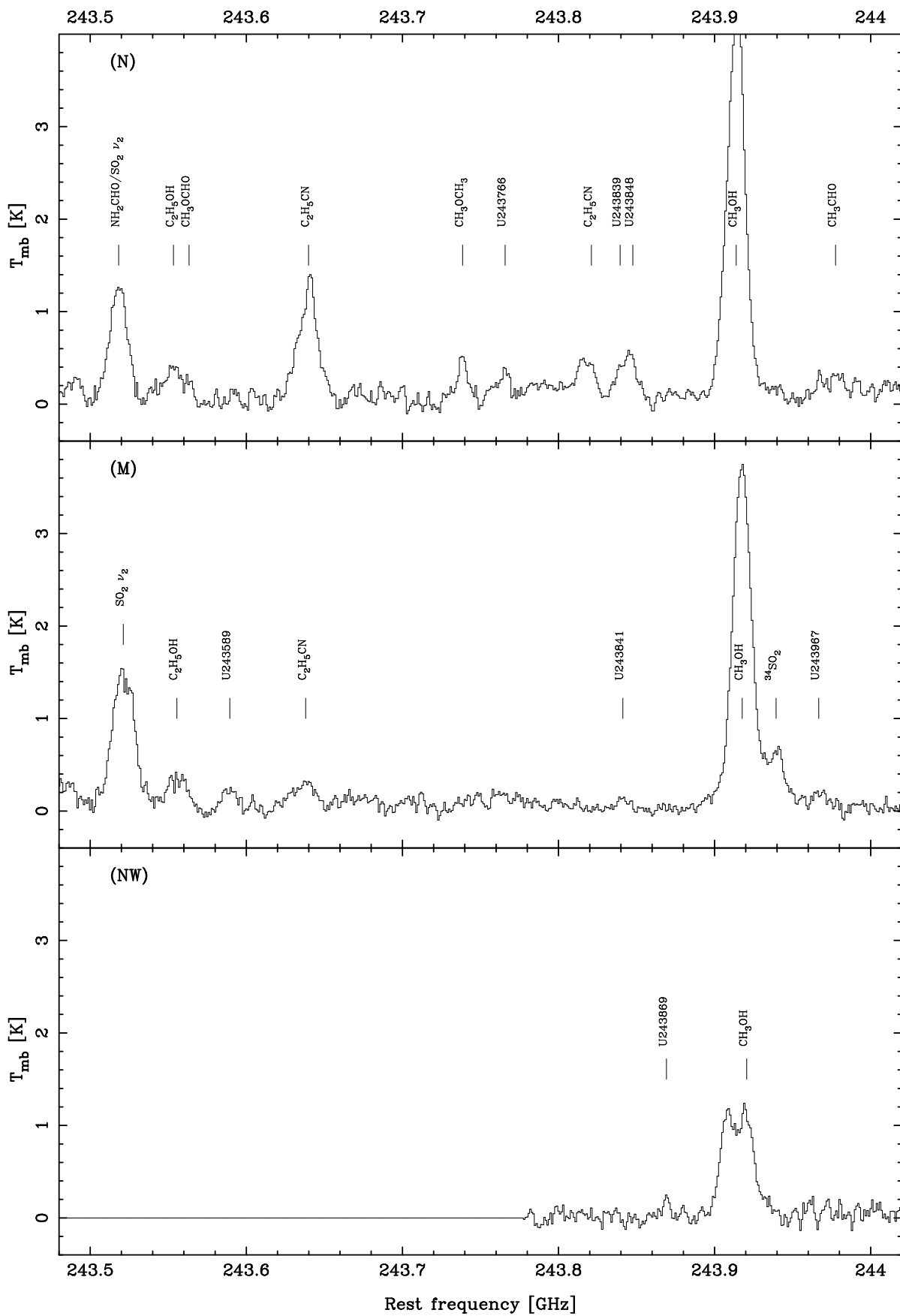


FIG. 1.—Continued

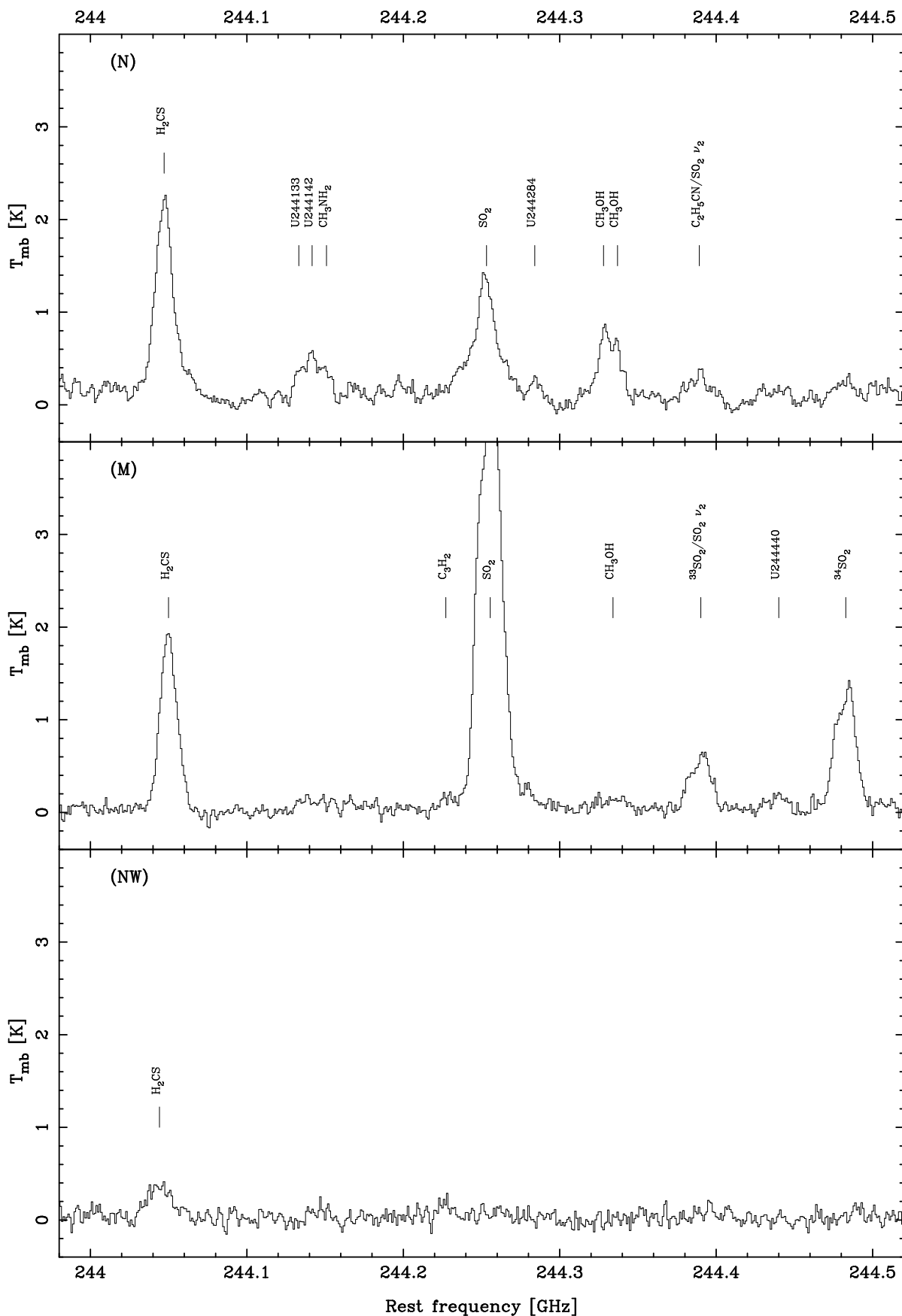


FIG. 1.—Continued

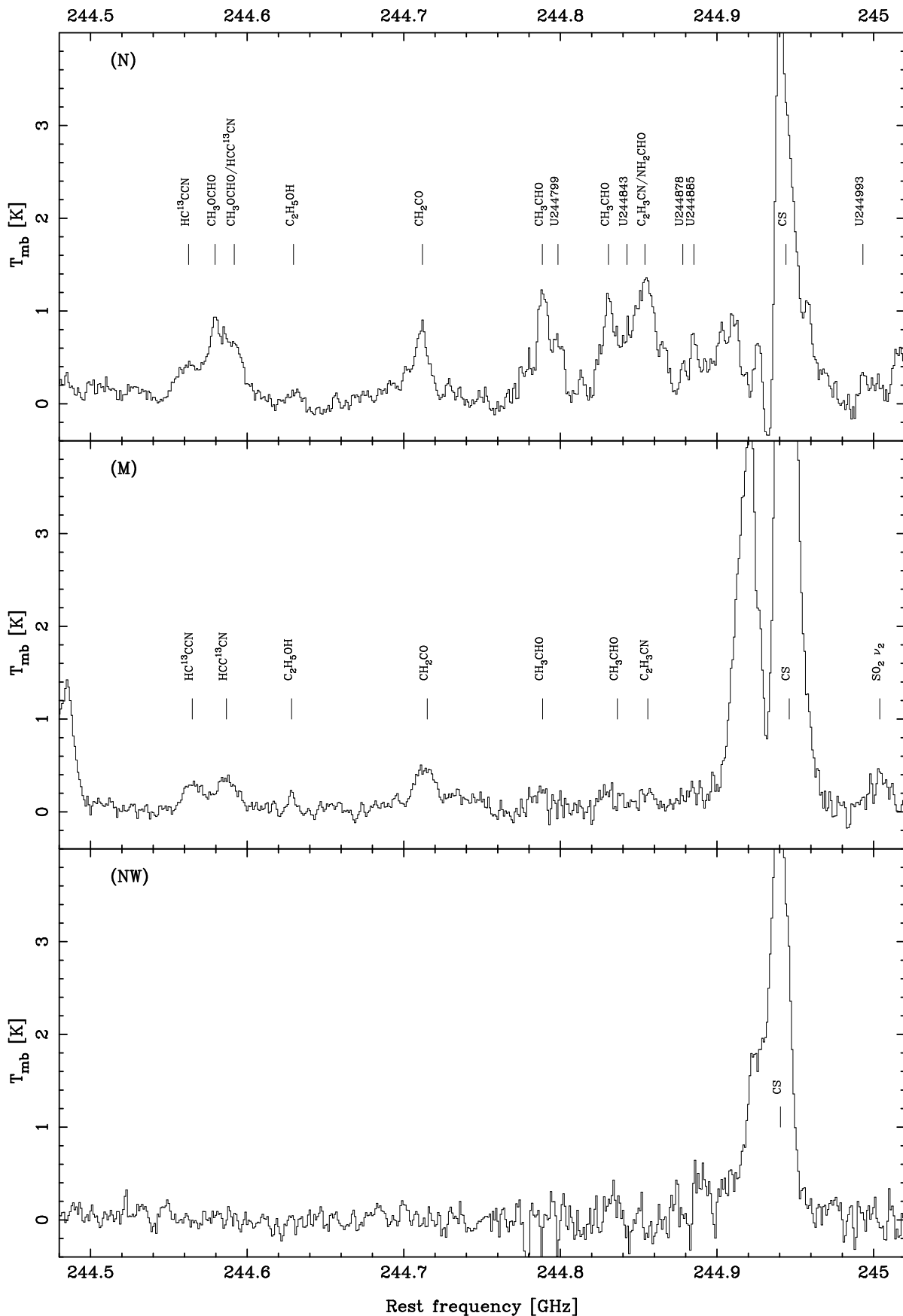


FIG. 1.—Continued

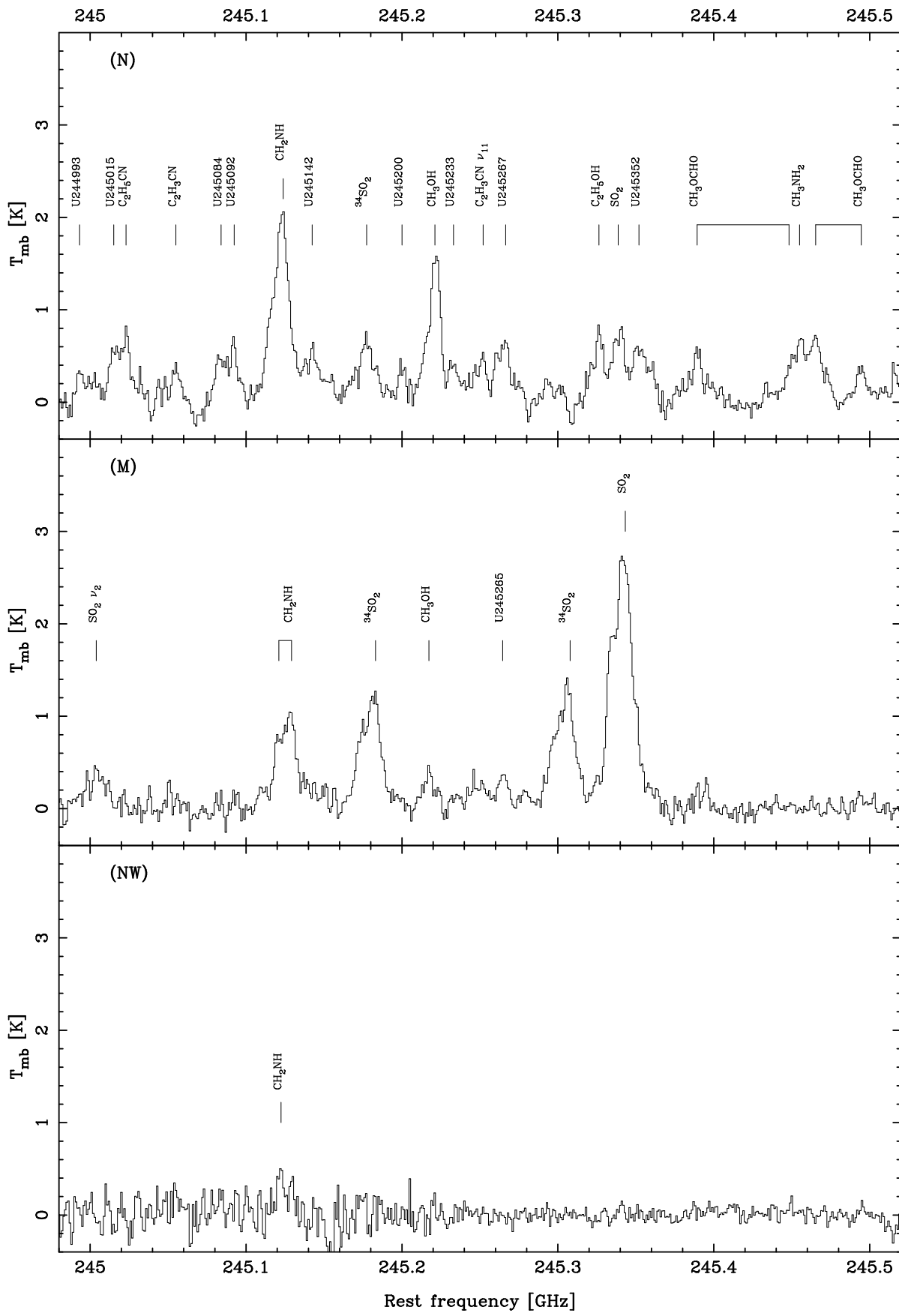


FIG. 1.—Continued

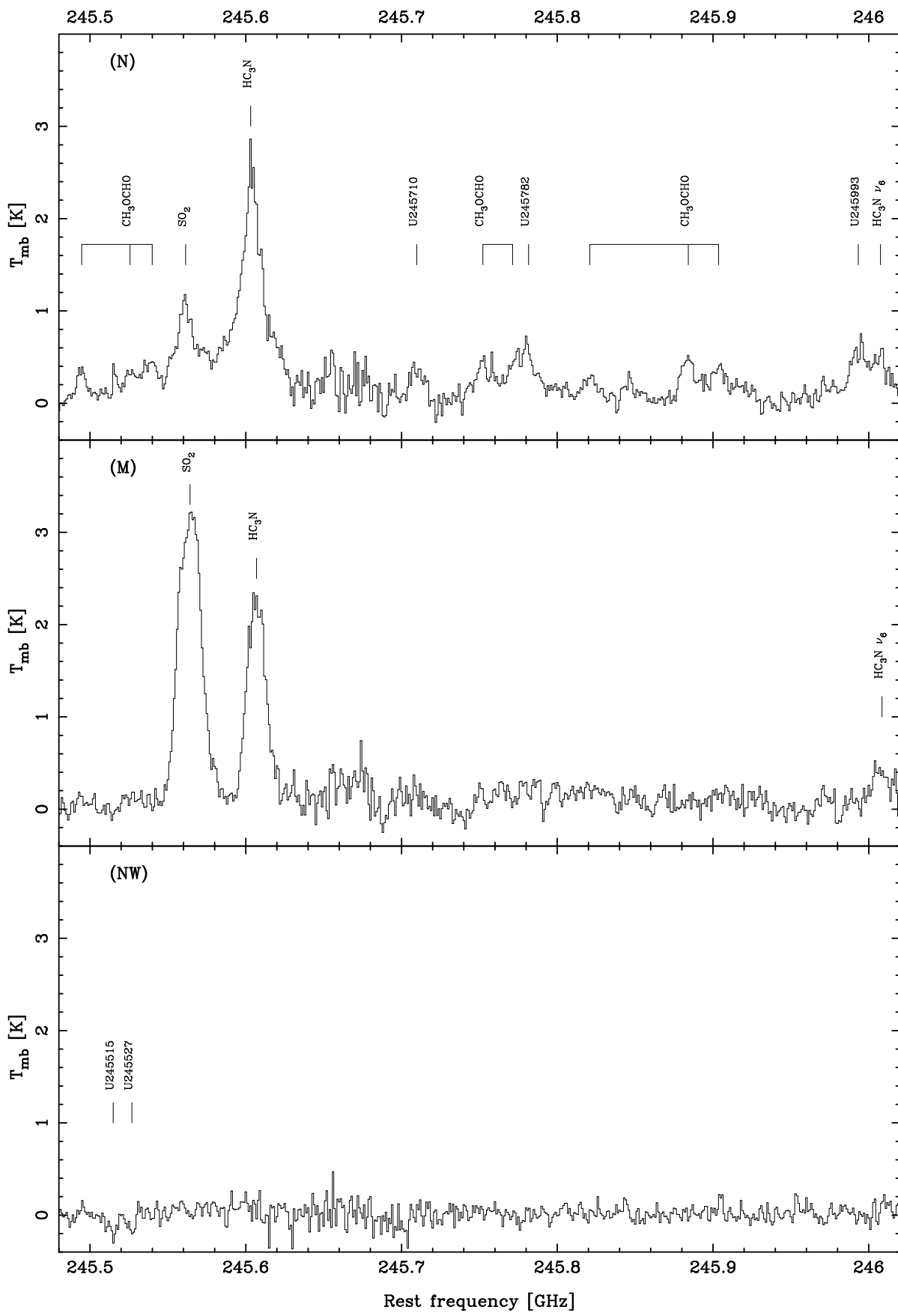


FIG. 1.—Continued

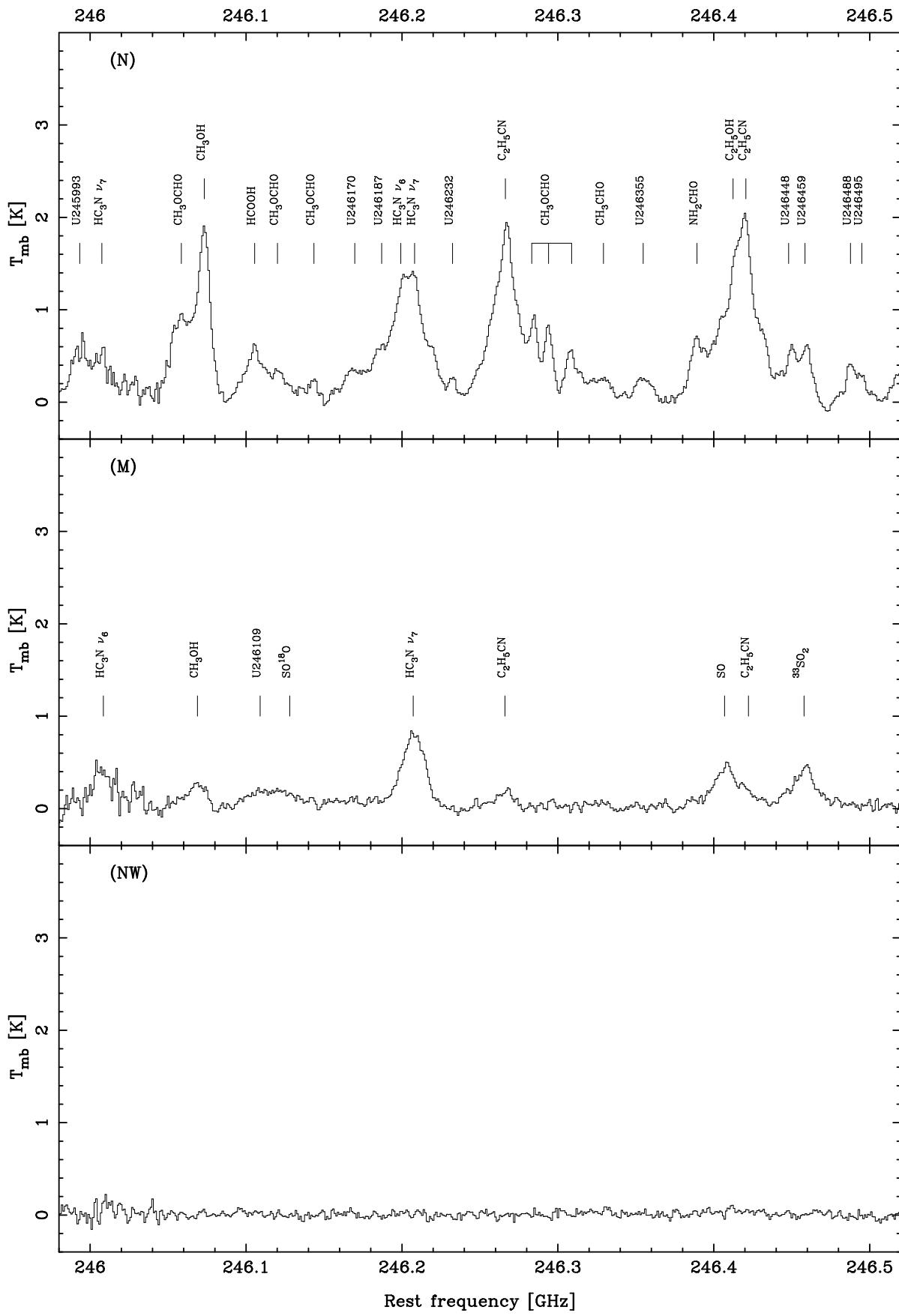


FIG. 1.—Continued

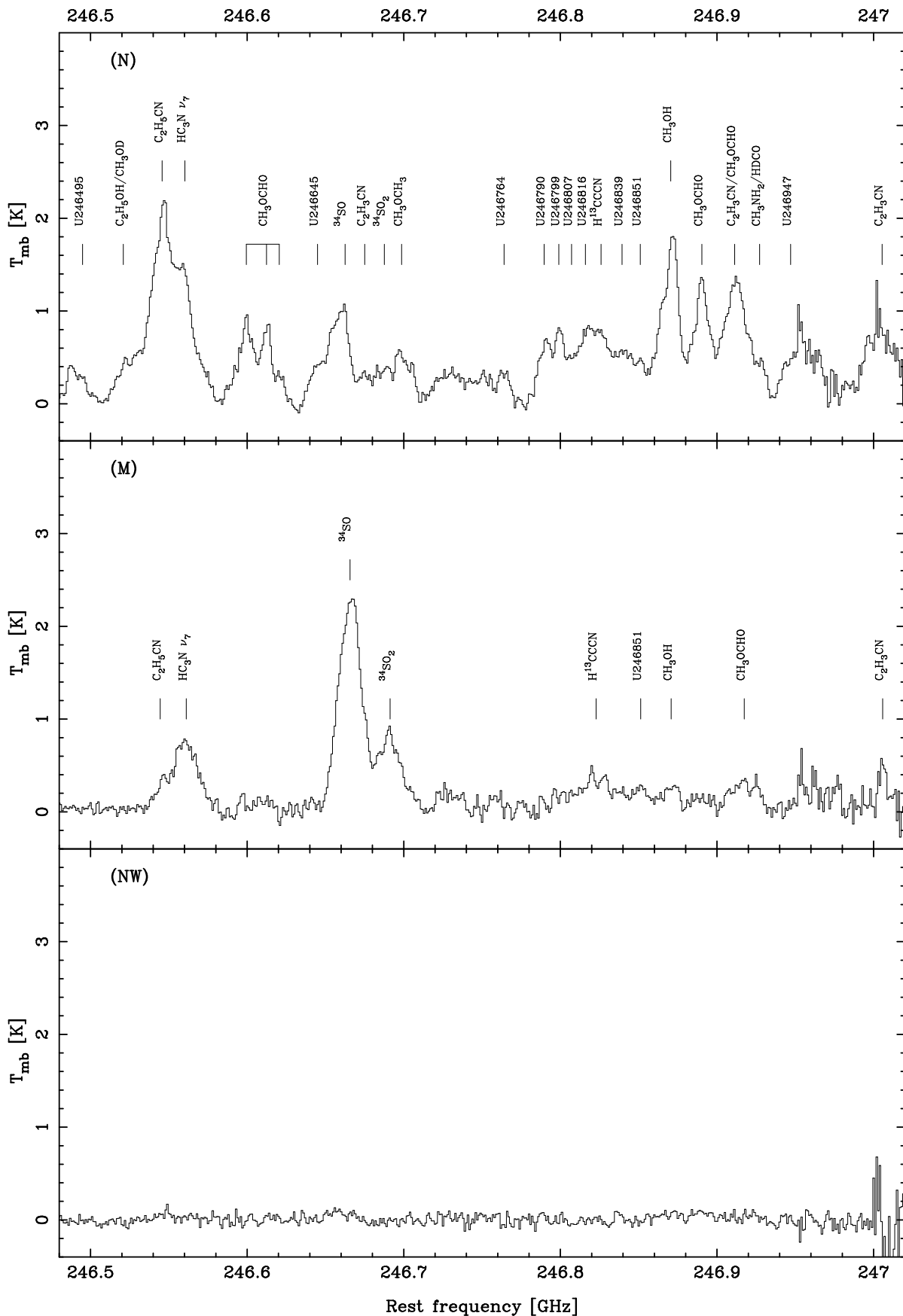


FIG. 1.—Continued

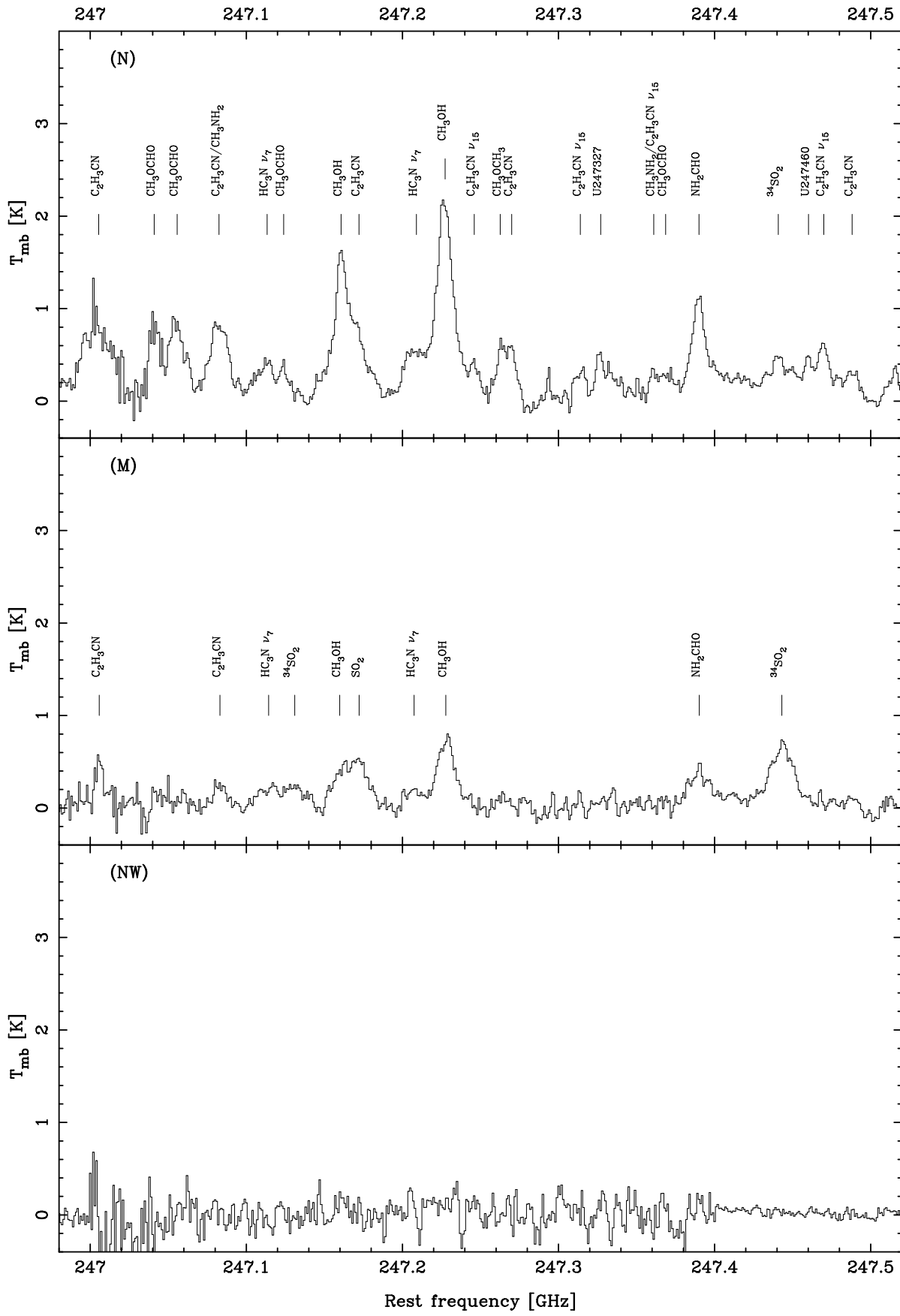


FIG. 1.—Continued

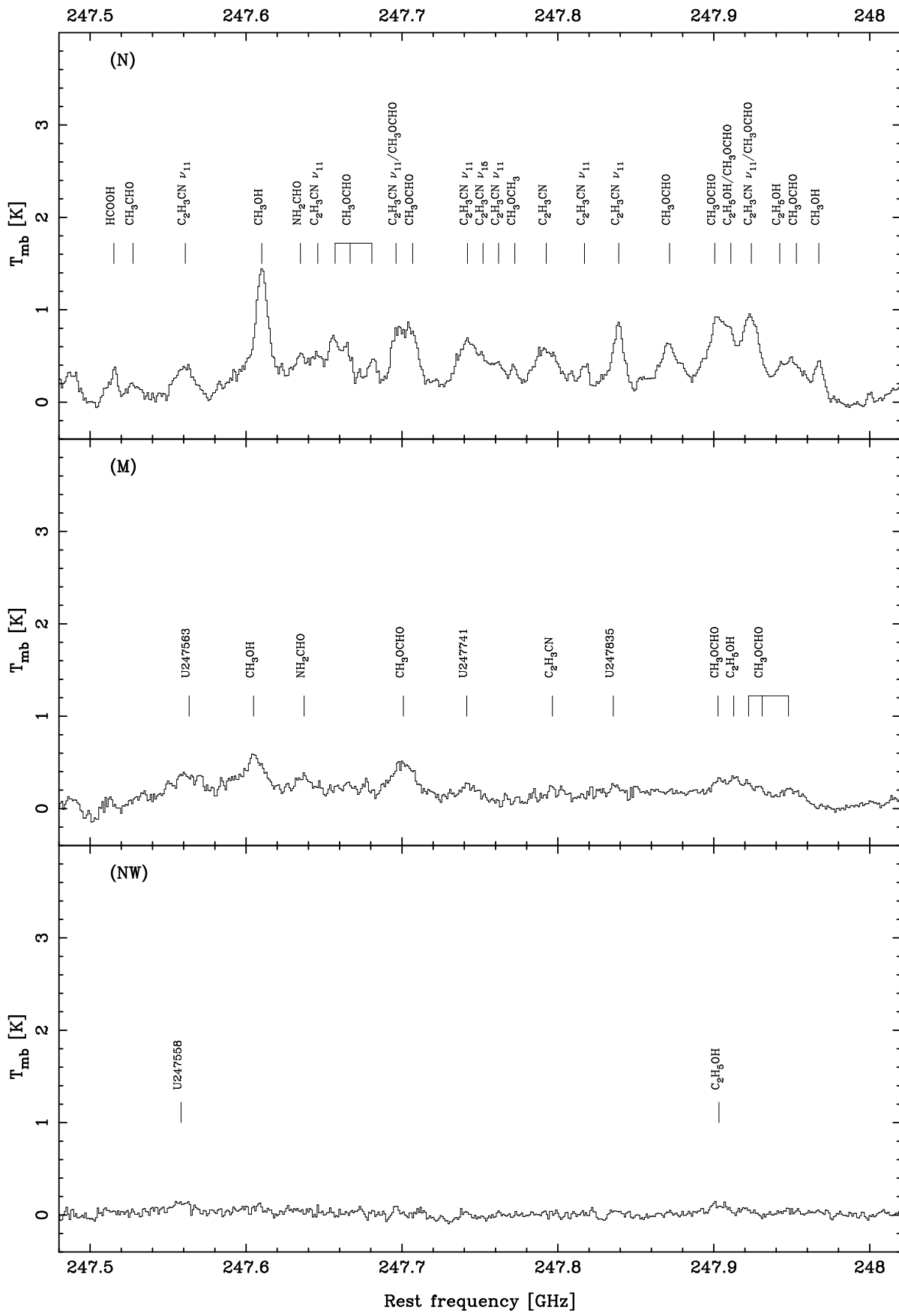


FIG. 1.—Continued

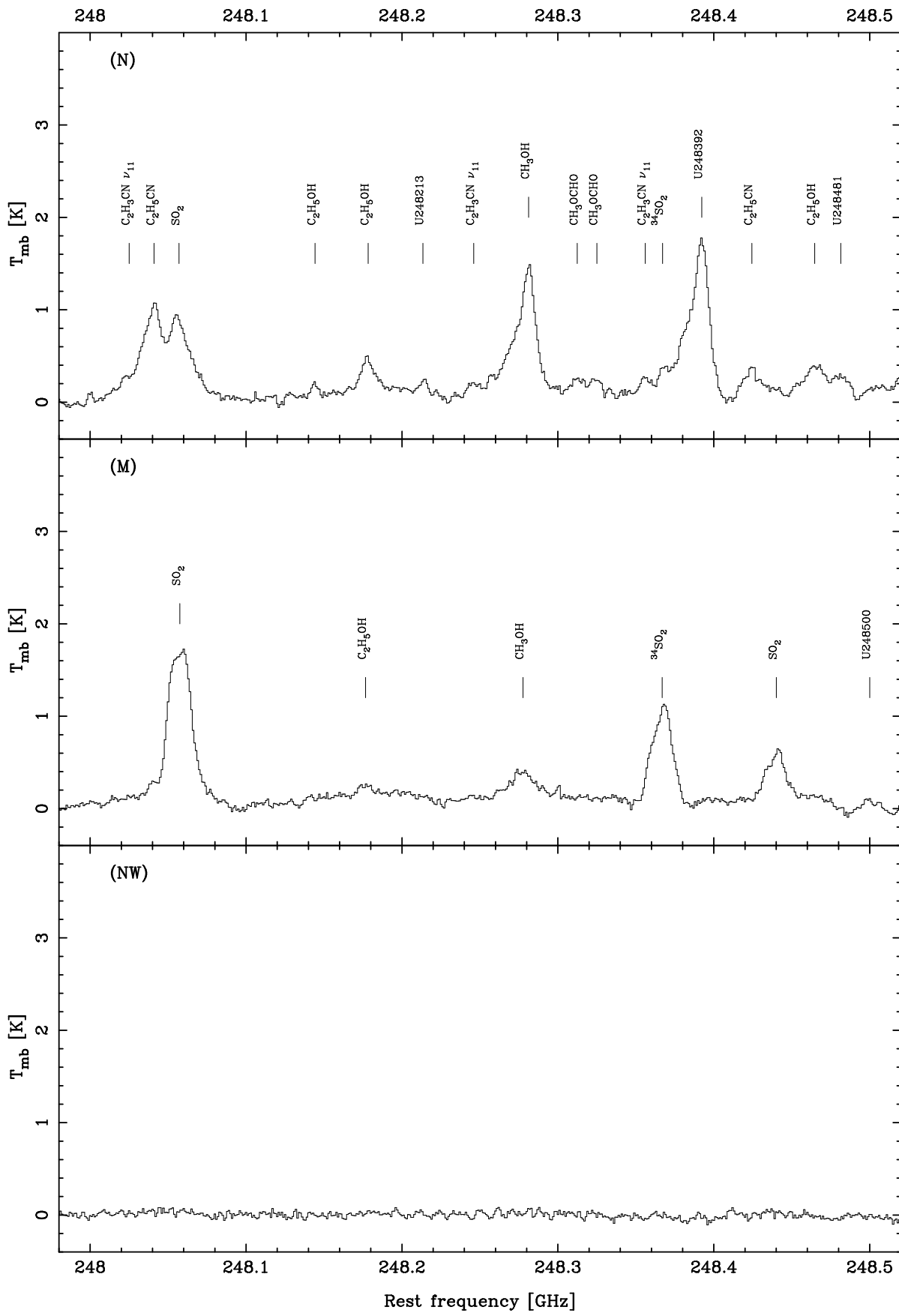


FIG. 1.—Continued

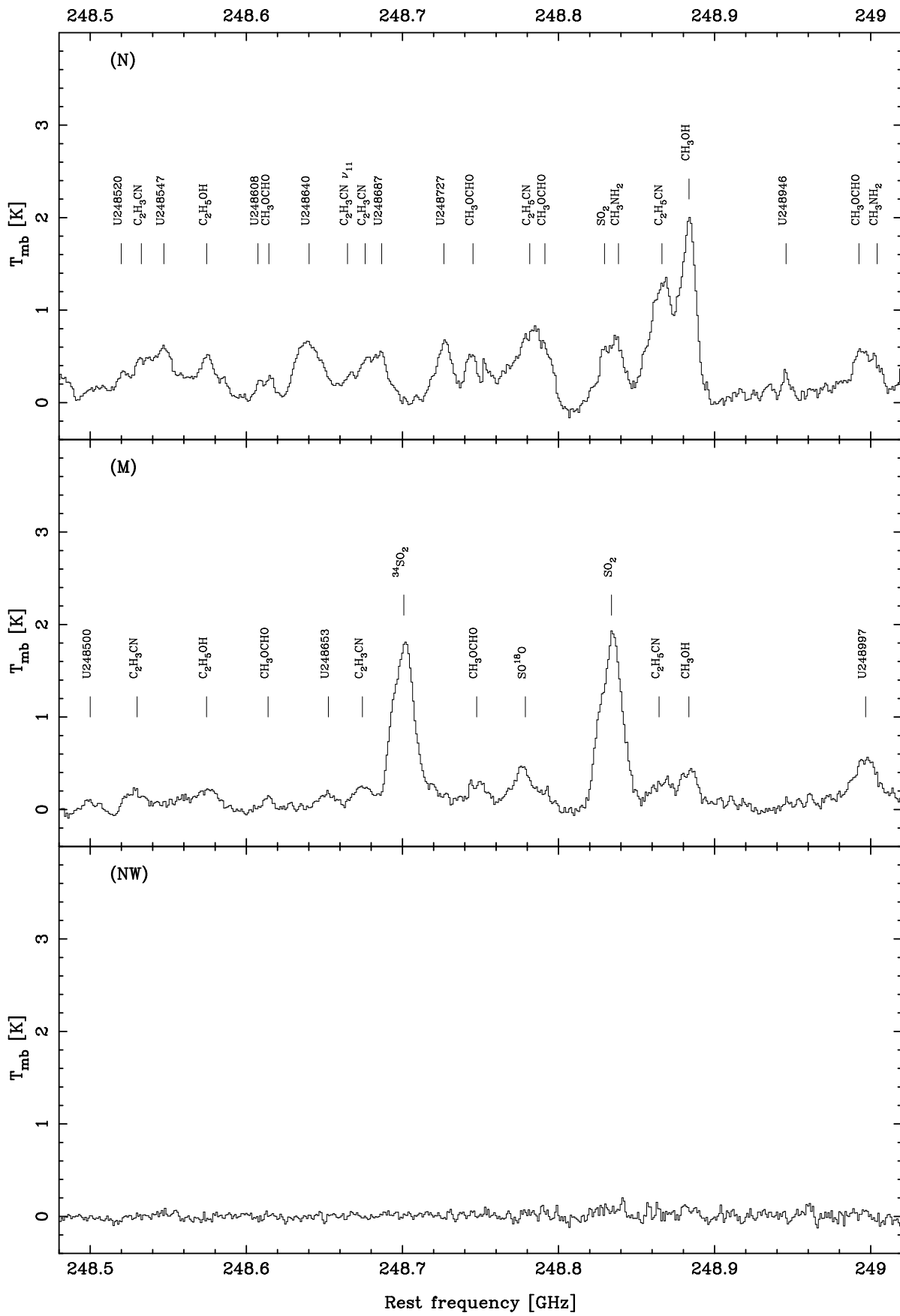


FIG. 1.—Continued

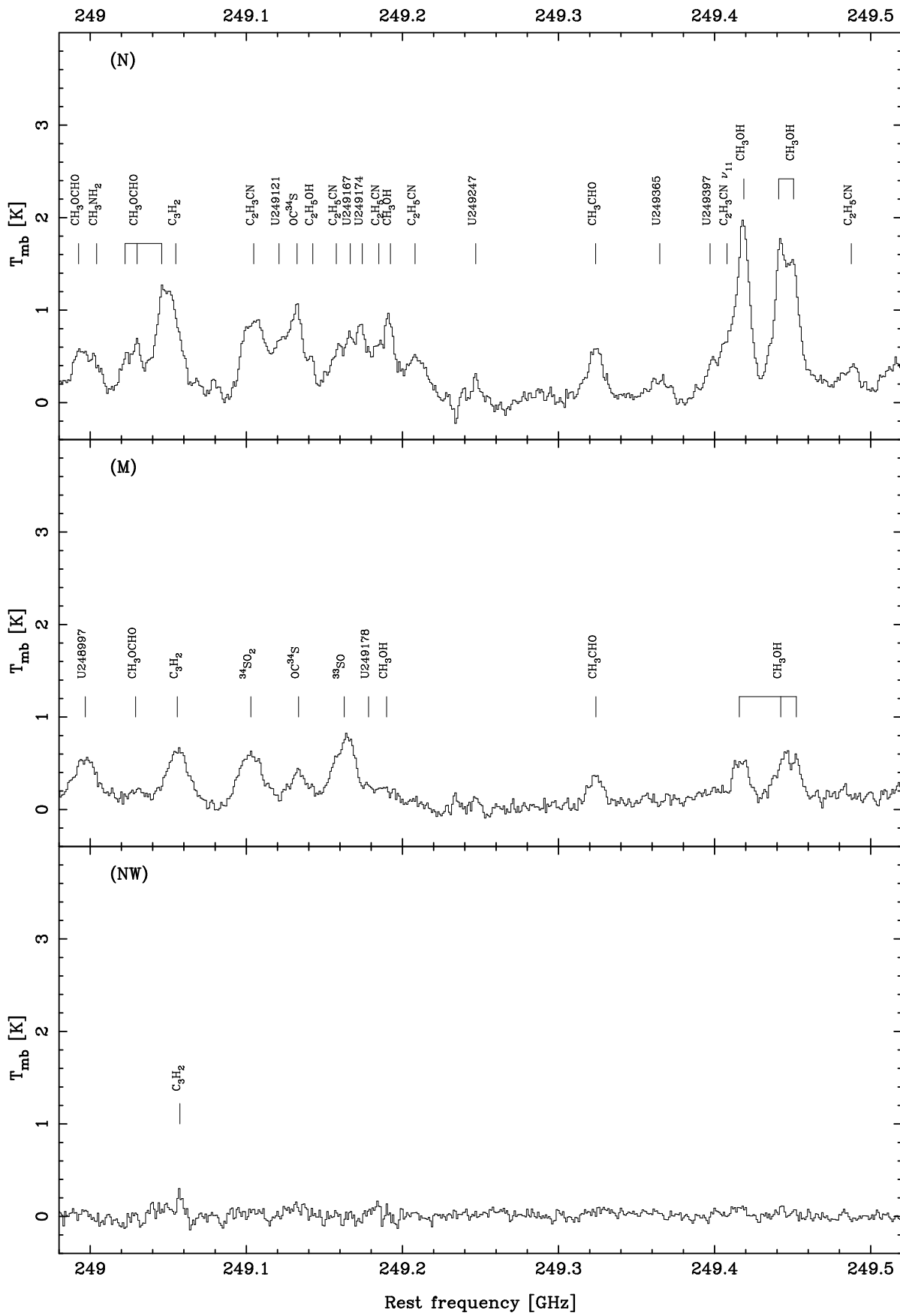


FIG. 1.—Continued

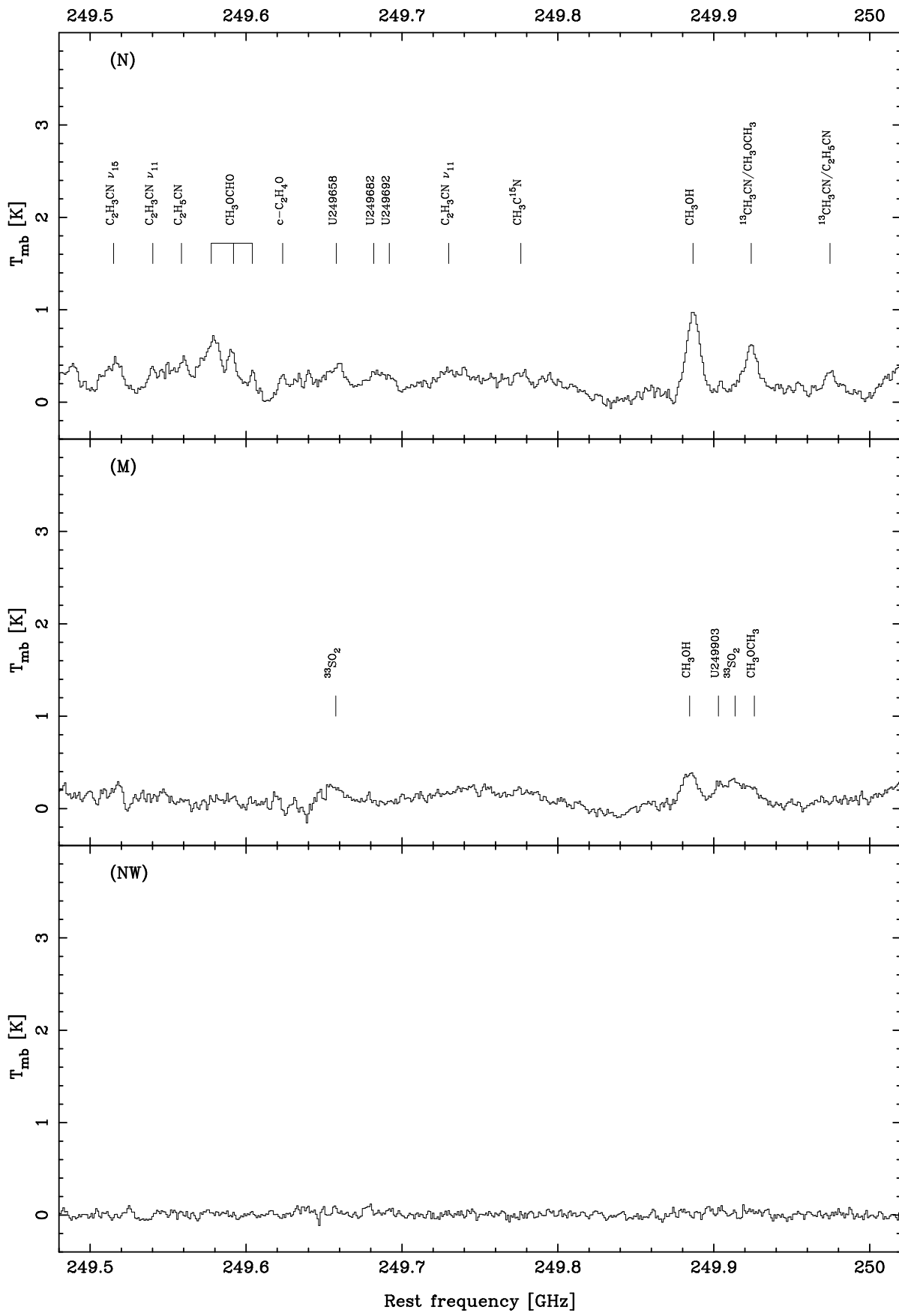


FIG. 1.—Continued

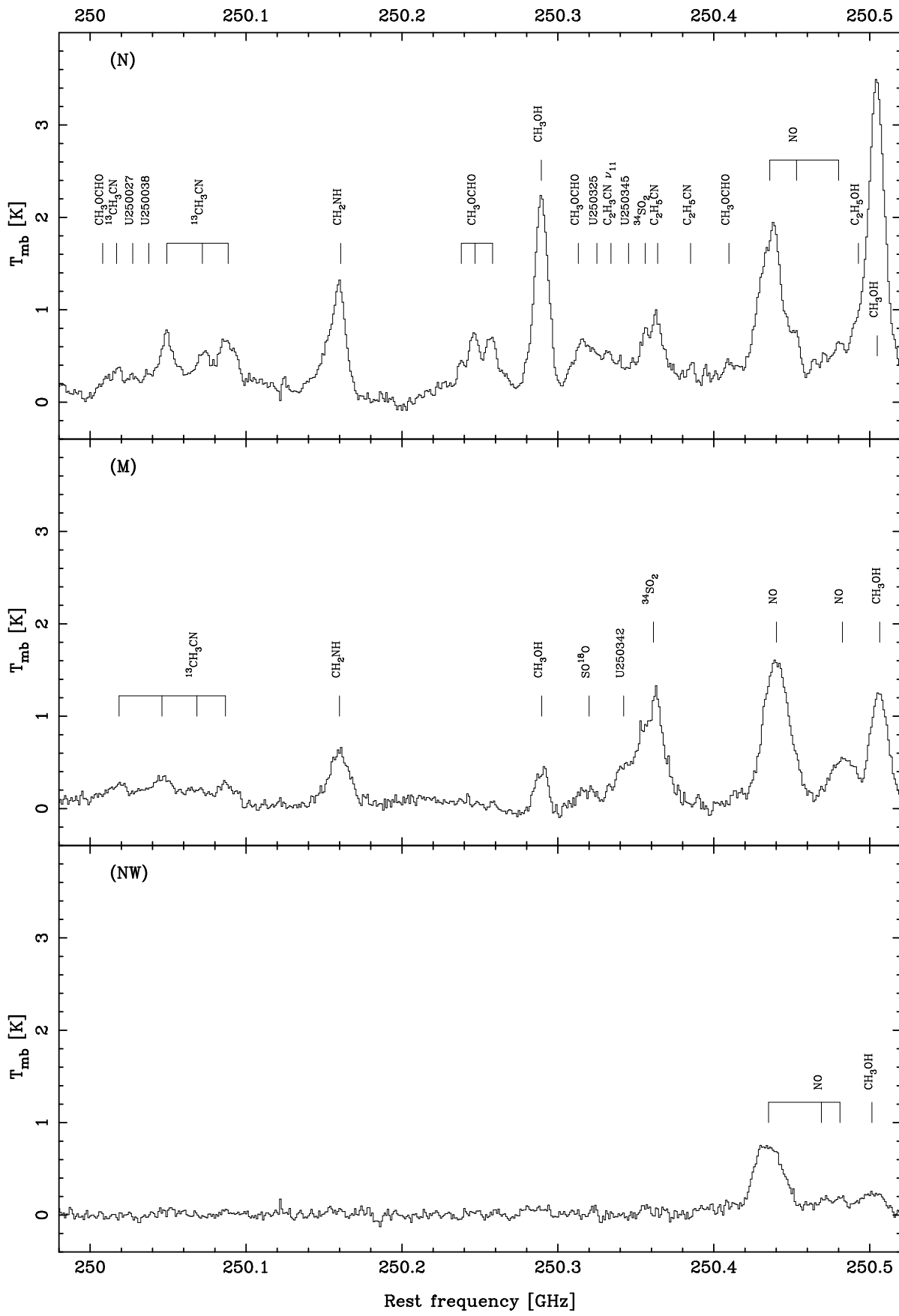


FIG. 1.—Continued

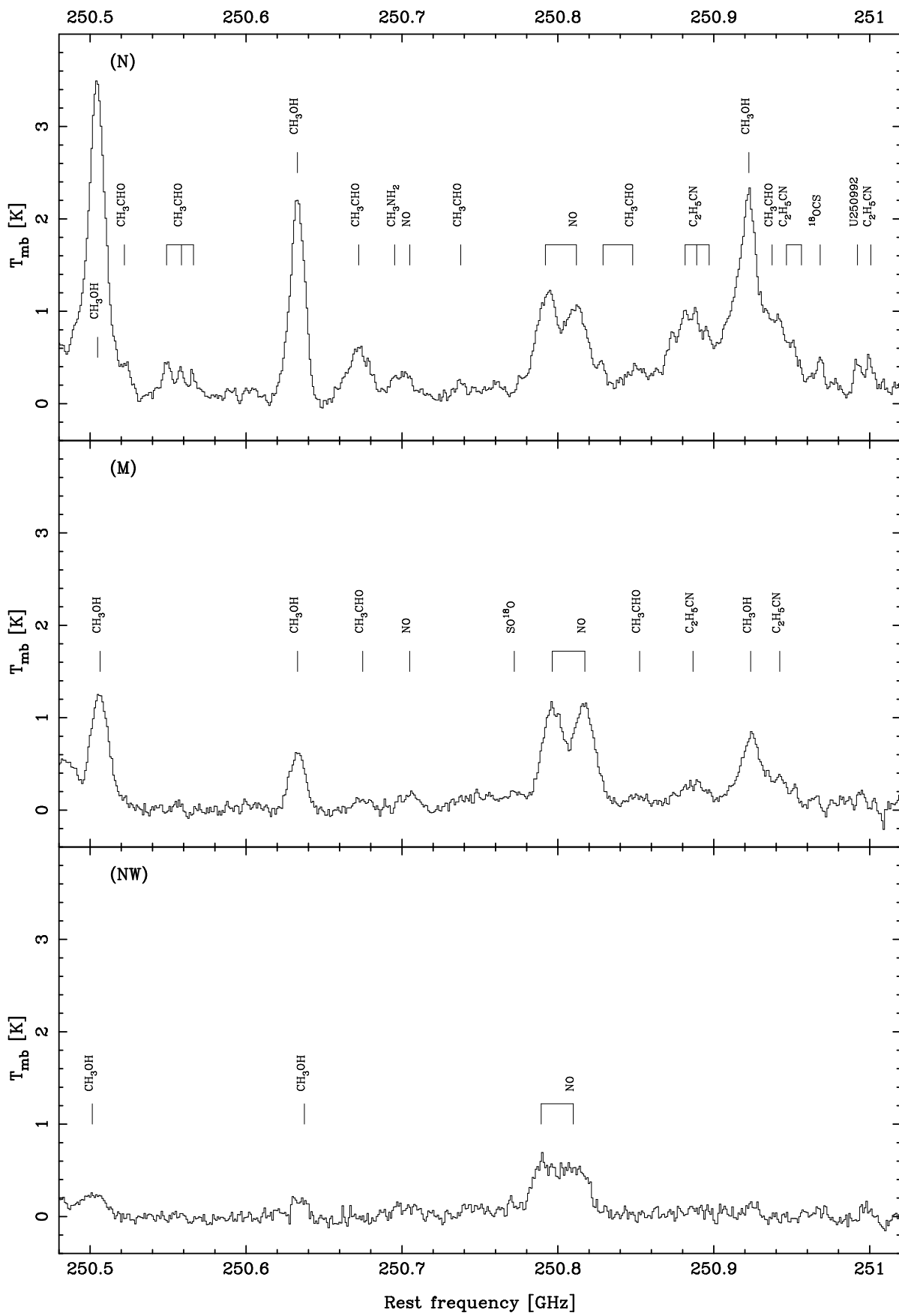


FIG. 1.—Continued

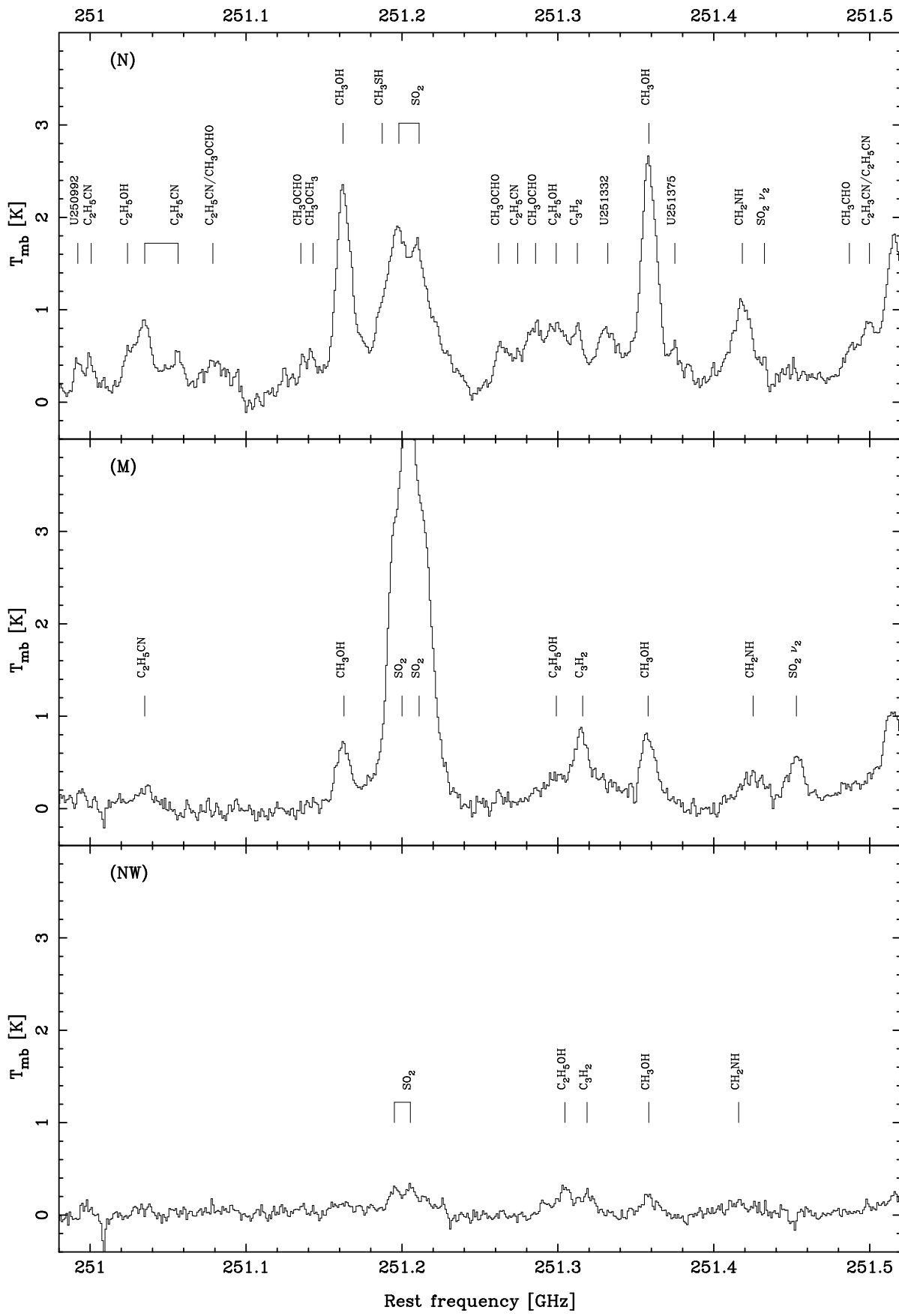


FIG. 1.—Continued

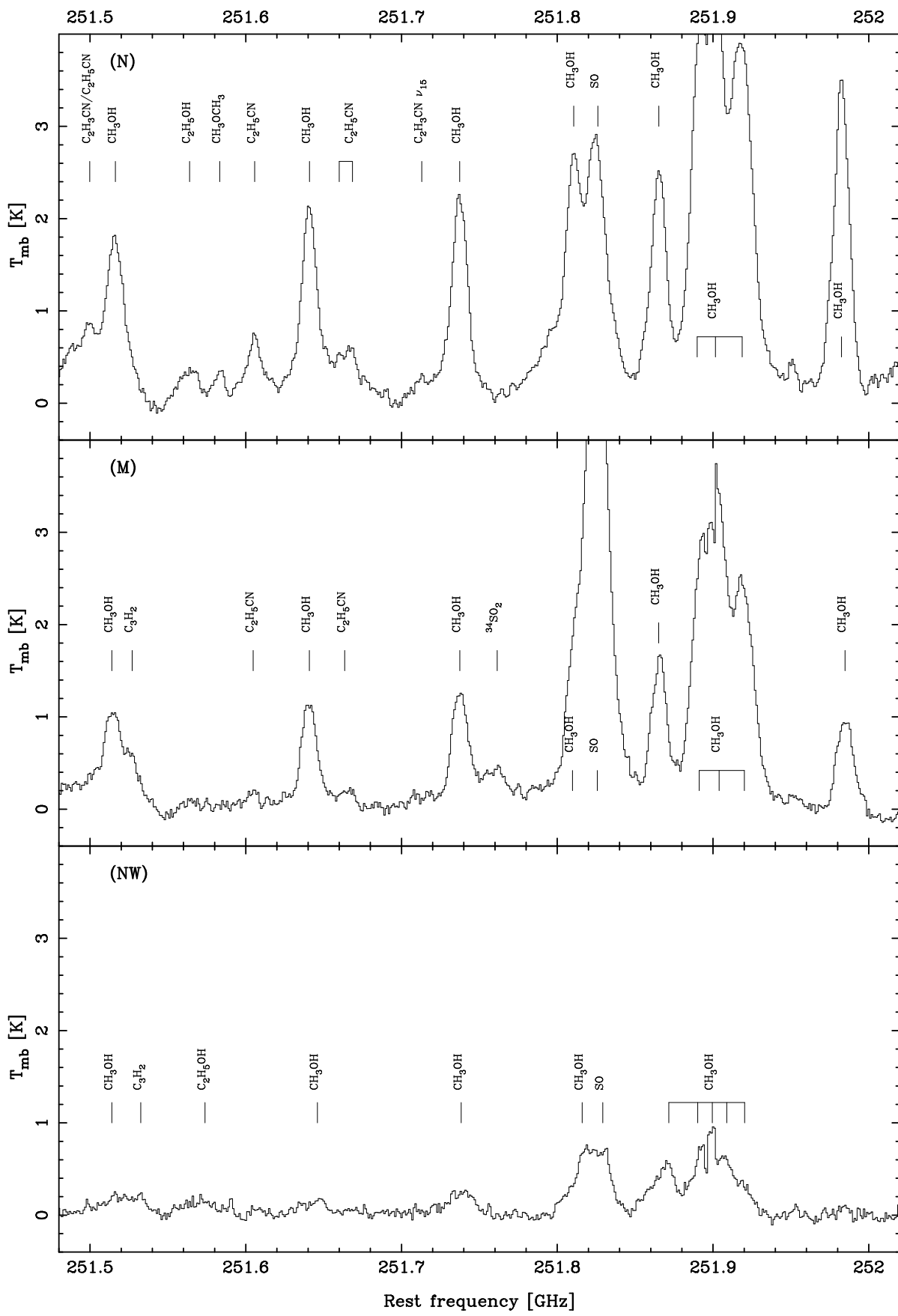


FIG. 1.—Continued

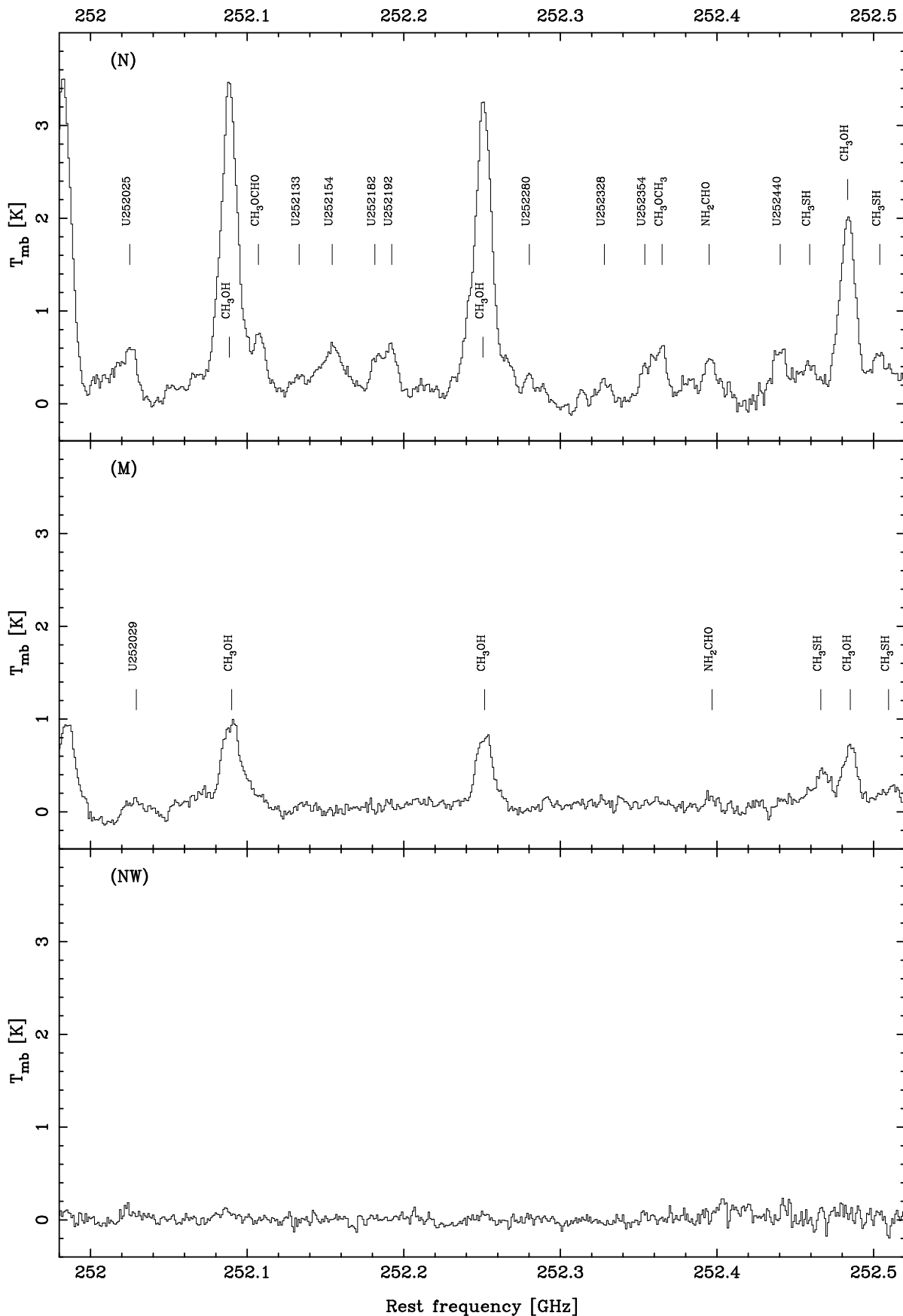


FIG. 1.—Continued

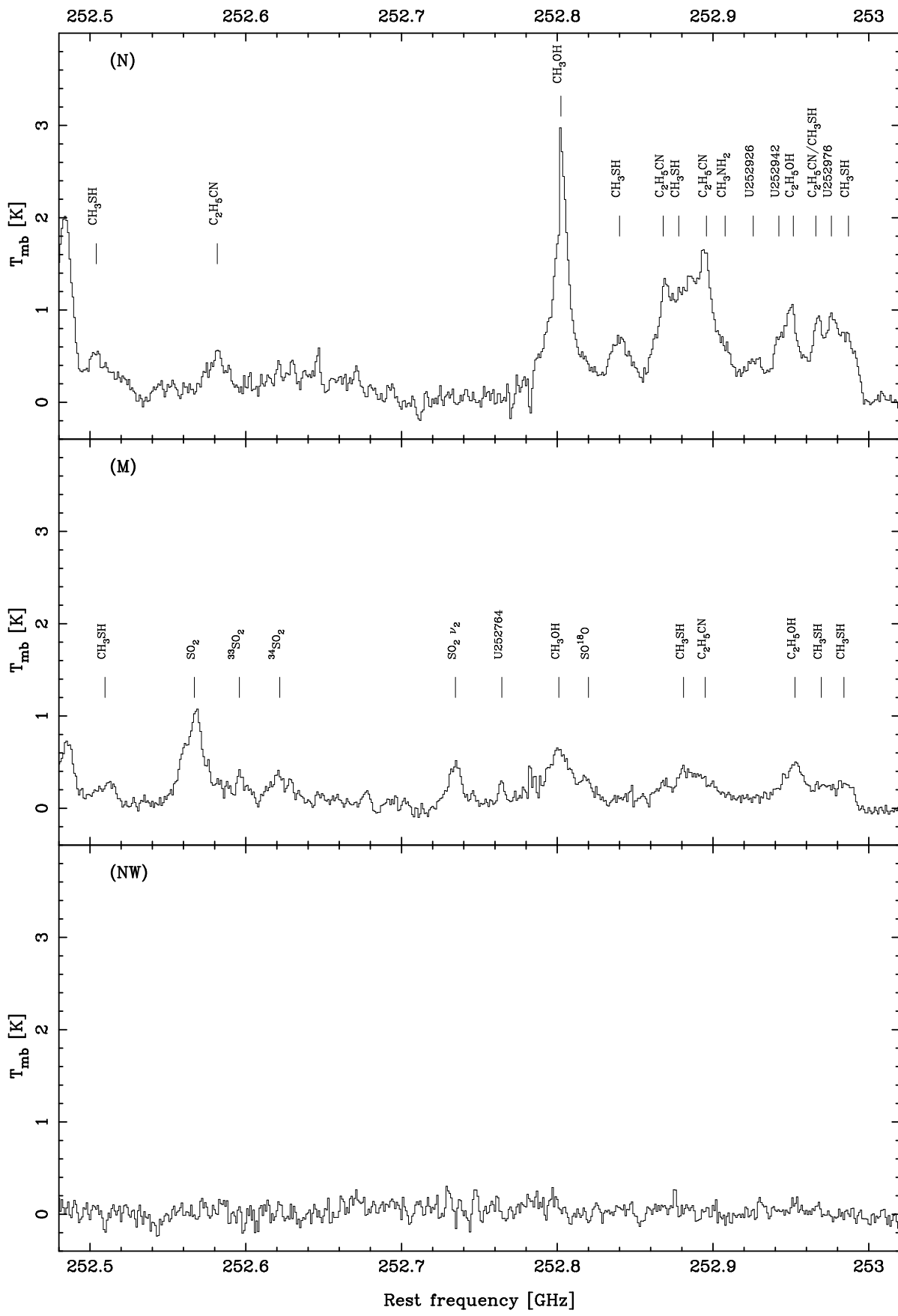


FIG. 1.—Continued

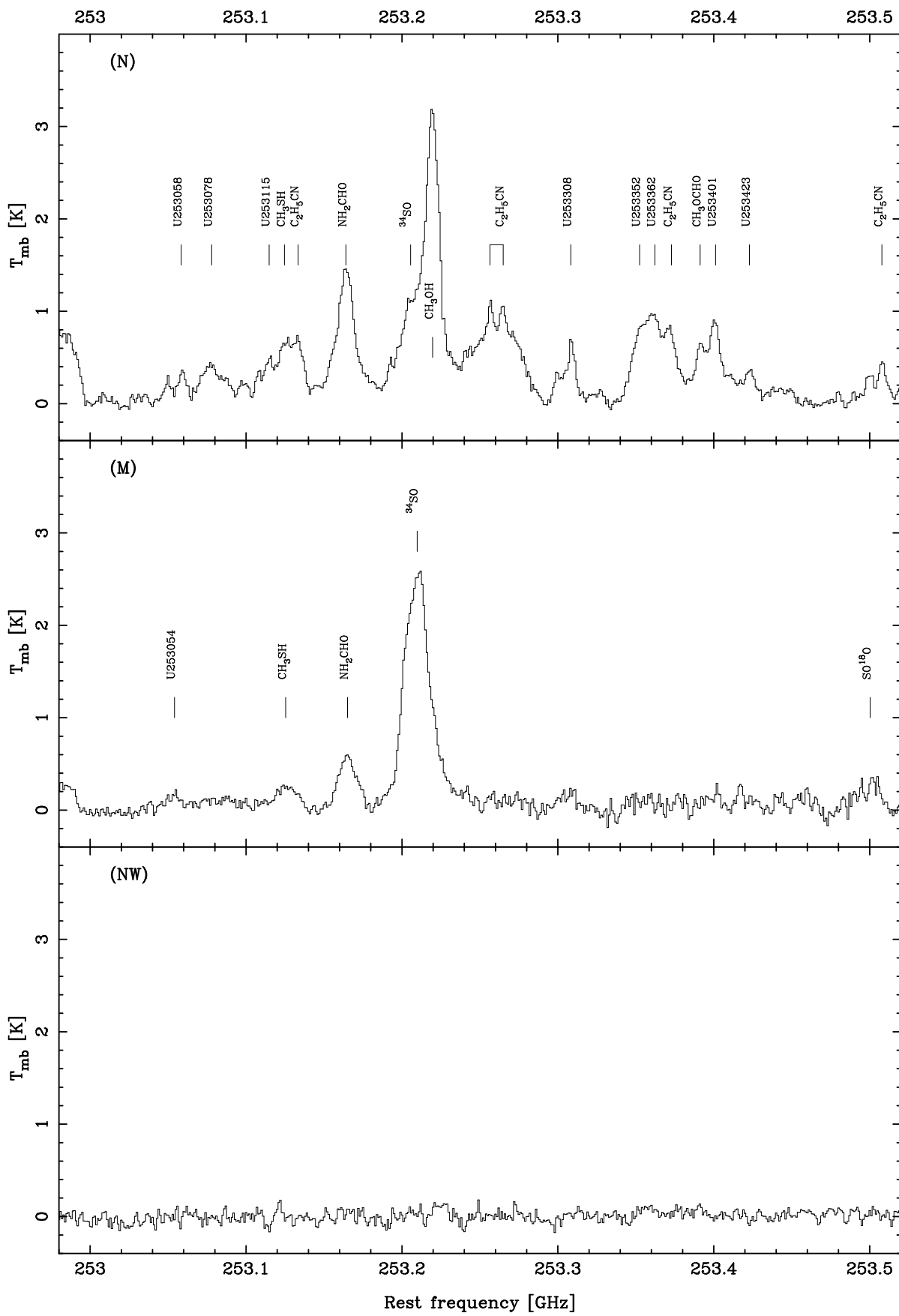


FIG. 1.—Continued

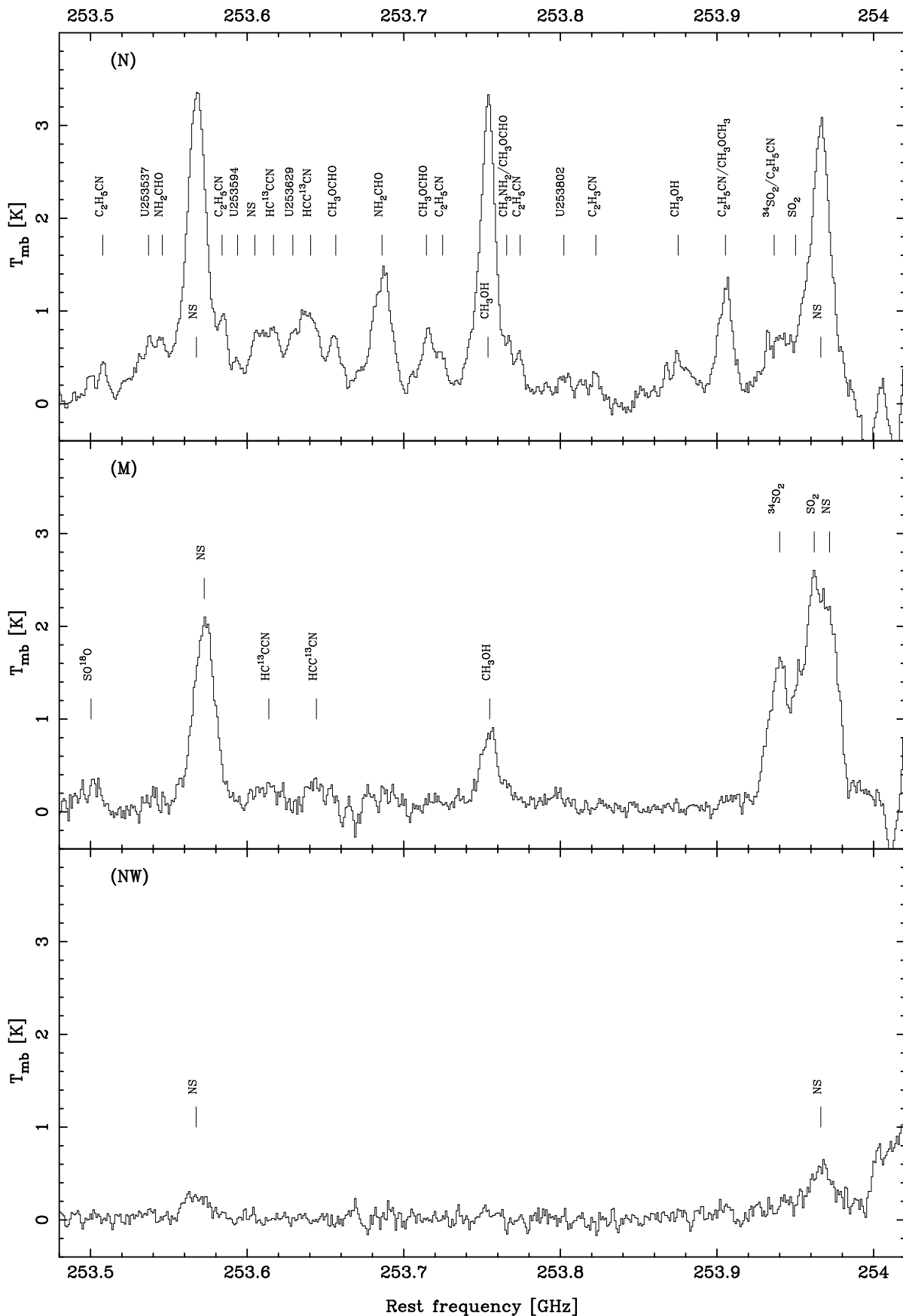


FIG. 1.—Continued

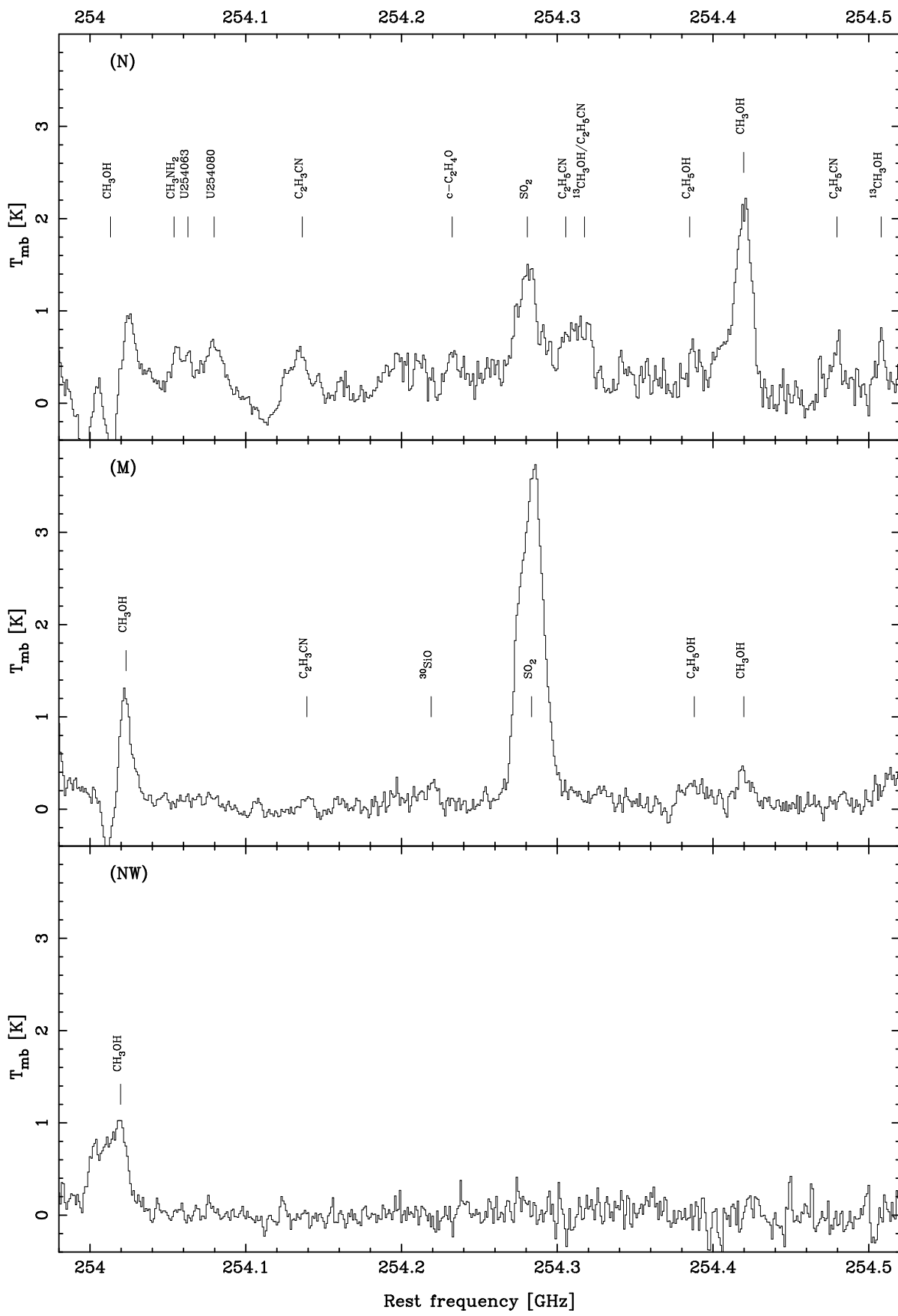


FIG. 1.—Continued

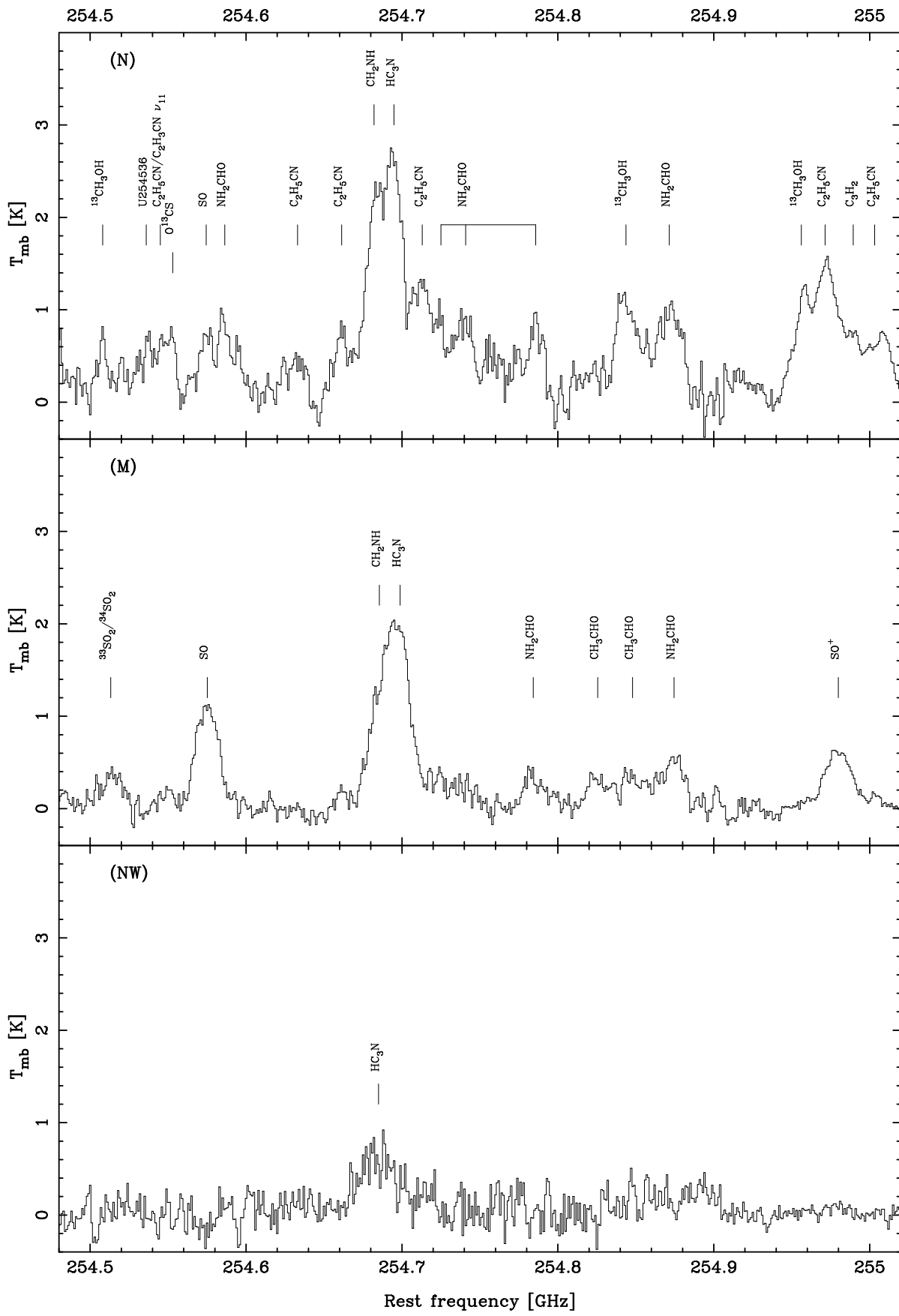


FIG. 1.—Continued

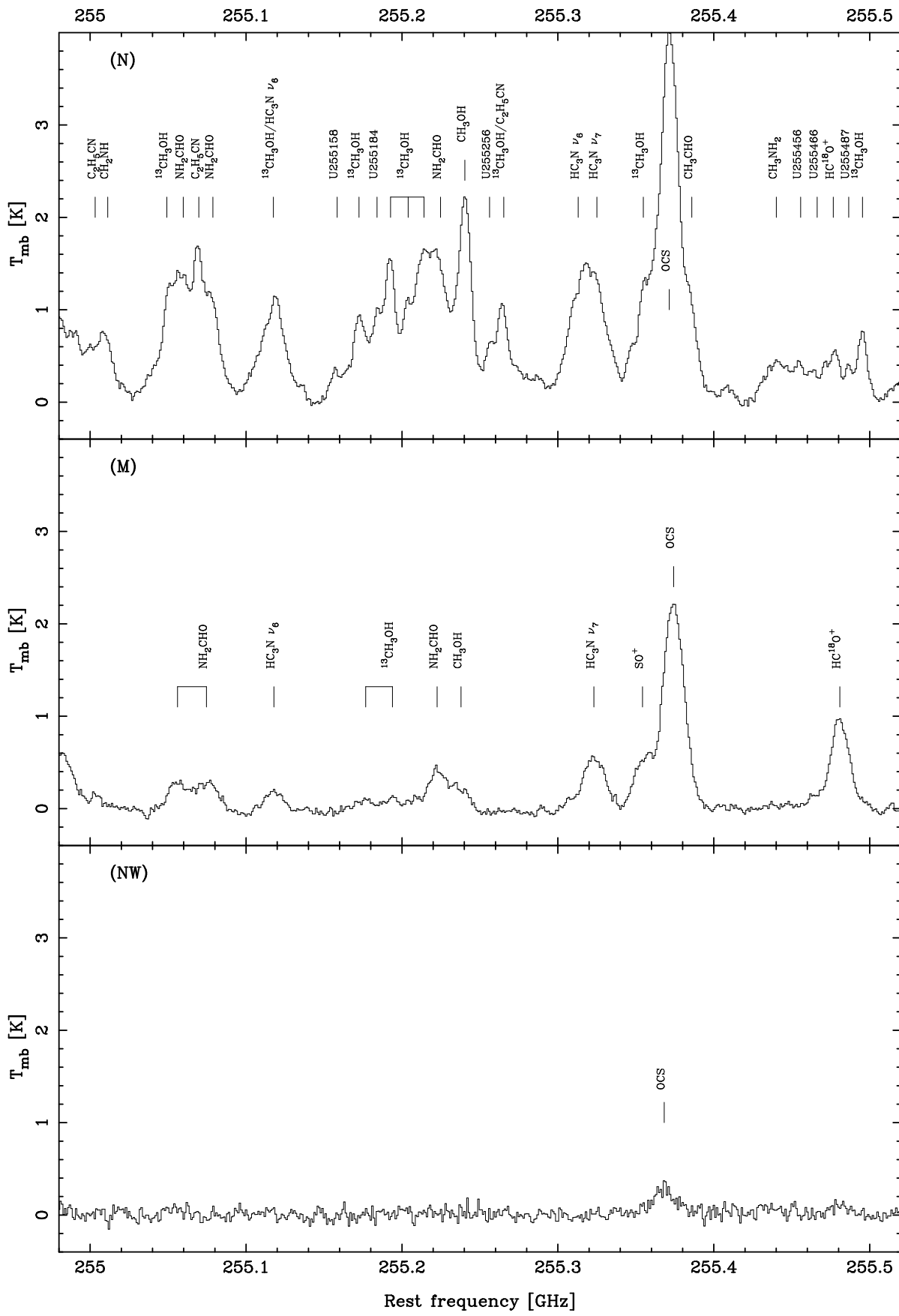


FIG. 1.—Continued

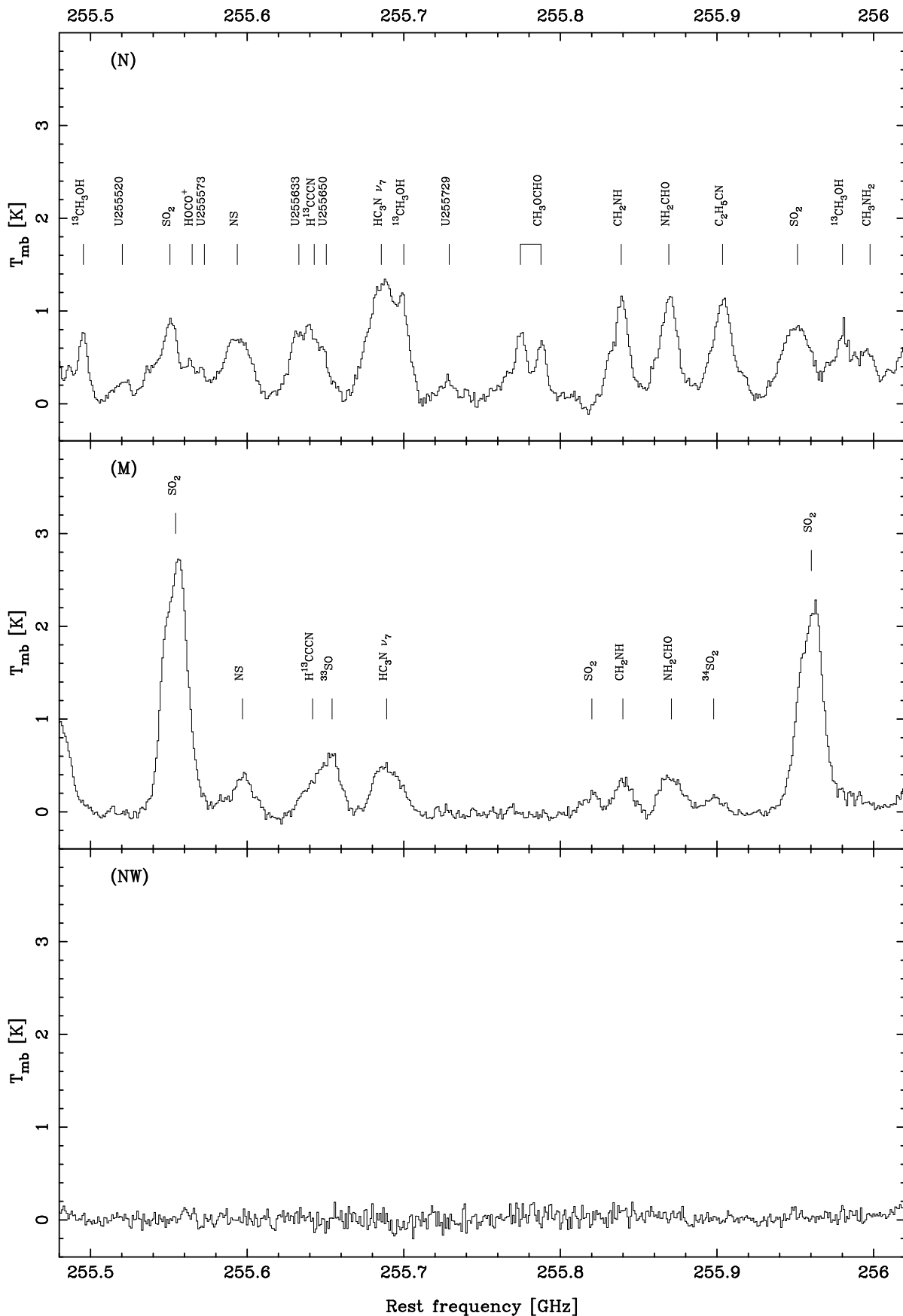


FIG. 1.—Continued

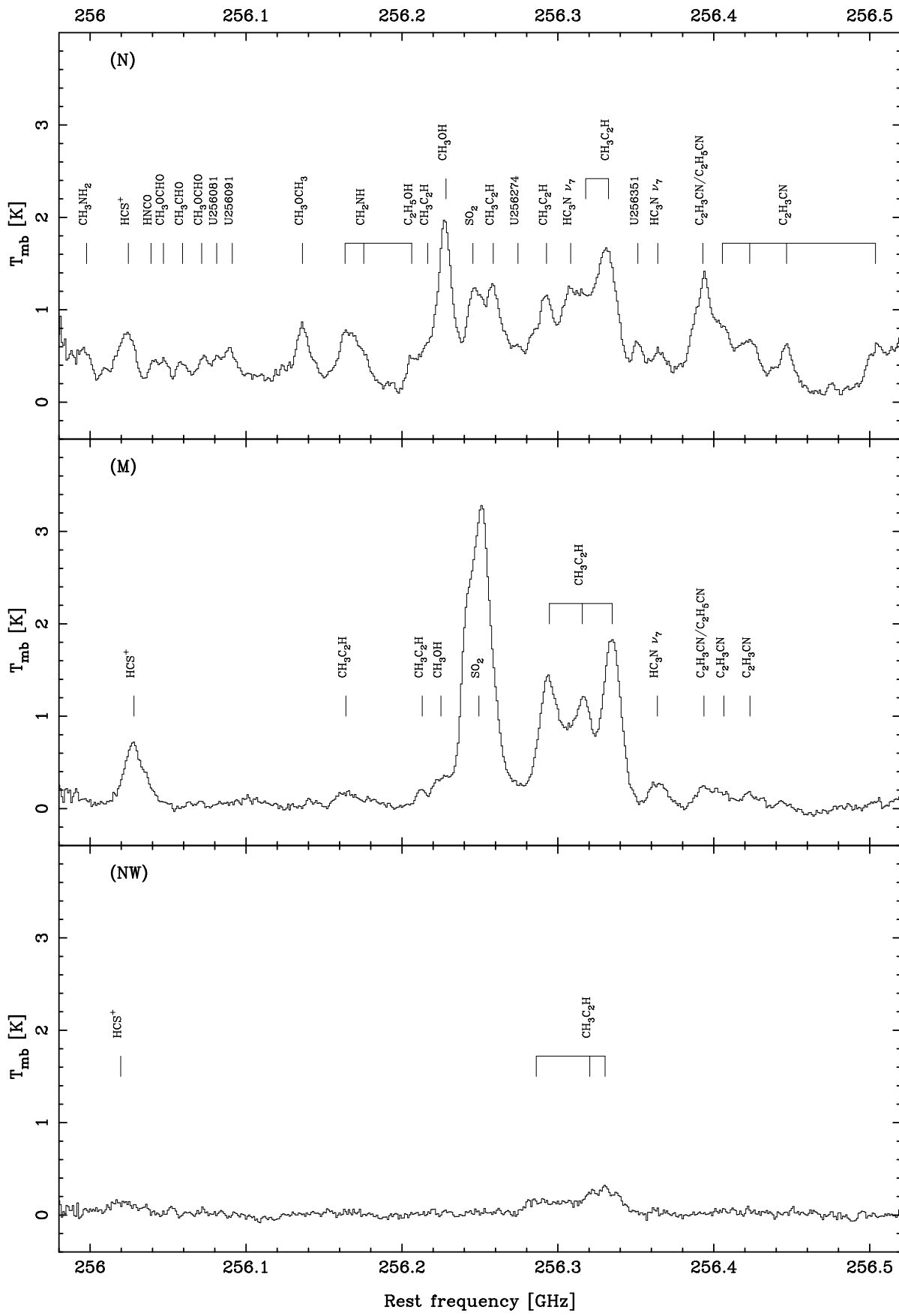


FIG. 1.—Continued

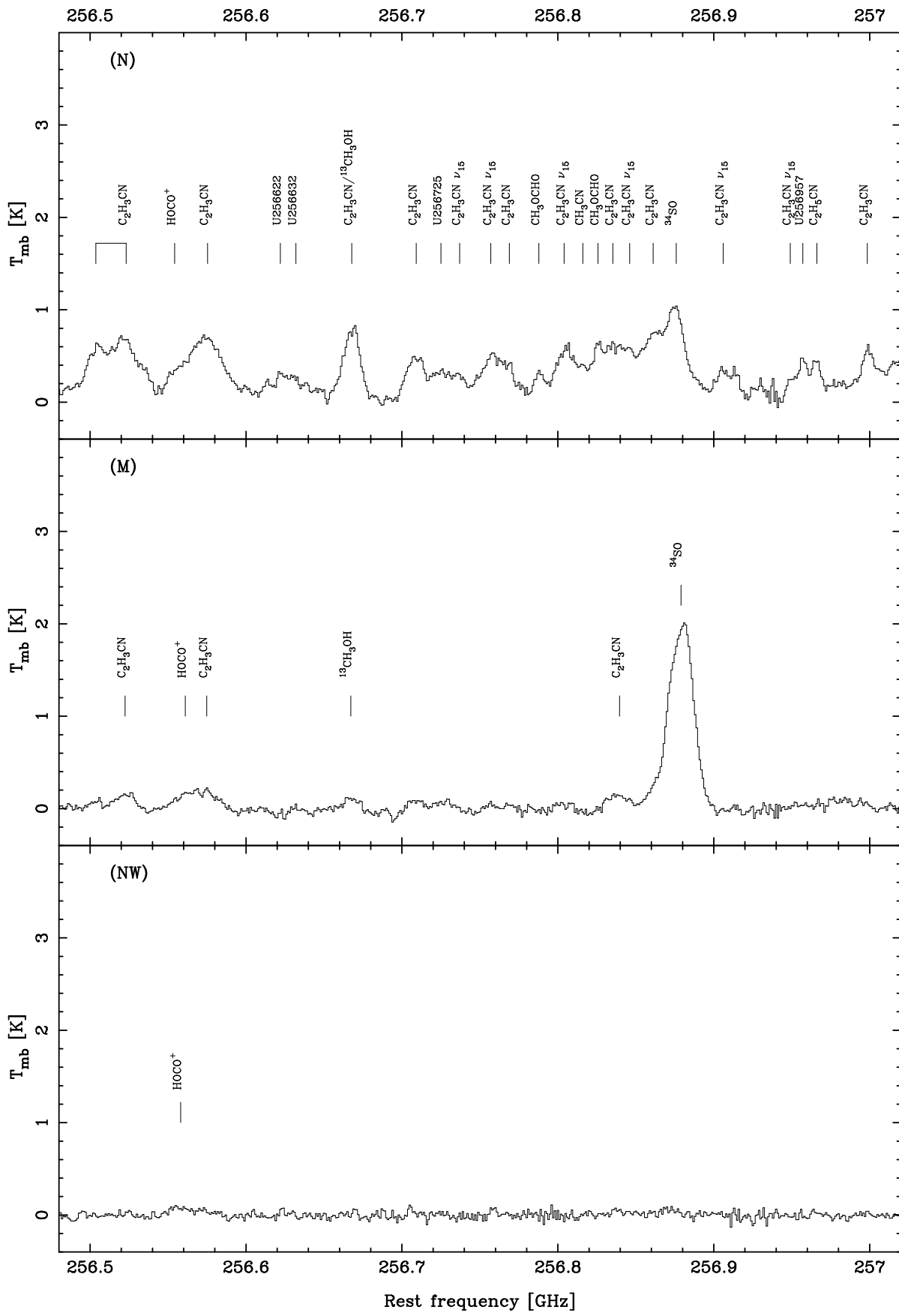


FIG. 1.—Continued

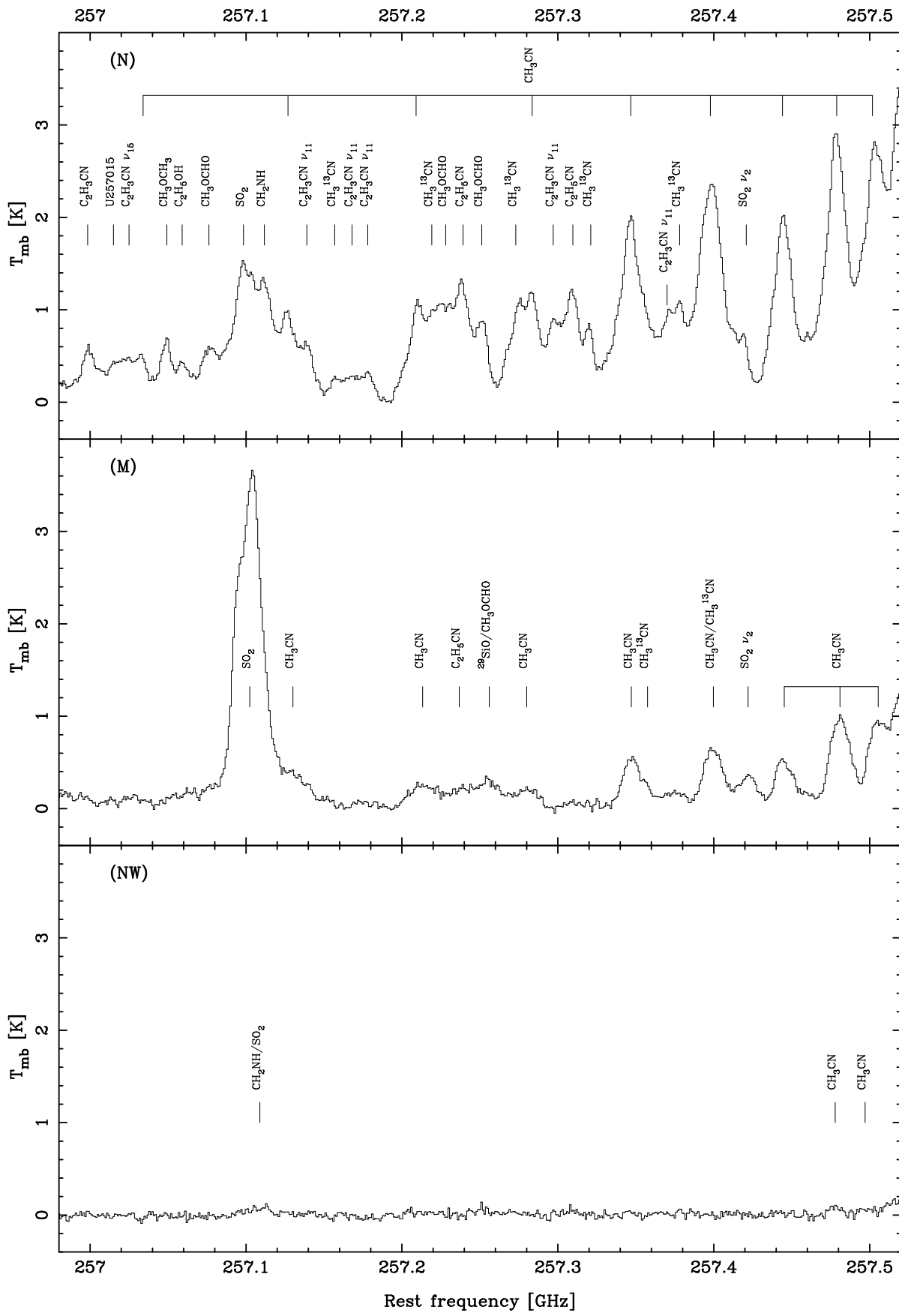


FIG. 1.—Continued

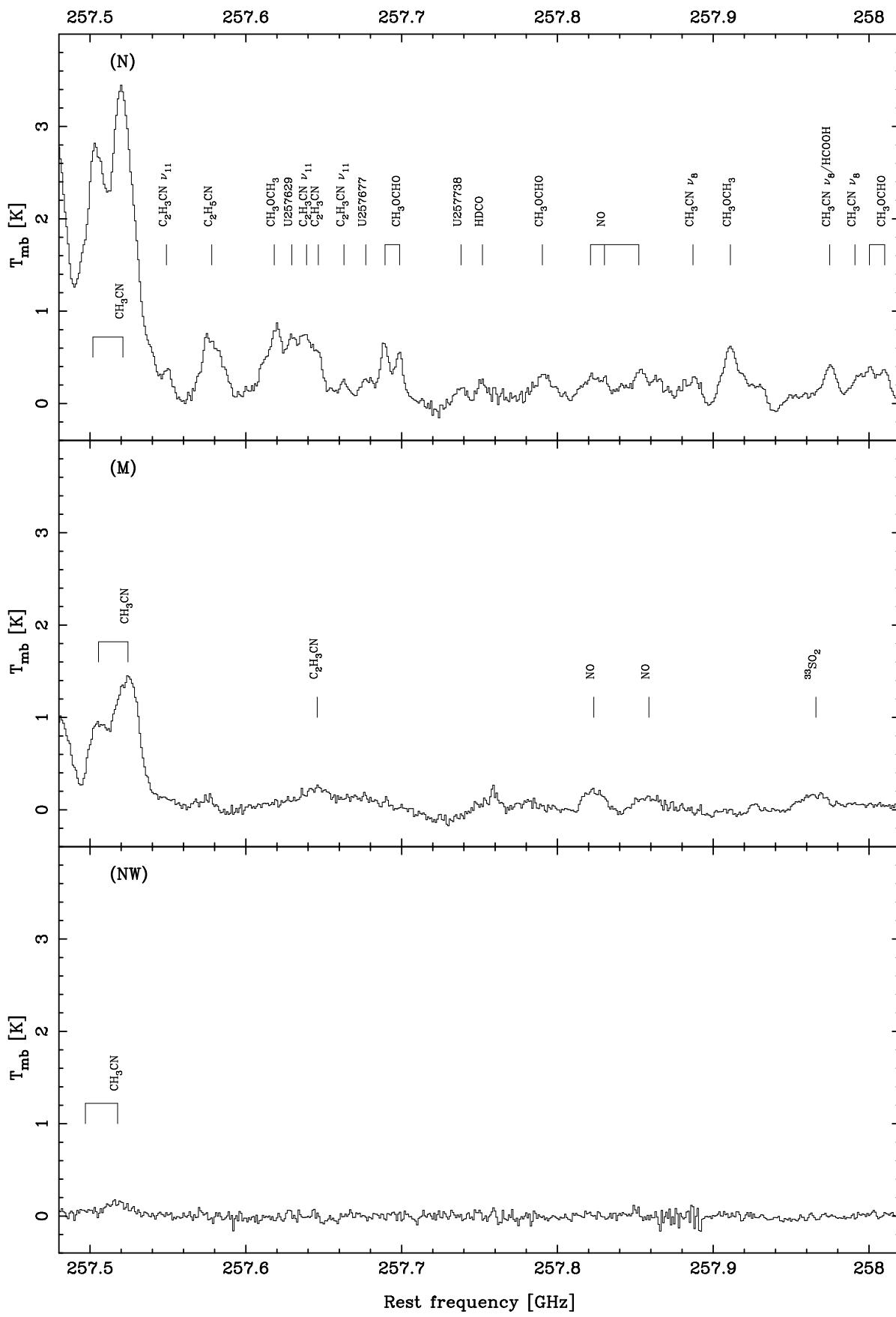


FIG. 1.—Continued

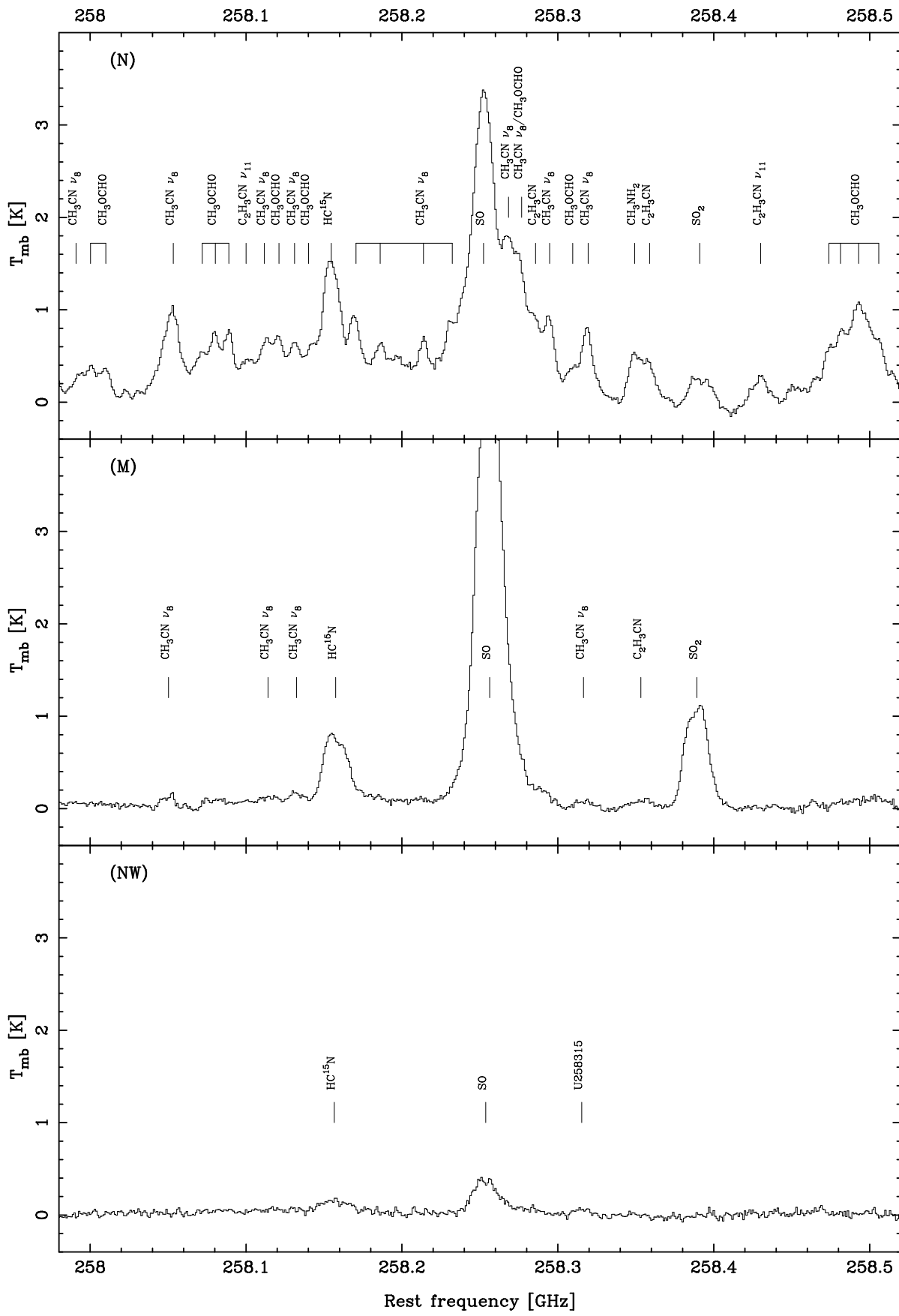


FIG. 1.—Continued

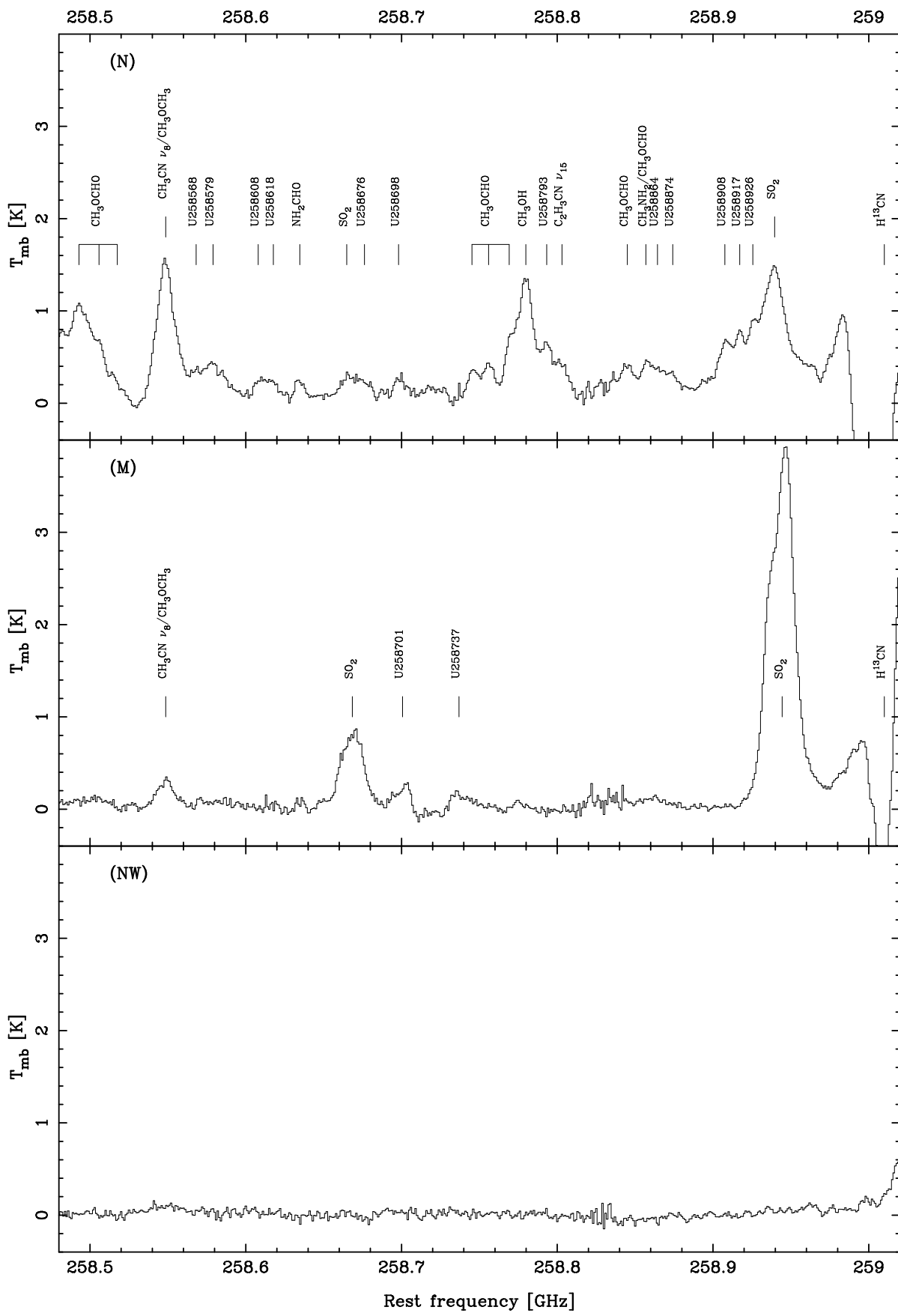


FIG. 1.—Continued

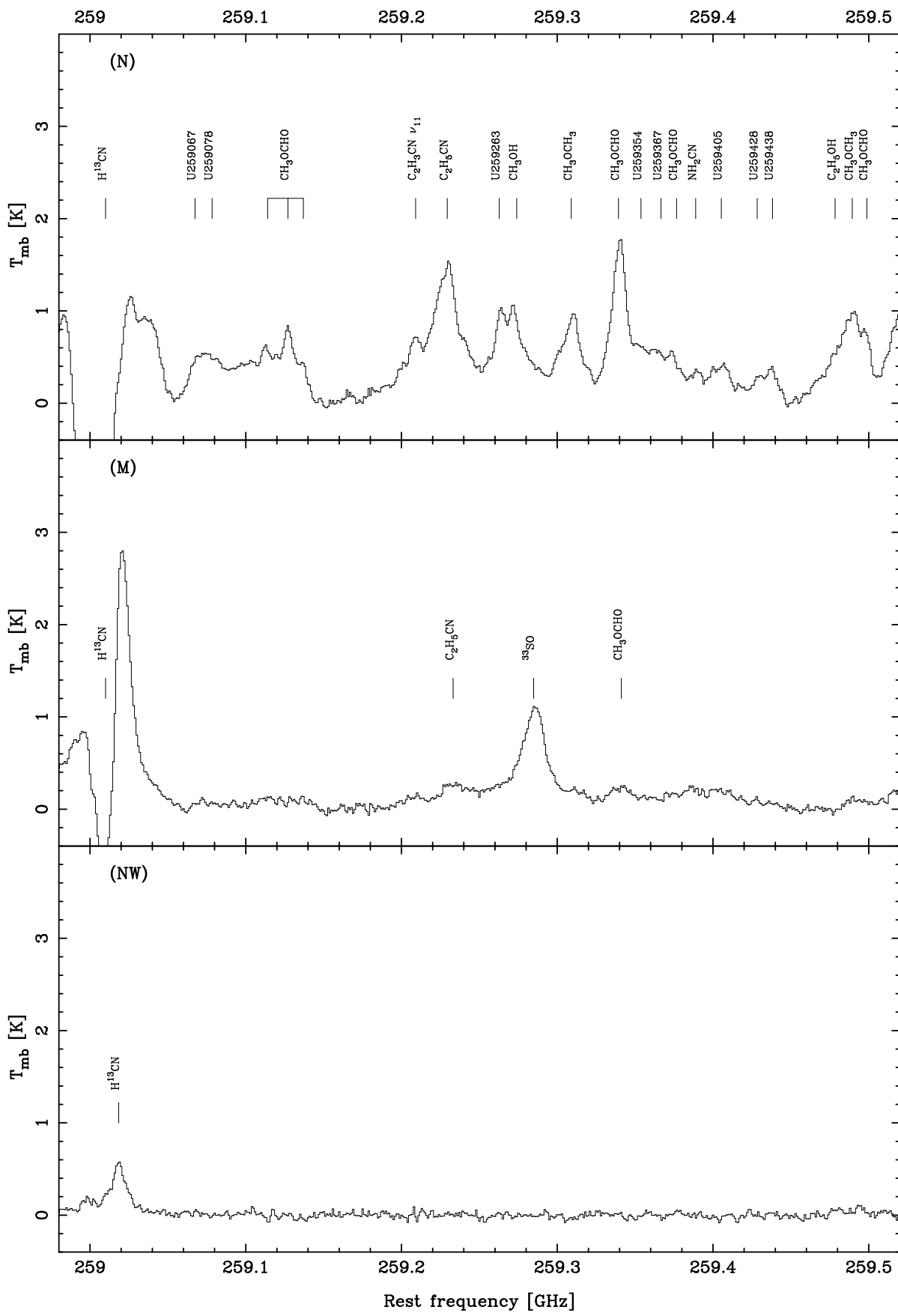


FIG. 1.—Continued

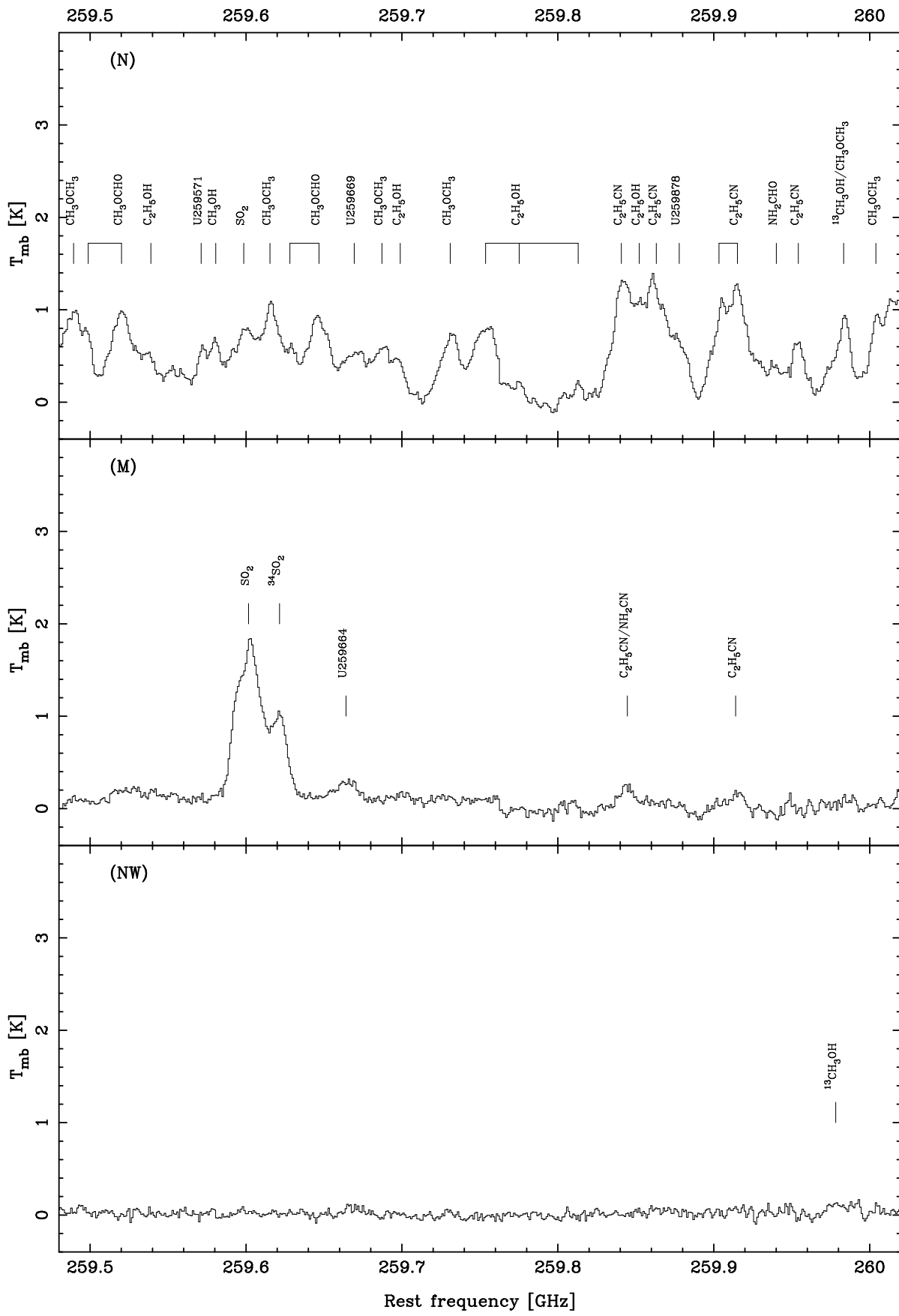


FIG. 1.—Continued

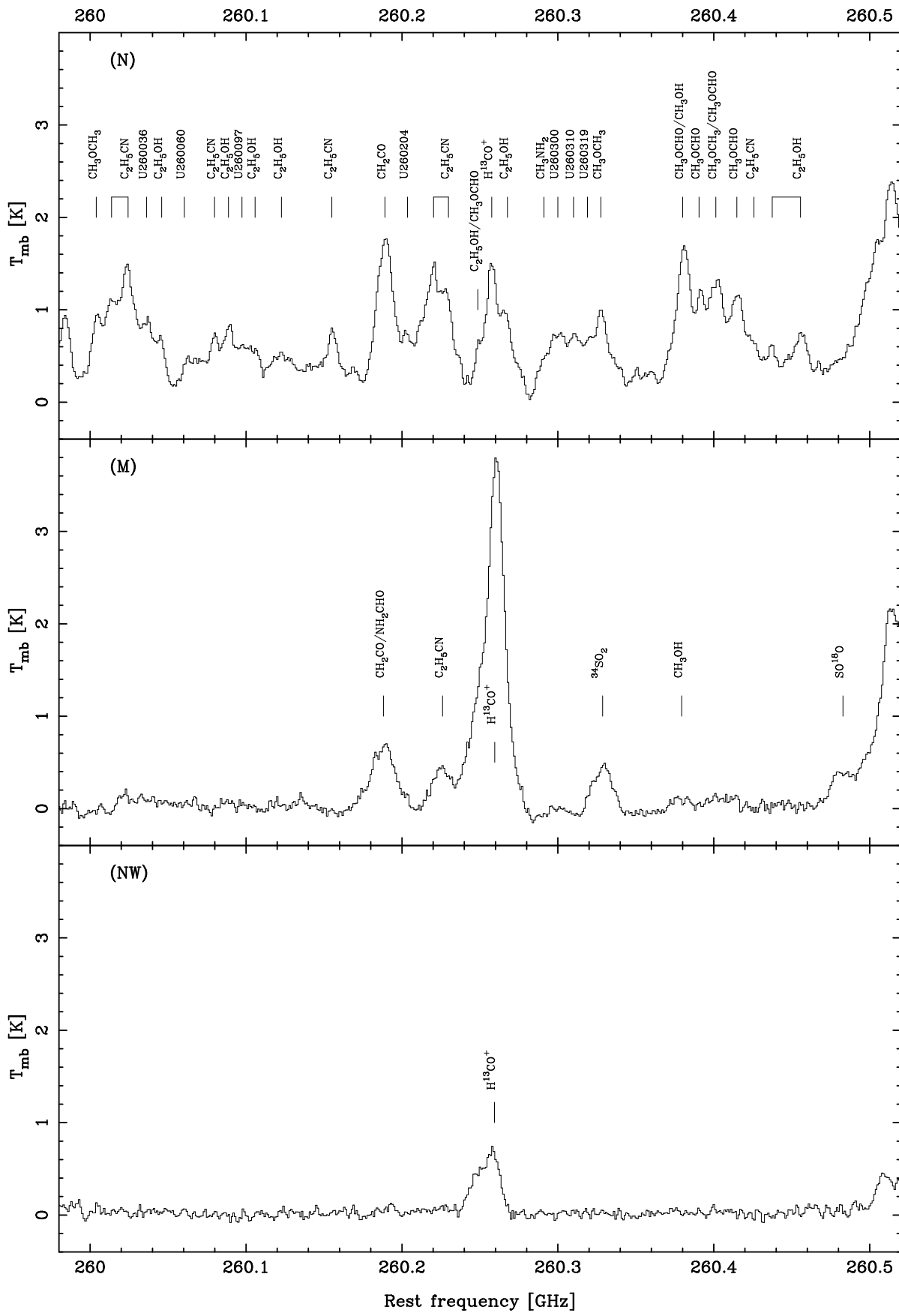


FIG. 1.—Continued

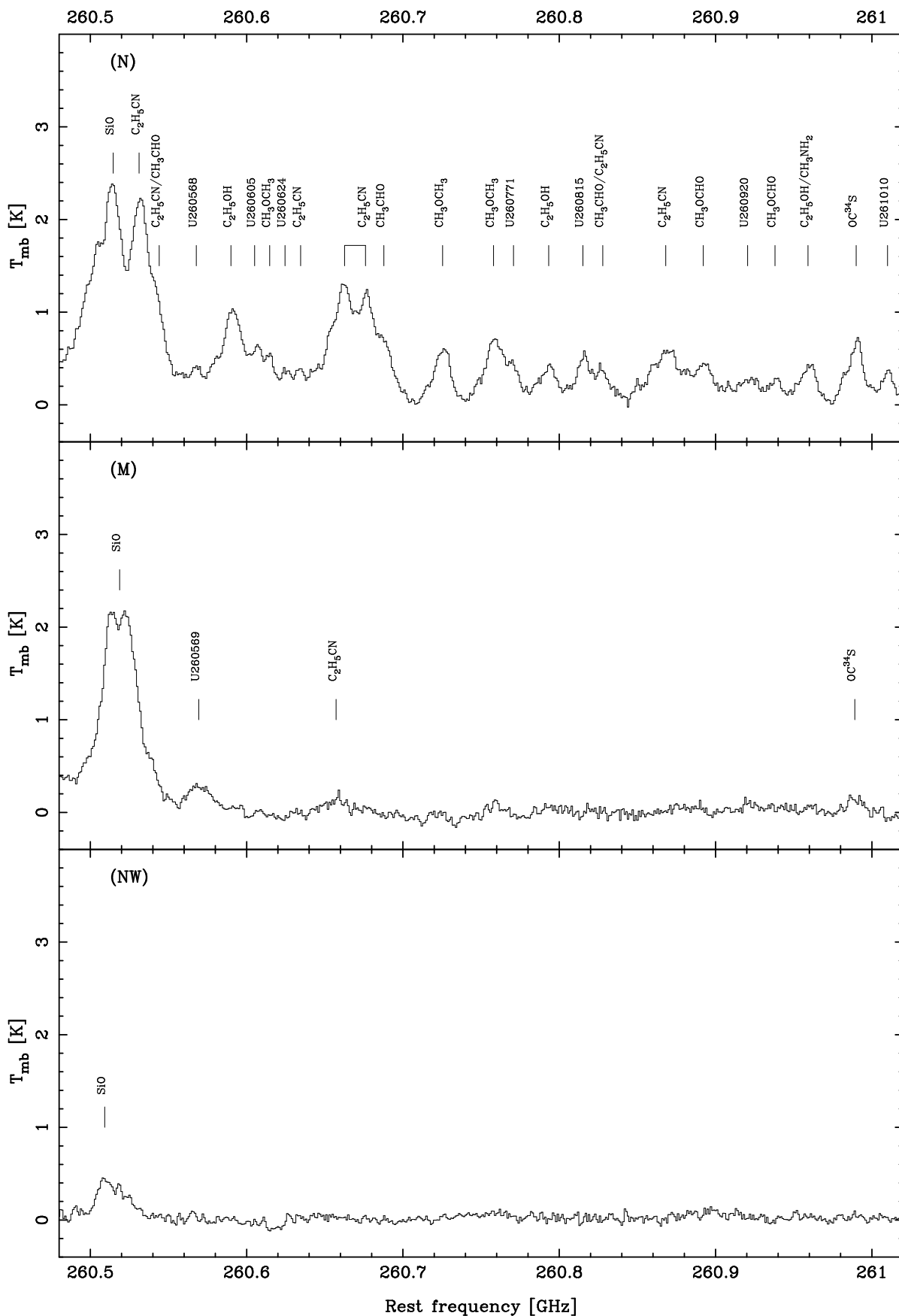


FIG. 1.—Continued

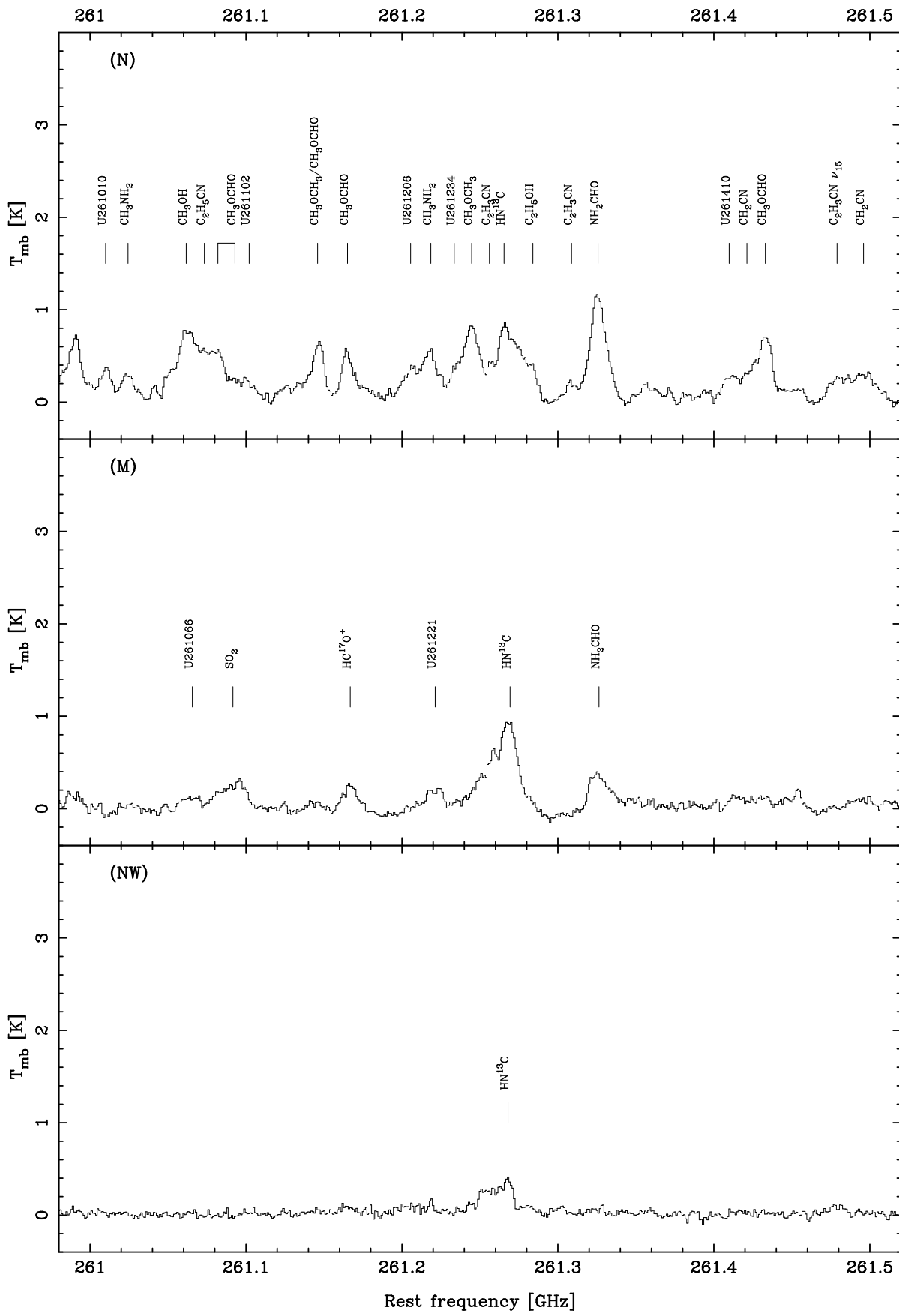


FIG. 1.—Continued

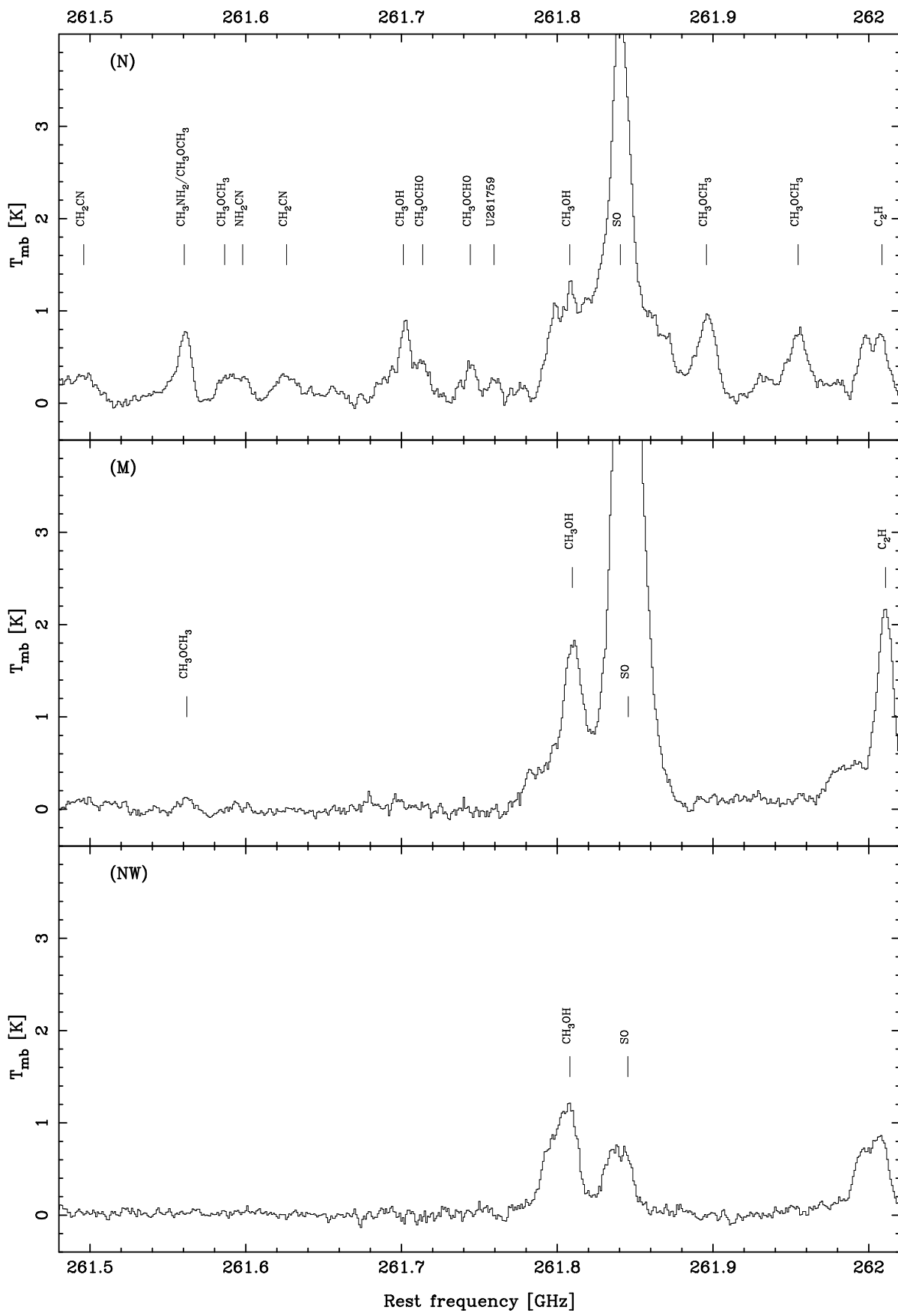


FIG. 1.—Continued

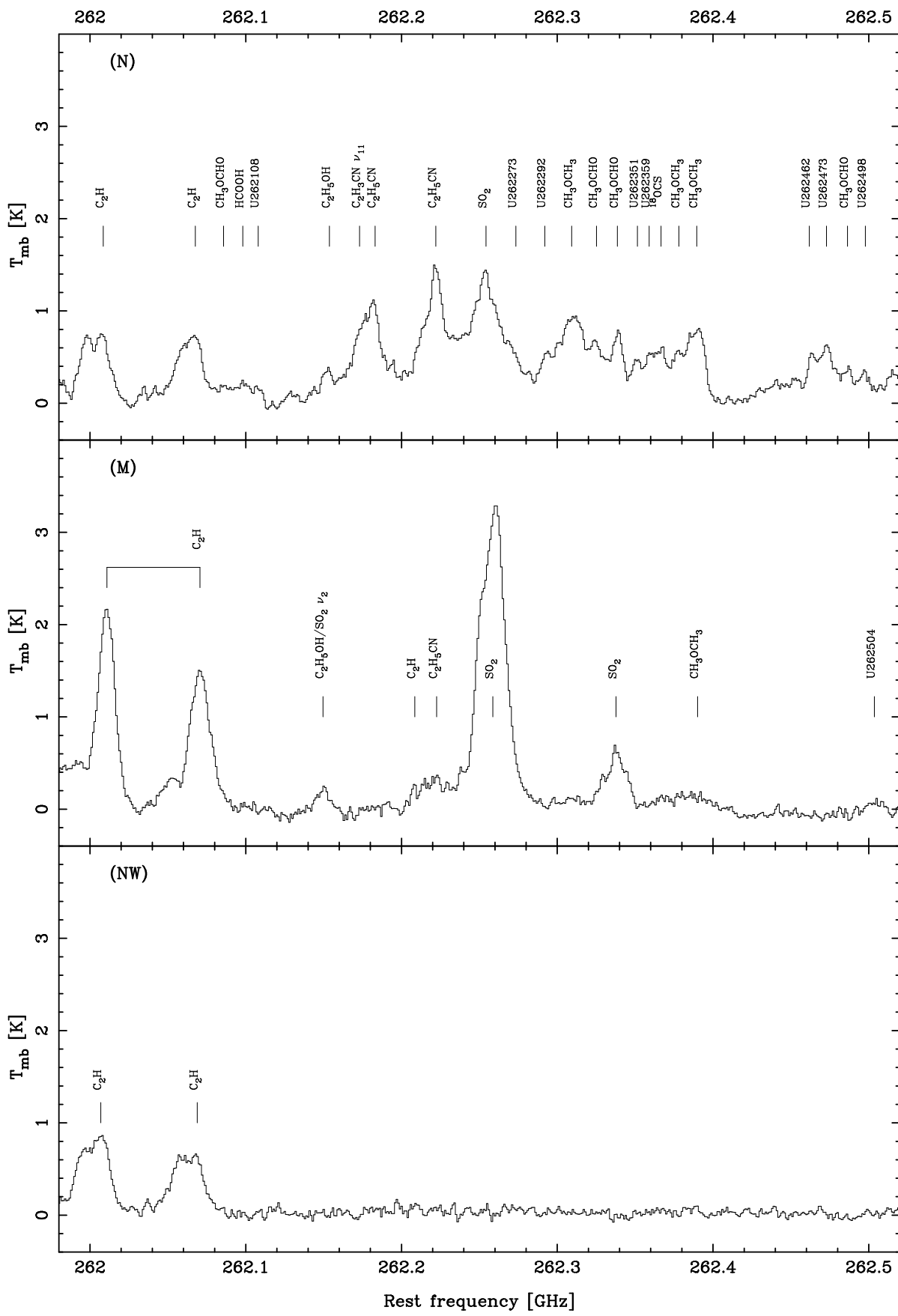


FIG. 1.—Continued

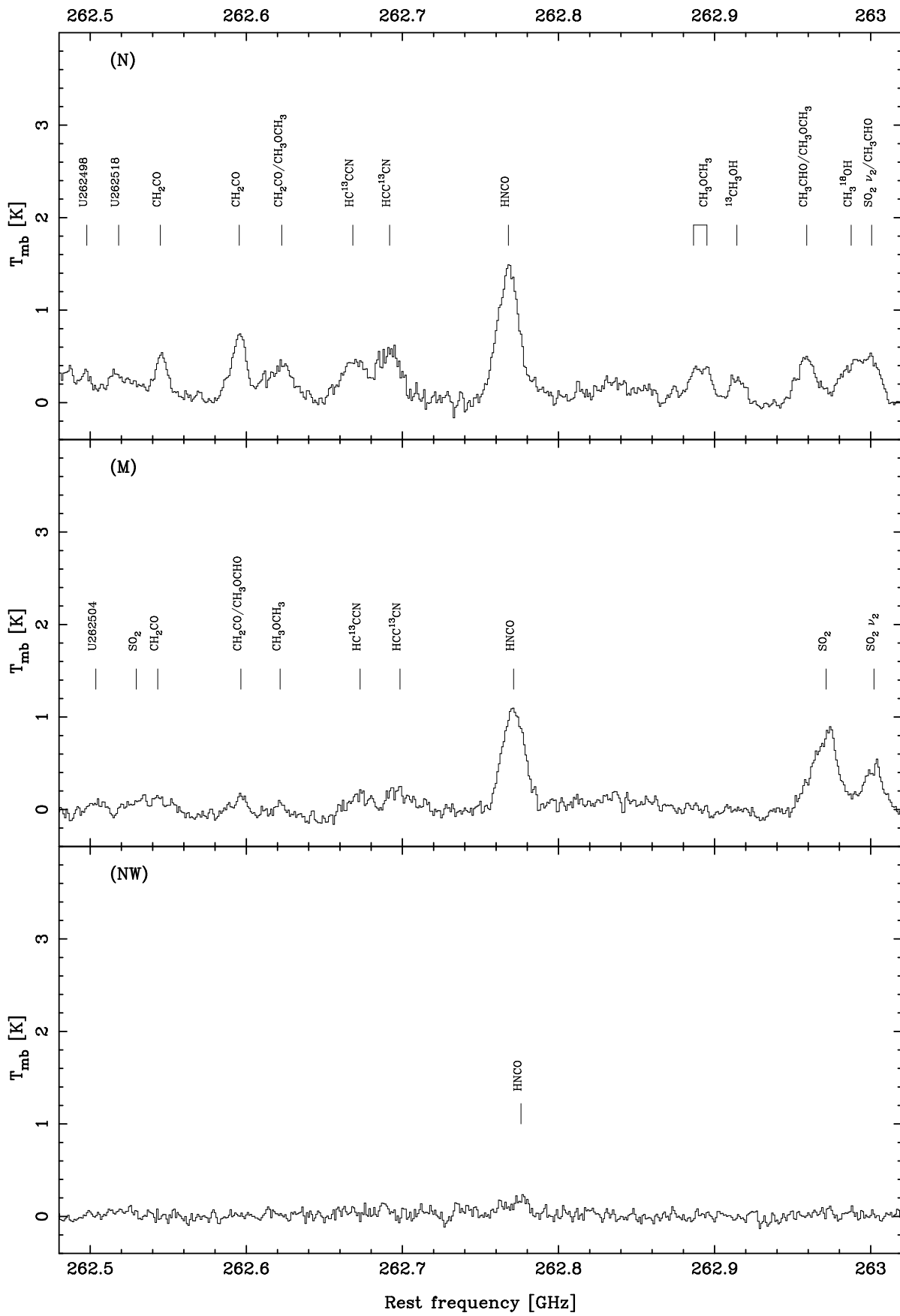


FIG. 1.—Continued

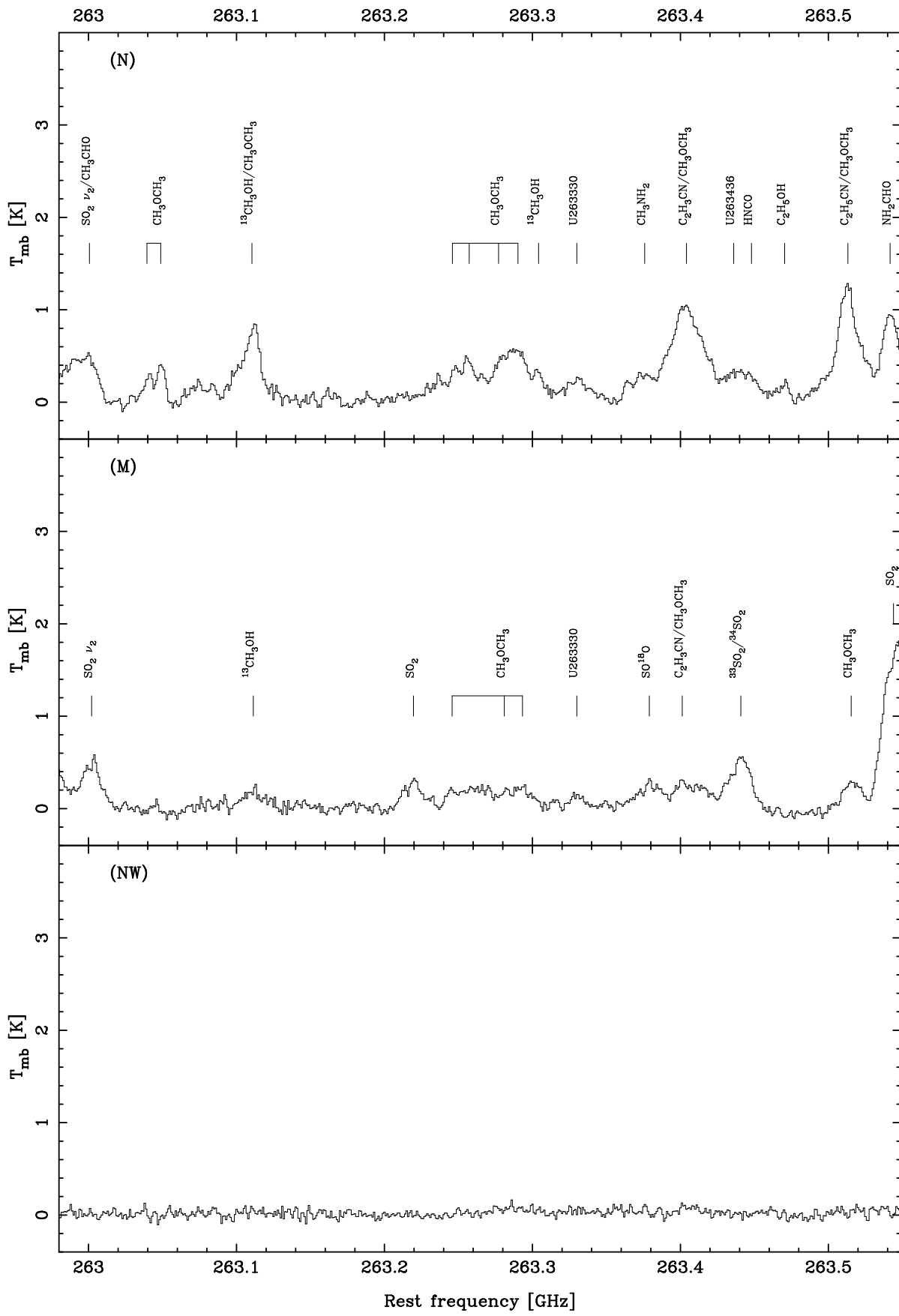


FIG. 1.—Continued

tions, and we therefore obtained an estimate of the continuum levels toward the sources from the baselines subtracted from the scans. The average continuum fluxes detected in the 22" beam were, adopting a sensitivity of 41 Jy K⁻¹ (T_A^{*}), 45 ± 12, 41 ± 8, and 7 ± 2 Jy toward N, M, and NW, where the error limits given are the standard deviations of the scatter between the individual scans. This flux level is consistent with the 50 Jy detected toward N by Goldsmith, Snell, & Lis (1987b) at a similar angular resolution.

Approximately 22% and 14% of the detected broadband flux toward N and M is caused by spectral line emission. In M, SO₂ emits 20% of the total spectral line flux through 125 lines (including all isotopomers), whereas in N the dominant sources of line emission are asymmetric organic molecules such as CH₃OH (13% of the total line emission, 152 lines), C₂H₅CN (10% of the line emission, 178 lines), and CH₃OCHO (8% of the line emission, 255 lines).

A few molecular transitions exhibit intermixed emission and absorption, e.g., H₂CO, and one transition from

CH₂NH is seen purely in absorption. In the complicated band of intermixed emission and absorption from CN(J = 2 → 1) occurring at a wide range of velocities in the 226.30–226.42 and 226.60–227.00 GHz regions, we have not fitted any Gaussians.

We would like to thank E. Herbst, J. C. Pearson, K. V. L. N. Sastry, I. Kleiner, F. J. Lovas, Th. Klaus, D. Cragg, M. Ikeda, and K. Takagi for fruitful discussions and for generously sharing spectroscopic data. We are grateful to the Jet Propulsion Laboratory for their spectral line catalog available on the World Wide Web. Thanks go to the SEST staff for help with the observations. A. N., P. B., and Å. H. gratefully acknowledge support from the Swedish Natural Science Research Council (NFR). T. J. M. is supported by a grant from PPARC and WMI by a NASA grant NAG 5-3653. We would like to thank the anonymous referee for several helpful and clarifying comments on the manuscript.

REFERENCES

- Anderson, T., Crownover, R. L., Herbst, E., & De Lucia, F. C. 1988, ApJS, 67, 135
 Anderson, T., Herbst, E., & De Lucia, F. C. 1990, ApJS, 74, 647
 Blake, G. A., Sutton, E. C., Masson, C. R., & Phillips, T. G. 1986, ApJS, 60, 357
 Cummins, S. E., Linke, R. A., & Thaddeus, P. 1986, ApJS, 60, 819
 Demaison, J., Cosléou, J., Bocquet, R., & Lesarri, A. G. 1994, J. Mol. Spec., 167, 400
 Dickens, J. E., Irvine, W. M., Ohishi, M., Ikeda, M., Ishikawa, S., Nummelin, A., & Hjalmarson, Å. 1997, ApJ, 489, 753
 Goldsmith, P. F., Snell, R. L., Hasegawa, T., & Ukita, N. 1987a, ApJ, 314, 525
 Goldsmith, P. F., Snell, R. L., & Lis, D. C. 1987b, ApJ, 313, L5
 Greaves, J. S., & White, G. J. 1991, A&AS, 91, 237
 Groner, P., Albert, S., Herbst, E., & De Lucia, F. C. 1997, ApJ, submitted
 Hoshino, Y., Ohishi, M., Ukai, T., Tsunekawa, S., & Takagi, K. 1996, ApJS, 104, 317
 Klaus, Th., Saleck, A. H., Belov, S. P., Winnewisser, G., Hirahara, Y., Hayashi, M., Kagi, E., & Kawaguchi, K. 1996, J. Mol. Spectrosc., 180, 197
 Kleiner, I., Lovas, F. J., & Godefroid, M. 1996, J. Phys. Chem. Ref. Data, 25, 4, 1113
 Kutner, M. L., & Ulich, B. L. 1981, ApJ, 250, 341
- Lafferty, W. J., & Lovas, F. J. 1978, J. Phys. Chem. Ref. Data, 7, 2, 441
 Lee, S. K., Ozeki, H., & Saito, S. 1995, ApJS, 98, 351
 Lovas, F. J. 1984, Spectral Line Atlas of Interstellar Molecules, National Institute of Standards and Technology (magnetic tape)
 ———. 1985, J. Phys. Chem. Ref. Data, 14, 2, 395
 Lovas, F. J., & Krupenie, P. H. 1974, J. Phys. Chem. Ref. Data, 3, 1, 245
 Mangum, J. G. 1993, PASP, 105, 117
 Nummelin, A., et al. 1998, in preparation (Paper II)
 Ohishi, M. 1992, in Chemistry and Spectroscopy of Interstellar Molecules, ed. D. K. Bohme et al. (Tokyo: Univ. of Tokyo Press), 23
 Ohishi, M., Ishikawa, S., & Kaiju, N. 1998, in preparation
 Plummer, G. M., Herbst, E., & De Lucia, F. C. 1987, ApJ, 318, 873
 Poynter, R. L., & Pickett, H. M. 1985, Appl. Opt., 24, 2335
 Saito, S., & Yamamoto, S. 1997, J. Chem. Phys., 107, 1732
 Sutton, E. C., Blake, G. A., Masson, C. R., & Phillips, T. G. 1985, ApJS, 58, 341
 Sutton, E. C., Jaminet, P. A., Danchi, W. C., & Blake, G. A. 1991, ApJS, 77, 255
 Towle, J. P., Feldman, P. A., & Watson, J. K. G. 1996, ApJS, 107, 744
 Turner, B. E. 1989, ApJS, 70, 539
 ———. 1991, ApJS, 76, 617
 Vogel, S. N., Genzel, R., & Palmer, P. 1987, ApJ, 316, 243